



HAL
open science

Supramolecular Chemistry and Self-Organization: A Veritable Playground for Catalysis

Loïc Leclercq, Gregory Douyere, Véronique Rataj

► **To cite this version:**

Loïc Leclercq, Gregory Douyere, Véronique Rataj. Supramolecular Chemistry and Self-Organization: A Veritable Playground for Catalysis. *Catalysts*, 2019, *Catalysts*, 9, pp.163. 10.3390/catal9020163 . hal-02978938

HAL Id: hal-02978938

<https://hal.univ-lille.fr/hal-02978938>

Submitted on 8 Feb 2023

HAL is a multi-disciplinary open access archive for the deposit and dissemination of scientific research documents, whether they are published or not. The documents may come from teaching and research institutions in France or abroad, or from public or private research centers.

L'archive ouverte pluridisciplinaire **HAL**, est destinée au dépôt et à la diffusion de documents scientifiques de niveau recherche, publiés ou non, émanant des établissements d'enseignement et de recherche français ou étrangers, des laboratoires publics ou privés.



Distributed under a Creative Commons Attribution 4.0 International License

Review

Supramolecular Chemistry and Self-Organization: A Veritable Playground for Catalysis

Loïc Leclercq *, Grégory Douyère and Véronique Nardello-Rataj *

Univ. Lille, CNRS, Centrale Lille, ENSCL, Univ. Artois, UMR 8181-UCCS-Unité de Catalyse et Chimie du Solide, F-59 000 Lille, France; gregory.douyere@gmail.com

* Correspondence: loic.leclercq@univ-lille.fr (L.L.); veronique.rataj-nardello@univ-lille.fr (V.N.-R.); Tel.: +33-32-043-4448 (L.L.); +33-32-033-6369 (V.N.-R.)

Received: 23 January 2019; Accepted: 30 January 2019; Published: 8 February 2019



Abstract: The directed assembly of molecular building blocks into discrete supermolecules or extended supramolecular networks through noncovalent intermolecular interactions is an ongoing challenge in chemistry. This challenge may be overcome by establishing a hierarchy of intermolecular interactions that, in turn, may facilitate the edification of supramolecular assemblies. As noncovalent interactions can be used to accelerate the reaction rates and/or to increase their selectivity, the development of efficient and practical catalytic systems, using supramolecular chemistry, has been achieved during the last few decades. However, between discrete and extended supramolecular assemblies, the newly developed “colloidal tectonics” concept allows us to link the molecular and macroscopic scales through the structured engineering of colloidal structures that can be applied to the design of predictable, versatile, and switchable catalytic systems. The main cutting-edge strategies involving supramolecular chemistry and self-organization in catalysis will be discussed and compared in this review.

Keywords: supramolecular architectures; adaptive chemistry; host–guest complexes; colloidal tectonics; homogeneous catalysis; heterogeneous catalysis; chemzymes; ionic liquids; nanoparticles

1. Introduction

Sixty years ago, Lehn, Pedersen, and Cram (1987 Nobel Prize) developed the concept of supramolecular chemistry, which focuses on the chemical systems made up of self-assembled molecular subunits through reversible noncovalent interactions (electrostatic effects, hydrogen bonds, metal coordination, aromatic stacking, hydrophobic and van der Waals forces) that force the spatial location and relative orientation of molecules towards each other [1]. This self-assembly allows for the construction of various structures, ranging from discrete supermolecules (i.e., dimers, trimers, tetramers) to extended supramolecular networks (i.e., highly complex materials crosslinked by reversible supramolecular interactions) [2]. This interdisciplinary field of research, reaching from chemistry to physics and biology, has found many applications in materials [3], medicine [4–6], pharmacy [7,8], data storage [9], catalysis [10–12], etc. In the context of catalysis, the tools of supramolecular chemistry (i.e., the molecular recognition and the self-organization via noncovalent interactions) are extremely important for the design and understanding of catalysts and catalysis [13]. This new discipline is named “supramolecular catalysis” [14].

Originally, this field was inspired by enzymatic systems that, unlike classical organic chemistry, catalyze reactions with high turnover and remarkable chemo-, regio-, and stereoselectivity under very mild conditions. Enzyme catalysis relies on the molecular recognition and on the stabilization of the transition state of a reaction [15]. Unfortunately, enzymes (i.e., proteins) are structurally complex and difficult to modify. In contrast, supramolecular catalysts offer good opportunities to

develop efficient and practical catalysts that may or may not have an enzyme equivalent in Nature (Figure 1) [16]. The first simple enzyme mimics were described by Cram et al. and used chiral host thiols (thiobinaphthyl crown ether) to catalyze transacylation (thiolysis) [17]. This catalyst uses the ability of a crown ether to bind the ammonium cation of the substrate and subsequently employs the nearby thiol function to cleave the ester. Classically, crown ethers, cryptands, and cyclodextrins (CDs), named “chemzymes”, have been extensively studied for their encapsulation properties and used as binding sites in supramolecular catalysts [18,19]. Nowadays, numerous cage-like receptors have been synthesized and applied in order to create microenvironments suitable for chemical transformations, e.g., a self-assembled capsule [20] or the so-called “tennis ball” structure [21]. The catalytic steps may be ensured via the use of organo- or organometallic catalytic residues [22,23]. All these systems are discrete and structurally well-defined, in which the use of receptors capable of recognizing guest molecules (substrates and/or catalysts) leads to benefits in terms of catalyst implementation and catalytic performance [24].

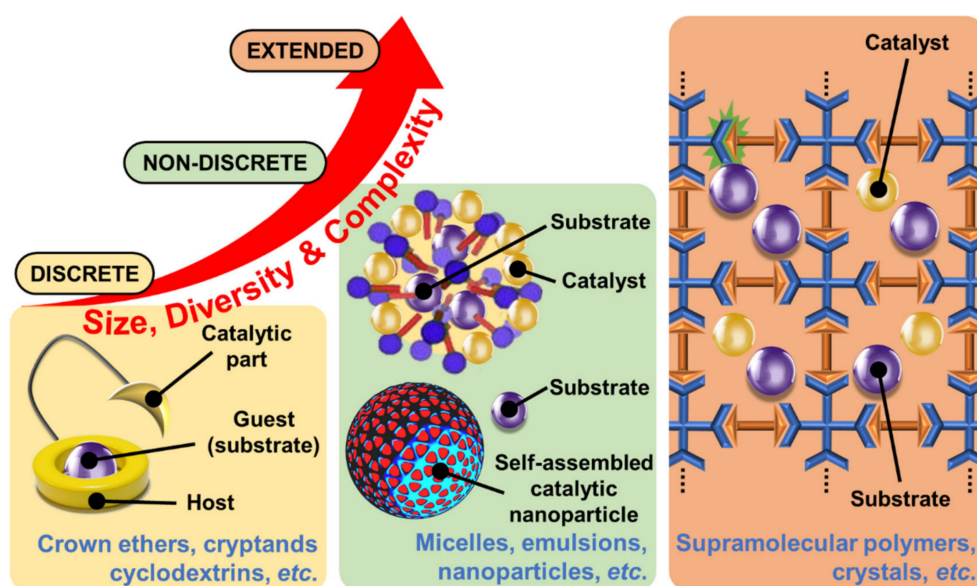


Figure 1. Some strategies for the engineering of catalytic systems from molecular building blocks by using supramolecular chemistry and self-organization.

In contrast, nondiscrete and structurally poorly defined systems, such as micelles, emulsions, and microemulsions, which are stabilized by molecular surfactants can also be used to accelerate biphasic liquid/liquid (L/L) reactions, which are clearly under mass transfer limitation due to the inadequate transport of reactants (Figure 1) [25]. Indeed, the use of molecular surfactants produces large interfacial areas and promotes the mass transfer. In comparison to the widespread phase transfer catalysis, such organized systems exhibit several advantages: (i) the presence of nanostructured dispersions in which the liquid/liquid interfacial area hugely favors the mass transfer between the nanodomains, and (ii) the compartmentalization of reactants and products that avoids or limits side reactions [26]. In addition, a reaction catalyst can also be concentrated into the interfacial layer to obtain very efficient catalytic reactions (i.e., “catalytic surfactants”) [27]. In such micro-heterogeneous systems, the presence of the catalyst jointly to mass transfer catalysis contributes to fast reactions. Despite all of the advantages brought about by the use of molecular surfactants, their presence complicates the phase separation, and, in some cases, a stable system (e.g., emulsion) is obtained instead of a biphasic system after cooling down the reaction mixture. Consequently, an important issue is the reversibility of the system leading to simple phase separation of the products [28].

On the other hand, extended supramolecular systems (e.g., macroscopic assembly, polymeric networks) can also be used to perform catalytic transformations (Figure 1). Indeed, physical gels and

self-assembled solvents have received an increased amount of attention because they represent an interesting case of supramolecular self-assembly [29,30]. These materials are formed from the ordered aggregation of molecules through noncovalent bonds to yield extended supramolecular materials that would contain catalytic units [31]. These systems may combine properties of homogeneous catalysts with heterogeneous ones (e.g., easy preparation, characterization, phase separation, and recycling) with an added value: their bottom-up, self-programmed construction [32]. For instance, room temperature ionic liquids (ILs) based on imidazolium salts have been used as self-assembled solvents to perform catalytic transformations due to a preorganized structuration [33]. When different molecules are dissolved in these networks, the creation of cavities that can accommodate the guest molecules provides a good platform for catalytic reactions [30,31].

Connecting the discrete and extended supramolecular assemblies, “colloidal tectonics” combines these two fields in order to obtain iterative self-assembling processes from molecules (named tectonic subunits) into self-assembled colloidal systems via a bottom-up edification (Figure 1) [34]. The assembling process is based on molecular recognition and operates at the level of the complementary tectons, providing an infinite variety of colloidal systems with predictable, versatile, and switchable properties [34]. As a result, these nanostructured systems can be useful for a vast array of applications, including catalytic facilitation systems, which are particularly useful for multiphasic systems (solid/liquid (S/L), liquid/solid/liquid (L/S/L), etc). These catalytic self-assembled colloidal systems (e.g., colloidal suspensions, Pickering emulsions, etc.) improve: (i) the performance of the catalytic systems, (ii) the mass transfer, (iii) the phase separation, (iv) the selectivity, and (v) the global ecological aspect of the process [35]. Despite all their benefits, the “colloidal tectonics” approach requires fine “programming” of tectons to make them amphiphilic and to allow for their self-organization, which results from the interactions at work between subunits of the system under consideration [34].

The objective of this contribution is to focus on the actual and potential use of self-assembled catalysts in the vast array of catalytic applications. We place emphasis on discrete and extended supramolecular assemblies endowed with catalytic activities. Through chosen examples, the strategies to obtain these supramolecular systems will be presented. Their catalytic applications will also be discussed. Finally, some future directions of investigation will be proposed. It is worth noting that, for the sake of clarity, only some typical examples are reported in this review. Therefore, the cited references are not intended to be an exhaustive list of all the works on the investigated topic but are portals to other publications.

2. Catalytic Systems Based on Discrete Supermolecules

The Nobel laureate Emil Fischer, who developed the philosophical roots of supramolecular chemistry, introduced the “lock and key” principle to describe the interactions between the enzyme and its substrate prior its chemical transformation. Following this concept, the development of synthetic mimics of active enzyme sites was considered. The simplest systems use a cavity that is capable of complexing molecules, leading to discrete assembly by way of nonbinding interactions and a functionalized moiety that can perform a chemical reaction. In this case, the reaction is triggered by the spatial proximity of the substrate and the catalytic group. Since the pioneer works of Cram and coworkers (see above) and the discovery, by Corey et al. in 1989, of oxazaborolidine catalysts, referred to as “chemzymes” due to the binding between the catalyst and substrate, a holy grail is to achieve the “syntheses” of various supramolecular systems with a catalytic function [36,37]. This research can take two forms: (i) the mimic of the catalytic features found in native enzymatic systems (ribonucleases, proteases, phosphatases, etc.) from new synthetic compounds, or (ii) the partial use of enzymatic properties (recognition) to create catalytic systems with varied reactivity.

N.B. In this section, only systems that use macrocyclic hosts will be described to highlight the main strategies involved in the field of catalytic systems based on discrete assemblies.

2.1. Concept

The mimic of natural enzymes, which works with remarkable regio- and stereoselectivities under very mild conditions, remains a major challenge. Therefore, artificial enzymes (or “chemzymes”), which are smaller and structurally much simpler than natural enzymes, can be used to obtain powerful and selective catalysis and to provide a simple model of enzyme models. Generally, the binding site is ensured by bio- or petro-sourced macrocyclic hosts, such as cyclodextrins (CDs), calixarenes (Cs), and/or crown ethers (nCn) (Figure 2) [38,39].

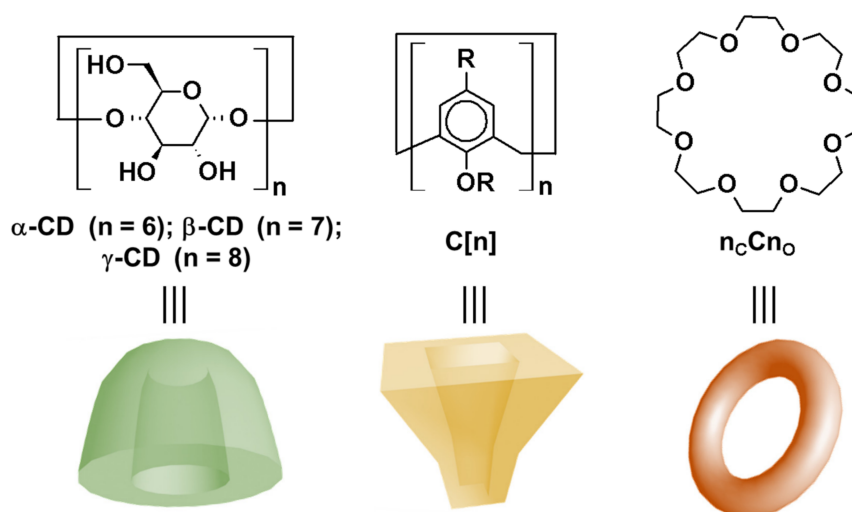


Figure 2. The structure and a schematic representation of different macrocycles (n_C = carbon number and n_o = oxygen number). CD, cyclodextrin; C, calixarene; nCn, crown ether.

CDs are water-soluble hosts able to accommodate a large variety of hydrophobic molecules [40]. Depending on the number of glucose residues, there are essentially three types of CDs: α -CD (six), β -CD (seven), and γ -CD (eight glucoses). Each type of CD has a cavity with slightly different sizes that confers on them a selectivity for well-sized molecules. Another synthetic host able to sequester hydrophobic molecules and ions is calixarene [41]. According to the residues' nature, calixarenes host–guest complexes can be obtained in an organic or a water environment. Finally, cyclic oligomers of ethylene oxide, named crown ethers, have the ability to strongly complex cations [42]. All these bio- or petro-sourced macrocyclic hosts can be used as “chemzymes” in order to mimic natural enzymes or to inspire new selective and efficient catalytic systems by way of their functionalization with an appropriate residue able to perform a chemical transformation (Figure 3).

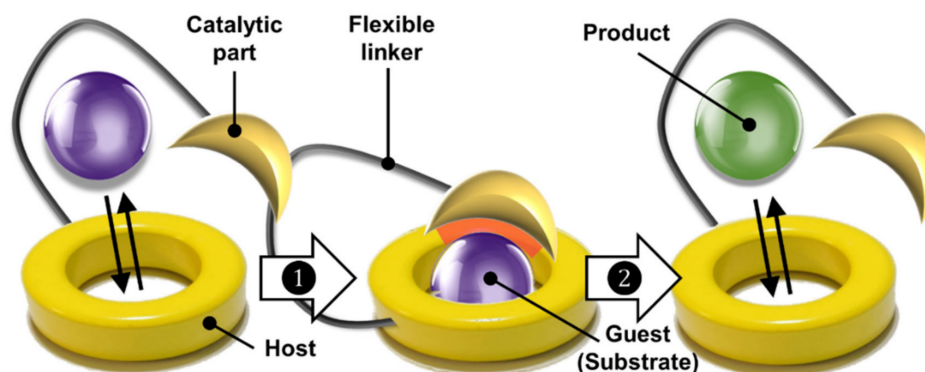


Figure 3. The general principle of “chemzymes” (1 = formation of the “chemzyme”–substrate complex and 2 = catalytic transformation).

The chemical reaction catalyzed by the “chemzyme” takes place in two sequential steps: (i) formation of the “chemzyme”–substrate complex using the host cavity; and (ii) catalysis allowing for the transformation of the substrate into a product. It is worth noting that the binding of the substrate (or substrates) is more or less specific depending on the “chemzyme”; the recognition is carried out according to the conformation and the chemical composition of the substrate. In this section, some typical systems that use macrocyclic hosts will be described.

2.2. Organocatalytic Systems

“Chemzymes” are widely used in organocatalysis, where the rate of a chemical reaction is increased by an organic catalyst, referred to as an “organocatalyst”, which consists of organic elements (carbon, hydrogen, oxygen, sulfur, etc.) and sometimes nonmetal elements found in organic compounds. For instance, in 1984, Breslow and coworkers proposed to use modified CD as a holoenzyme mimic for benzoin condensation (Figure 4) [43,44]. This “chemzyme”, based on functionalized β - or γ -CD, catalyzes the condensation with a rate increase of about 7-fold.

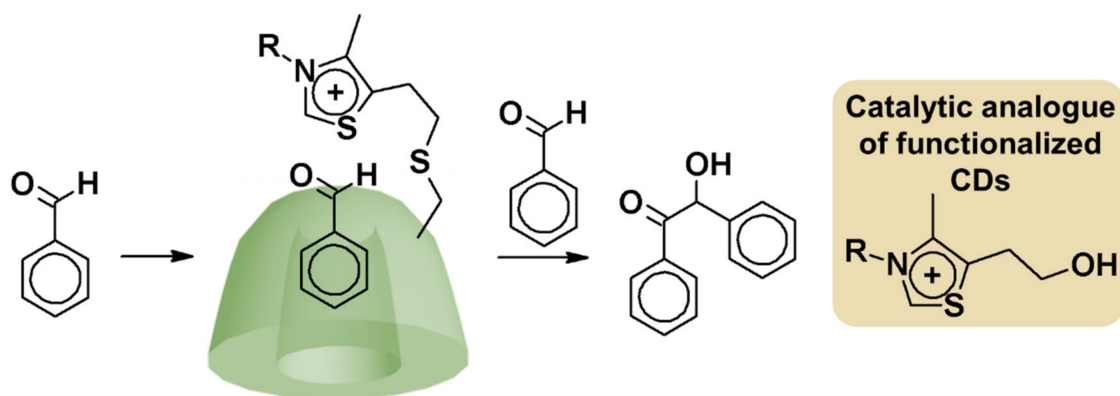


Figure 4. Benzoin condensation catalyzed by thiazolium-functionalized β - and γ -CD (R = Et or Bn).

In more detail, Breslow and coworkers performed kinetic studies of the benzoin condensation performed using thiazolium salts functionalized or not by β - or γ -CD (the structure of the catalytic analogue, i.e., thiazolium salts alone, is presented in Figure 4) [44]. Note that the various rate constants, k_{rel} , given in the following discussion are expressed relatively to 3-ethyl-5-(2-hydroxyethyl)-4-methyl-1,3-thiazolium, (i.e., the catalytic analogue with the *N*-ethyl group). For thiazolium salts alone, the benzoin condensation is more effective with *N*-benzyl than with residue *N*-ethyl ($k_{rel} = 20$). In contrast, when β -CD is linked to the thiazolium salt, an acceleration of the rate up to 2.5-fold compared to a control experiment ($k_{rel} = 2$ or 50 for β -CD attached to *N*-ethyl or *N*-benzyl residues, respectively). In contrast, in the presence of functionalized γ -CD, which can hold both benzaldehydes due to its larger cavity, k_{rel} increases until 9 and 150 (γ -CD linked to *N*-ethyl or *N*-benzyl residues, respectively). The authors also reported the effect of free β - and γ -CD in the presence of catalytic analogues on the reaction rates. These results prove that β -CD was a mild inhibitor while γ -CD only led to about a 2-fold increase in the rate. All these results prove that catalytic systems based on functionalized CDs work very well when the binding and the catalytic sites are linked to a flexible residue. Indeed, this flexible link allows us to bind the substrate into the CD cavity in a more appropriate geometry prior to the catalytic transformation. This assertion is perfectly supported by the outstanding catalytic activity observed when the thiazolium group is linked to the large γ -CD cavity combined with the flexible catalytic part. Therefore, this catalyst clearly behaves as an artificial enzyme.

However, it is worth noting that “chemzymes” without CD are also possible. For instance, Zhao et al. developed an enzyme/coenzyme mimic system using modified polyethylenimines as enzyme surrogates, and hydrophobic thiamine analogues (imidazolium or thiazolium cations) as

coenzyme mimics (Figure 5) [45]. A very efficient catalytic system was obtained: up to 3300-fold rate accelerations compared to a control experiment without polyethylenimines.

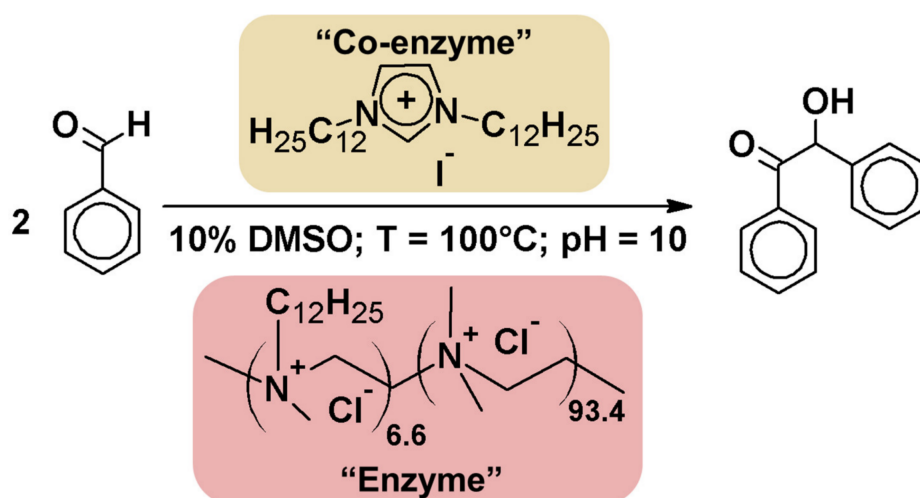


Figure 5. Benzoin condensation catalyzed by an artificial enzyme with imidazolium as coenzyme mimics. T, Temperature.

In 1989, Breslow et al. proposed the use of a modified CD to mimic the ribonuclease A [46]. As the two amino acids involved in the hydrolysis of RNA are histidine, the authors attached two imidazole rings on the primary face of β -CD (Figure 6) [47,48]. As expected, this “chemzyme” catalyzed the hydrolysis of a cyclic phosphate: the hydrolysis rate was enhanced 120 times compared to the uncatalyzed reaction. In addition, 5-*tert*-butyl-2-hydroxyphenyl hydrogen phosphate was the main product of the hydrolysis catalyzed by the “chemzyme”, whereas a similar reaction, performed in solution with sodium hydroxide, produced an equimolar mixture of both isomers (4-*tert*- and 5-*tert*-butyl-2-hydroxyphenyl hydrogen phosphate). The authors found that both imidazoles operate simultaneously, with one imidazole function protonated and the other unprotonated [49]. This mechanism is almost identical to that of the natural enzyme.

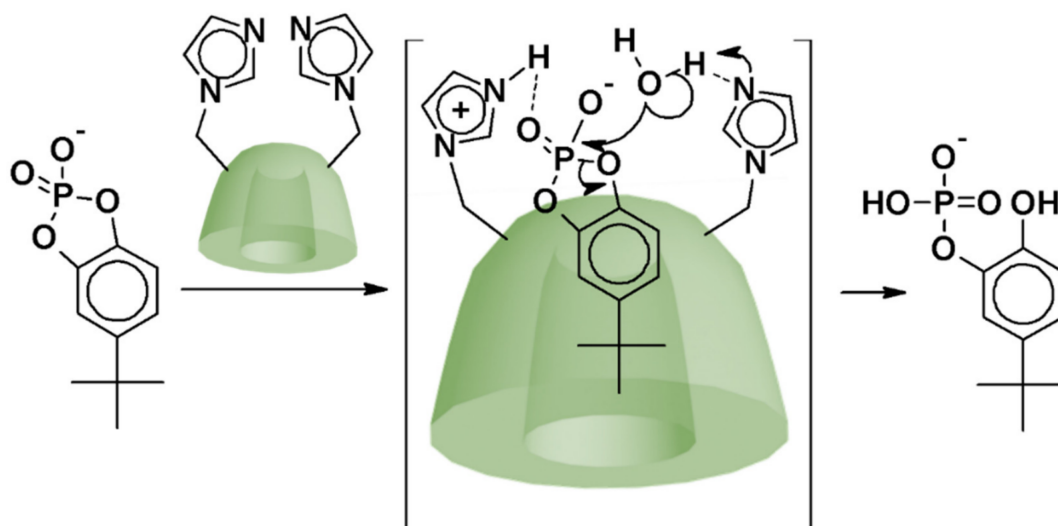


Figure 6. Bisimidazole-functionalized β -CD for the hydrolysis of a cyclic phosphate.

It is worth noting that the same functionalized β -CD can be used in the selective intramolecular condensation of ketoaldehyde to aldol (Figure 7) [50]. Generally, the intramolecular aldol condensation of dialdehydes carrying a *tert*-butylphenyl residue is almost random using simple imidazole

buffer catalysis. However, with the bisimidazole-functionalized β -CD, the authors reported a 97% preference for a single regiochemistry after cyclization. This very good regioselectivity was ascribed to the geometric preferences of these catalysts due to substrate binding inside the CD cavity. Therefore, this catalyst behaves as an artificial enzyme that is able to mimic enzymatic behavior. This assumption is supported by the selectivity decrease when the reaction is catalyzed by the monoimidazole-functionalized β -CD.

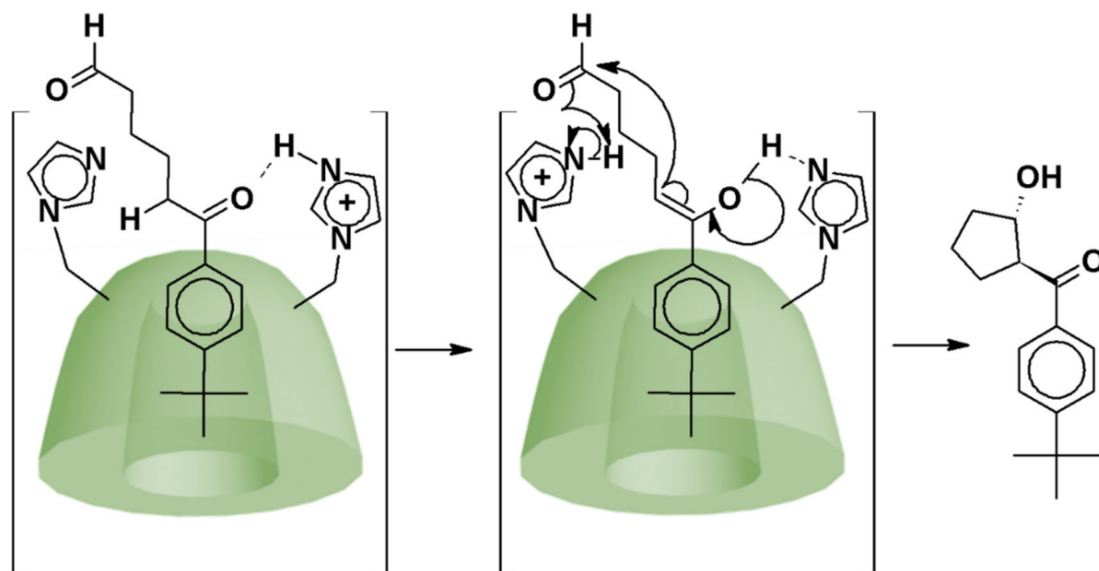


Figure 7. Intramolecular condensation of ketoaldehyde to aldol catalyzed by the bisimidazole-functionalized β -CD.

In 2005, Bols and coworkers reported on a “chemzyme” that mimics the glycosidase [51]. The substrate studied was 4-nitrophenyl- β -glucopyranoside. In the presence of cyanohydrin β -CD, the substrate was complexed and the proximity of the substrate and alcohol residue of the modified CD triggered the osidic cleavage (Figure 8). This reaction follows the well-known Michaelis–Menten kinetics.

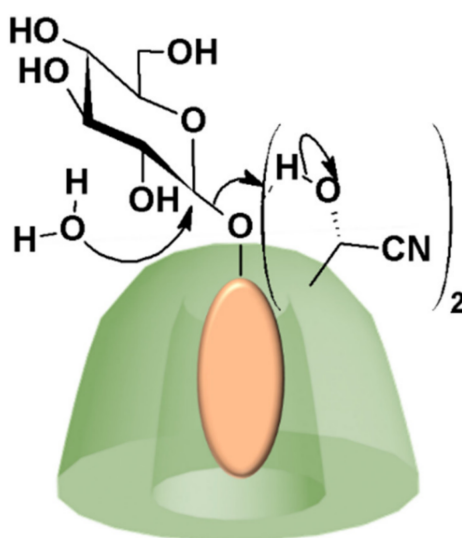


Figure 8. A “chemzyme”, based on cyanohydrin β -CD that mimics the mode of action of a glycosidase.

However, it is also possible to perform organocatalytic reactions away from the usual conditions of natural enzymes. For instance, in 2016, Galia and coworkers reported on the ring-opening

polymerization of ϵ -caprolactone in the presence of wet β -CD (Figure 9) [52]. The reaction was performed in batch reactors pressurized with Ar, CO₂, or N₂. In such conditions, the native β -CD was able to improve the polymerization rate. For instance, at a β -CD: ϵ -caprolactone molar ratio around 1:100 at 120 °C, the monomer conversion after 24 h increased from 4 to 99% with the pressure change (from 0.1 to 13 MPa). This effect is completely independent of the nature of the compressing gas. The MALDI-TOF analyses proved that the polymerization was initiated by the high energy water molecules inside the β -CD cavity. Therefore, wet β -CD at 13 MPa can catalyze the ring opening of ϵ -caprolactone and the polymerization's water molecules. The authors concluded that wet β -CD can be used to mimic lipase under high-pressure conditions.

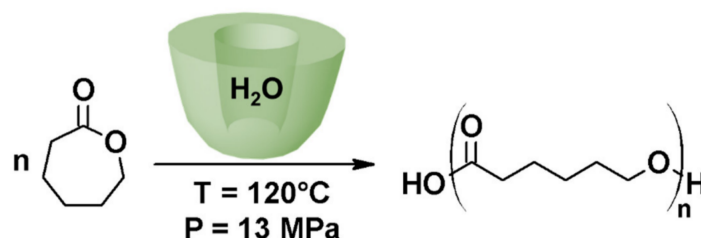


Figure 9. A “chemzyme”, based on native β -CD, that mimics the mode of action of a lipase under high-pressure conditions. P, pressure.

It is worth noting that calixarenes can also be used to obtain “chemzymes”. For instance, an archetype was the dinuclear C[4]-Cu(II) complex able to cleave the 2-hydroxypropyl-*p*-nitrophenyl phosphate (10^4 rate enhancement) and ethyl-*p*-nitrophenyl phosphate (2.7×10^4 rate enhancement) [53]. The rate enhancement compared to the mononuclear reference complex was attributed to the efficient synergic action of the two Cu(II) centers as well as the phosphate esters on the C[4] scaffold being well-preorganized (Figure 10).

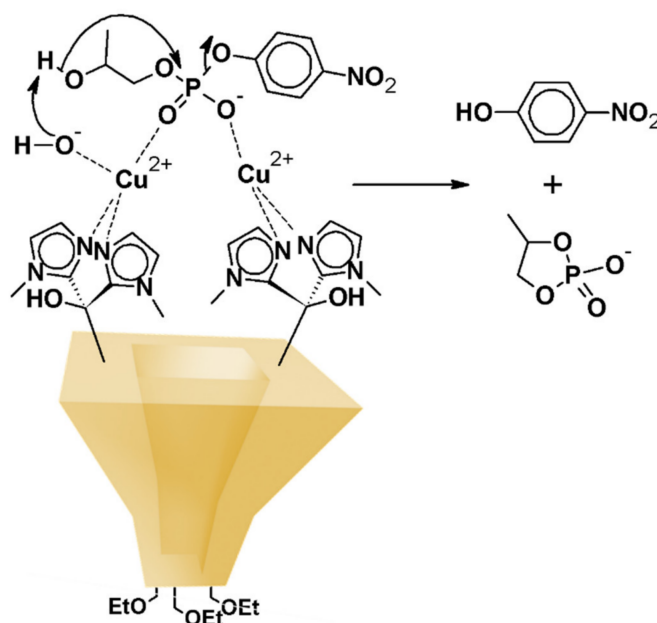


Figure 10. The cleavage of 2-hydroxypropyl-*p*-nitrophenylphosphate by a C[4]-Cu(II) complex.

Similar C[4]-bearing imidazole groups at different positions on the wide rim were also used for the enzyme-like release of *p*-nitrophenol from *p*-nitrophenyl esters in buffered solution (Figure 11) [54]. It is worth noting that the nucleophilic assistance of the imidazole moieties was confirmed by the PM3 semi-empirical method.

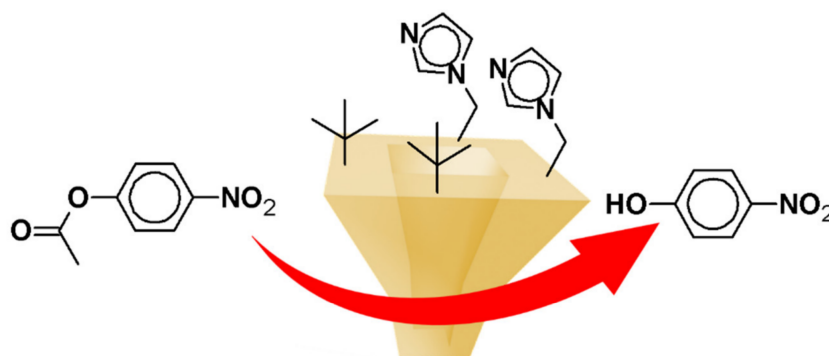


Figure 11. The hydrolysis of *p*-nitrophenyl by modified C[4].

Finally, the complexation capacities of crown ethers were applied in the construction of a dinuclear barium (II) complex and applied for the cleavage of esters and amides (Figure 12) [55]. One of them binds and activates the nucleophile while the other binds the amide or ester through the carboxylate, leading to an easy cleavage.



Figure 12. Transesterification by a dinuclear barium complex.

2.3. Organometallic Systems

The methodology used to mime an enzyme can be also applied in the context of organometallic catalysis. Therefore, the complexing properties of CD can also be exploited in the design of new homogeneous catalysts to perform hydroformylation, hydrogenation, etc. Some selected but typical examples will be discussed in this subsection. For the sake of clarity, only typical systems used for hydroformylation reactions are reported in this section.

For instance, it is worth noting that biphasic hydroformylation using water-soluble rhodium catalysts is advantageous with regard to catalyst recovery and product separation. For instance, the Ruhrchemie/Rhône-Poulenc process (1984), used for the hydroformylation of propene in butyraldehyde and isobutyraldehyde in the ratio 96:4, is the first commercially available two-phase system in which the rhodium catalyst is present in the aqueous phase due to the use of water-soluble phosphine [56]. Unfortunately, higher olefins cannot be converted at competitive and commercial rates due to their immiscibility with water (i.e., the catalytic phase) [57]. To overcome this limitation, Monflier and coworkers proposed to use CDs as supramolecular carriers [58]. However, in the presence of β -CD, it was found that the linear-to-branched aldehydes ratio (l/b) is always lower than that observed without the mass-transfer promoter (1.8 versus 2.8 without CD) due to the formation of inclusion complexes between β -CD and the tris-(3-sulfo-phenyl)-phosphine, TPPTS, ligand. This inclusion induces a displacement of the equilibria between the different catalytic species, leading to the phosphine low-coordinated rhodium species being poorly selective towards the formation of the linear aldehyde [59]. This drawback can be overcome by the use of α -CD [60]. In 2005, cationic α -CDs bearing 2-hydroxy-3-trimethylammonio-propyl groups were used to perform biphasic hydroformylation of higher olefins [61] (Figure 13).

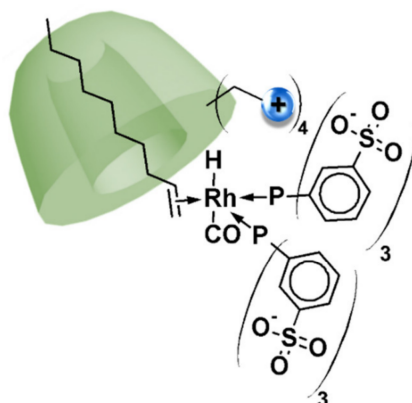


Figure 13. Rhodium complexes noncovalently bound to cationic α -CD bearing 2-hydroxy-3-trimethylammoniopropyl groups to perform biphasic hydroformylation of higher olefins.

The authors reported that the cationic α -CDs greatly improved the reaction rate, the chemoselectivity, and, surprisingly, the linear-to-branched aldehydes ratio (from 2.8 without CD to 5.4 with cationic α -CD). This effect was ascribed to the in-situ formation of new catalytic supramolecular species obtained by ion-exchange between the catalyst ligand and the cationic α -CD.

It is worth noting that, using an appropriate CD, it is also possible to complex phosphine, leading to water-soluble self-assembled ligands. The resulting ligands are capable of coordinating various metals, such as platinum, palladium, and rhodium, leading to second-sphere ligands. This second-sphere can be used to modify the selectivity of a given reaction due to steric hindrance. In the case of hydroformylation, adamantyl-substituted phosphines (e.g., di(1-adamantyl)benzylphosphine) were chosen as CD-interacting guests [62]. In the presence of methylated- β -CDs, a second-sphere ligand was formed, leading to a significant improvement in the reaction rate as well as regioselectivity in the homogeneous and biphasic hydroformylation of allyl alcohol and 1-octene, respectively (l/b up to 4.5, Figure 14).

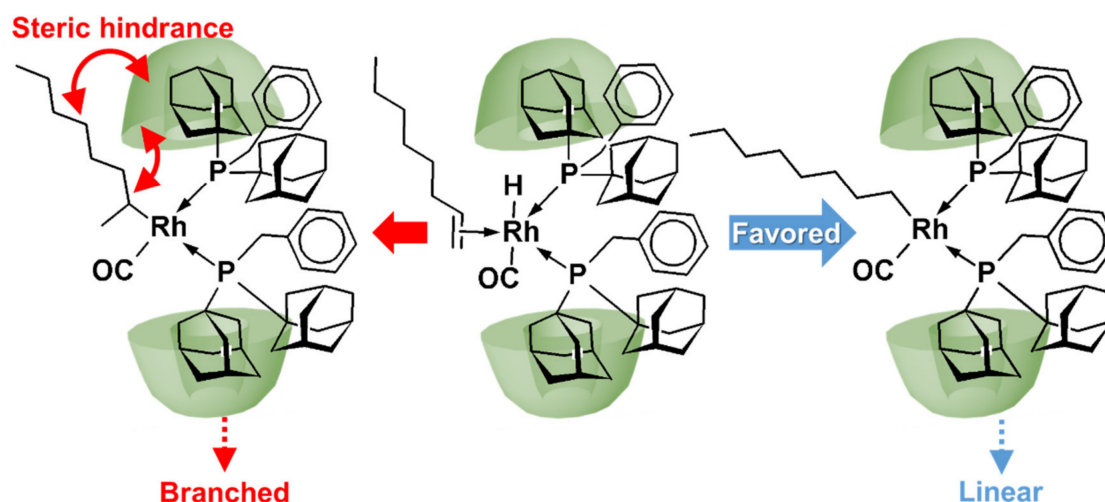


Figure 14. Supramolecular CD-based phosphorus as a first- and second-sphere ligand of rhodium.

The CD dimers can also be used to bind a substrate and a ligand (i.e., a catalyst) [63]. Under such conditions, the proximity between the catalyst and the substrate results in a highly efficient aqueous hydroformylation of higher olefins (Figure 15). It is worth noting that this water-soluble self-assembled ligand (i.e., a CD dimer/phosphine complex) also acts as a second-sphere ligand (see above).

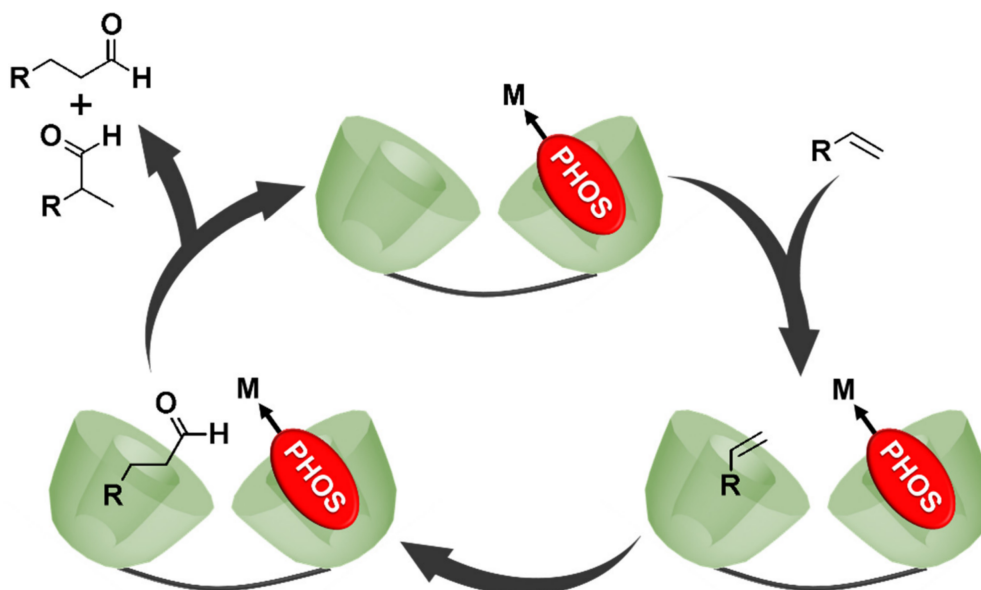


Figure 15. A CD dimer as a supramolecular reaction platform for hydroformylation.

Nowadays, numerous phosphines, based on a CD skeleton, have been developed to act as mass-transfer agents and as coordinating species towards transition metals. Obviously, to act as mass-transfer agents, the availability of the CD cavity is crucial. With respect to this assertion, Monflier and coworkers have been developing clever systems. For instance, in 2010, a diphenylphosphine based on a β -CD skeleton was used as a switchable catalyst for hydroformylation reactions [64]. Indeed, in aqueous solution, the self-inclusion of the phosphine occurs. The opposite holds with an organic solvent (Figure 16).

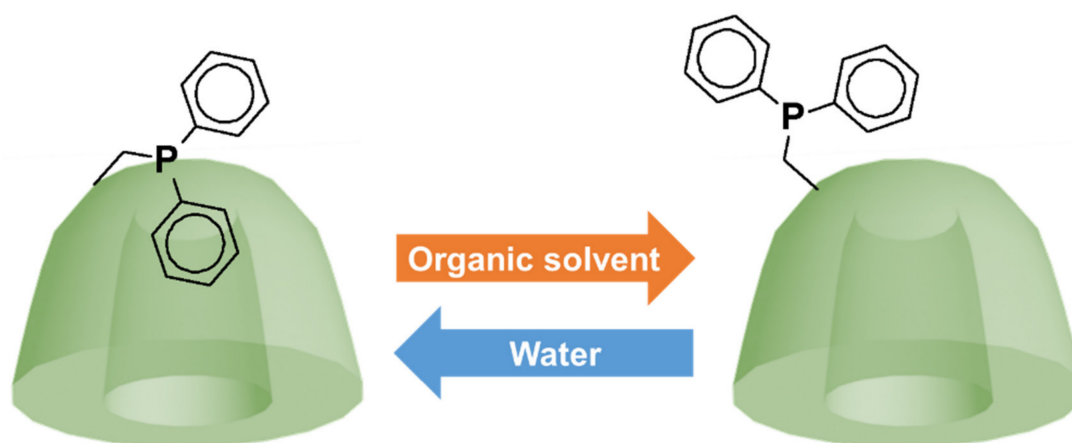


Figure 16. Permethyated β -CD phosphine conformation as a function of solvent.

Based on this principle, the self-inclusion can be controlled by the presence of guest molecules. Indeed, in the presence of a guest inside the cavity of a water-soluble CD-phosphine allowed for perfect control of the regioselectivity during aqueous hydroformylation reactions (Figure 17) [65].

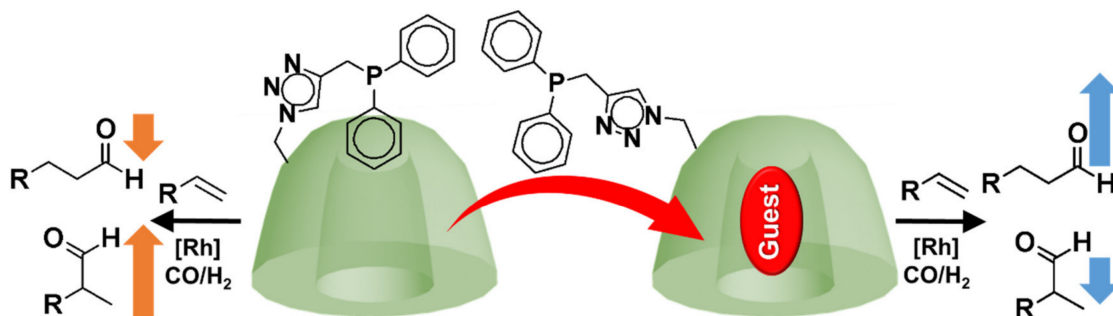


Figure 17. Cyclodextrin–phosphine with a guest-tunable conformation for biphasic, aqueous, and rhodium-catalyzed hydroformylation.

In 2017, a water-soluble 3,3'-disulfonatodiphenyl phosphine based on a β -CD skeleton was used in the hydroformylation of higher olefins [66]. This ligand was connected to the primary face of the β -CD by a dimethyleneamino spacer. As intra- and intermolecular inclusion of the sulfophenyl group in the β -CD cavity in aqueous solution is very important to ensure the smooth running of the catalytic cycle, the authors estimated the association constant related to the β -CD/sulfophenyl group couple (Figure 18). As this binding constant is sufficiently low, the inclusion process was easily displaced upon coordination to rhodium complexes. Therefore, these Rh-complexes, coordinated by a β -CD-based phosphine and applied in the hydroformylation of higher olefins, proved to be far more successful and efficient than a system consisting of supramolecularly interacting phosphine and CD. Indeed, the catalytic activity was up to 30-fold higher. Unfortunately, the chemo- and regioselectivities remained unchanged.

Finally, it is worth noting that the use of CD-based ligands is not limited to hydroformylation reactions. Indeed, all catalytic reactions involving organometallic complexes (e.g., hydrogenation [67], Heck reactions [68], Suzuki coupling reactions [69], etc.) can use these cavity-shaped ligands for their complexation and catalytic properties. For more information on these CDs, which are capable of acting both as first and second coordination sphere ligands towards various transition metals, we advise the reader to refer to the reviews of Hapiot and Armspach and coworkers [70–73].

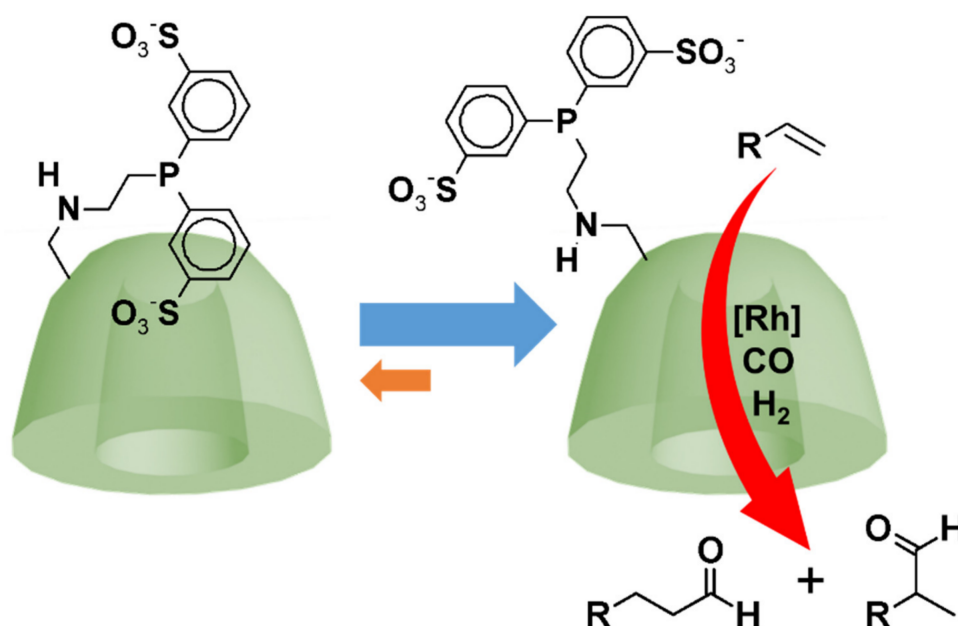


Figure 18. The principle of hydroformylation of higher olefins mediated by a CD-based organometallic catalyst.

3. Catalytic Systems Based on Nondiscrete and Structurally Poorly Defined Assemblies

Before we immerse ourselves into nondiscrete and structurally poorly defined assemblies based on colloidal chemistry (micelles, emulsions, and microemulsions), let us concentrate our attention on different concepts that have appeared in the last few years that enable us to perform a catalytic reaction in biphasic systems.

3.1. Concept

Catalytic biphasic systems usually entail water-in-oil or oil-in-water media for affording organic reactions in an aqueous environment. However, due to the immiscible nature of water and oil, all these systems require vigorous stirring to increase the interfacial area between the catalyst and/or the organic reactant(s). Unfortunately, even if the catalyst is operating under conditions that normally give a high catalytic activity, the observed reaction rate is lowered by the inadequate transport of reactants: the reaction rate is under mass-transfer limitation. To solve this issue, molecular surfactants can be used to promote mass transfer and to produce a large interfacial area. The use of surfactants allows for the formation of nondiscrete and poorly defined structures: micelles, emulsions, and microemulsions (μ ems). All of these nano- or micro-heterogeneous media can be used to perform a catalytic reaction (Table 1). Generally, micellar solutions require <5% of surfactant, microemulsions >10% depending on the Winsor type (see below), and emulsions 0.5–5%. However, it is worth noting that many papers report emulsions and micellar systems out of these reported ranges [74]. In terms of the solubilization efficiency of hydrophobic compounds, microemulsions and conventional emulsions are better than micellar solutions (1–30% versus <1%). However, this again depends on the systems used. For instance, the solubilization in microemulsions clearly depends on the Winsor-type system (see below).

It is worth noting that the classification chosen here is not exhaustive at all and that examples of systems with undefined or biased catalytic mechanisms are common. In such a situation and for the sake of clarity, only some typical examples of surfactant-type catalysts, that act in a dual role both as a surfactant to increase the local concentration of organic substrates in colloidal aggregates (i.e., nano- or microreactors) and as a catalyst to activate the substrates, are reported in this section.

Table 1. The principal difference between micellar solutions, emulsions, and microemulsions.

| Properties | Micellar solutions | Microemulsions | Emulsions |
|--------------|--|---------------------------------------|--|
| Shape | Spherical, cylindrical... ¹ | Droplets or bicontinuous ² | Spherical, cylindrical... ⁴ |
| Size | 4–10 nm | 5–100 nm | 0.1–25 μ m |
| Aspect | Transparent | Transparent | Turbid |
| Stability | Thermodynamic | Thermodynamic | Kinetic |
| Separation | No | No ³ | Yes |
| Formation | Spontaneous | Spontaneous | With energy |
| Viscosity | Fluid | Fluid | Fluid to viscous |
| Cosurfactant | No | Yes/No ² | No |

¹ Depending on the packing parameter (PP, see below). ² Depending on the Winsor type. ³ Assuming no change in composition, pH, temperature, and pressure. ⁴ See references [75,76].

3.2. Micelles and Emulsions

In aqueous solutions, molecular surfactants are compounds that lower the surface tension of the air/water interface. As an excess of surfactants occurs in the superficial layer, these molecules can promote the formation of well-organized monolayers. Then, once the surface is saturated, these amphiphilic molecules aggregate in the bulk phase to form aggregates above the critical aggregation concentration (CAC) as a consequence of the hydrophobic effect [77]. The simplest aggregate that can be obtained is micelles, where the hydrophobic tails form the core of the aggregate and the hydrophilic heads are in contact with the surrounding water molecules. However, other types of aggregates can also be formed, such as deformed micelles (e.g., cylindrical or worm-like micelles)

or other structures (e.g., bilayers, vesicles). The shape of the aggregates depends on the packing of the molecules, which is directly correlated to the chemical structure of the surfactants, namely the balance between the hydrophilic head and the hydrophobic tail. A measure of this is the packing parameter (PP), which often well-predicts the type of aggregates formed by a surfactant in an aqueous medium. The PP is defined as the ratio of the chain volume, v_s , to the volume projected by the optimal headgroup area, a_s , and the critical chain length, l_s (Figure 19) [78].

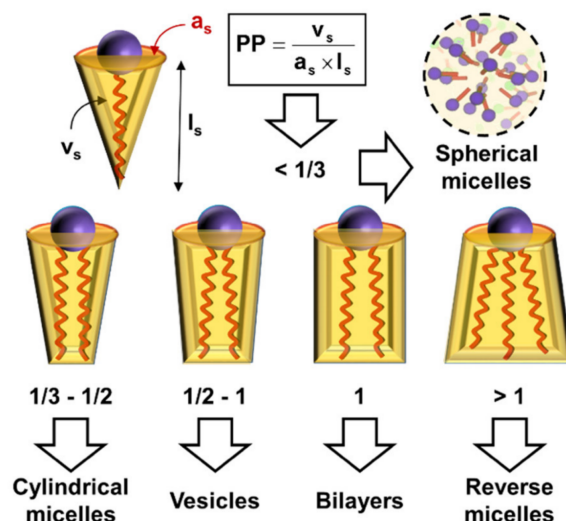


Figure 19. Relationships between the PP, the shape of the surfactant, and the self-assembled structure in aqueous media when $PP < 1$ or in organic solvents for $PP > 1$.

Consequently, in aqueous solutions, a small PP indicates a small tail attached to a large headgroup, leading to direct spherical or cylindrical micelles, and a large PP indicates large tail(s) connected to a smaller headgroup, leading to a vesicle or bilayer. In contrast, for $PP > 1$, the self-assembled structures in organic solutions are reverse micelles. It is worth noting that all of these self-assembled structures (except for vesicles) are spontaneously formed. Therefore, these aggregates are thermodynamically stable (except for vesicles that are kinetically stable). In aqueous solutions, direct micelles can also be used to dissolve lipophilic substrates in the hydrophobic micelle core, leading to swollen micelles and to a higher substrate concentration than in the surrounding water. The opposite holds for the inverted micelles, which allow for the solubilization of hydrophilic molecules. Under such conditions, the reaction rate is greatly accelerated by the higher concentration of reagents inside the micelles. Unfortunately, despite the low concentration of surfactant needed to obtain micelles, the quantity of solute in this colloidal medium is very low [79].

In order to accommodate more hydrophobic molecules, the system needs more surfactants to obtain the so-called emulsions. Unfortunately, in these systems, phase separation occurs and an external energy input (e.g., stirring or sonication) is needed to form them. Over time, emulsions tend to revert to the stable state of the phases comprising the emulsion. Therefore, their stability refers to the ability to resist change in their properties over time. In consequence, all emulsions are thermodynamically unstable but kinetically stable mixtures of the two immiscible liquid phases. The nature of emulsions (i.e., oil-in-water, O/W, or water-in-oil, W/O) depends on the volume fraction of both phases and the type of surfactant present (Figure 20). Surfactants tend to promote dispersion of the phase in which they do not dissolve very well. For instance, surfactants, which dissolve better in water than in oil, tend to form O/W emulsions (i.e., they promote the dispersion of oil droplets throughout a continuous phase of water).

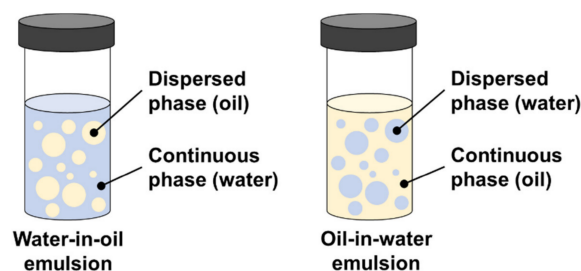


Figure 20. Classical types of emulsion.

Since the incorporation of surfactants in aqueous media has been proved to enhance the reactivity of water-mediated reactions via the formation of micelles or emulsions, the use of surfactants as catalysts in water is widespread and has been studied for a number of different transformations in water. In addition, the compartmentalization of reactants, products, and catalysts leads to a better stability of these species. Some typical examples are reported in this section.

The pioneer works of Kobayashi, Engberts, and coworkers, at the end of the 1990s, to perform reactions using surfactant-combined catalysts in order to promote interfacial transformations, have been of interest to numerous research teams. Indeed, the breakthrough came in the period 1997–1999 with the one-pot, multicomponent, and acid-catalyzed condensations (i.e., aqueous aldol [80,81], Mannich-type [82,83], and Diels–Aders reactions [84]) using Brønsted or Lewis acid catalytic surfactants, such as *p*-dodecylbenzenesulfonic acid, scandium trisdodecyl sulfate, and copper or zinc didodecyl sulfate, in aqueous media and under mild reaction conditions. This concept was extended, some years later, to the condensation of aldehydes, amines, and Danishefsky’s diene or allyltributyltin [85]. These organic reactions in an aqueous environment are cheap, safe, globally eco-friendly, and operate under mild reaction conditions. Moreover, these acid–surfactant-combined catalysts give good yields (up to 100%) compared to systems that use organic solvents (<10% in methanol or dichloromethane). Indeed, emulsion droplets are formed in situ from catalytic amounts of these catalytic surfactants and reaction substrates. These hydrophobic droplets, although dispersed in water, act as a protecting shell for the water-labile substrates, such as silyl enolates, preventing their hydrolytic decomposition (Figure 21).

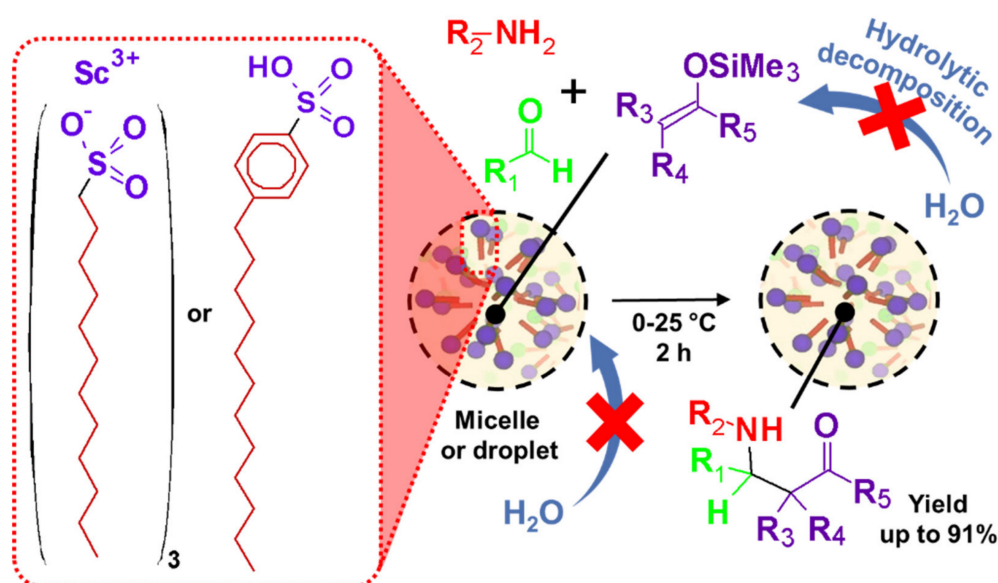


Figure 21. Lewis or Brønsted acid–surfactant-combined catalysts (scandium trisdodecylsulfate or *p*-dodecylbenzenesulfonic acid) for the synthesis of β -amino carbonyl compounds from three-component Mannich-type reactions of aldehydes, amines, and silyl enolates.

Some years later, all of these advantages prompted Kobayashi and coworkers to develop dehydration reactions in a water environment. For instance, in 2001, these authors reported the acid-catalyzed direct esterification of carboxylic acids with alcohols as a model reaction (Figure 22) [86].

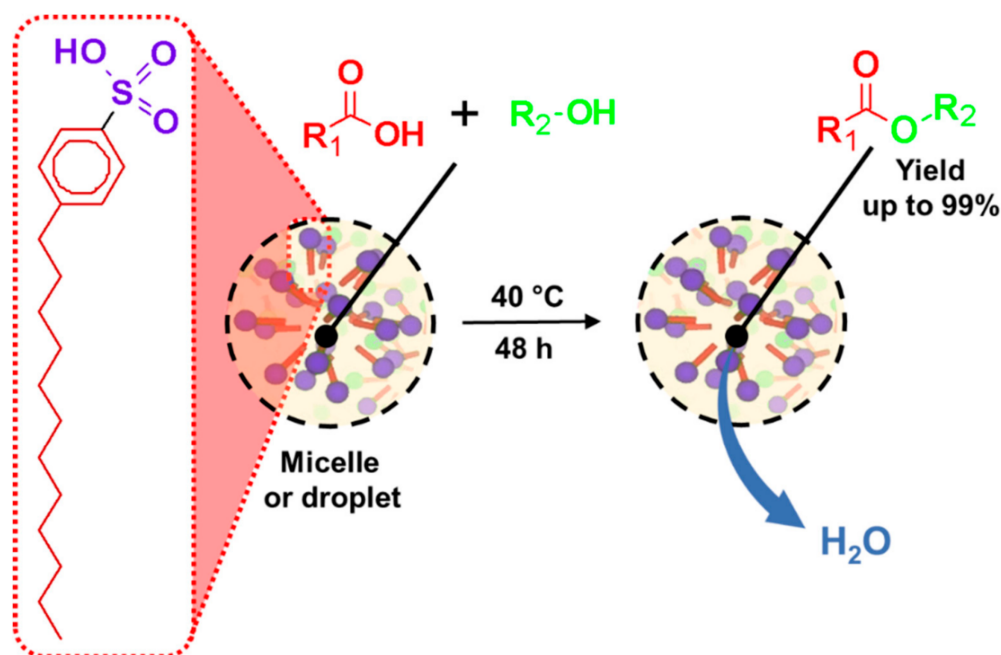


Figure 22. Brønsted acid–surfactant-combined catalyst, *p*-dodecylbenzenesulfonic acid, for esterification in a water environment.

Indeed, the direct esterification is difficult to carry out in aqueous solution, since water generated during the reaction needs to be excluded to shift the equilibrium. For instance, azeotropic distillation is used to remove water molecules generated during the reaction. Based on this ascertainment, the authors proposed the use of surfactant-type catalysts and organic substrates (e.g., carboxylic acids and alcohols) in an aqueous environment in order to obtain a compartmentalization of reactants and products (e.g., esters) inside the hydrophobic micelle core. In addition, the use of acidic surfactants would concentrate the catalytic species (i.e., protons) onto the surface droplets. In this system, the hydrophobic products remain in the micelle core, whereas the water molecules are expelled out of the droplets due to the lipophilic nature of their interior. As a result, the dehydration reactions efficiently proceed even in the presence of a large amount of water as a solvent. The surfactant-type Brønsted acid can be used for direct selective esterification in an aqueous environment. The results have proved that the esterification catalyzed by *p*-dodecylbenzenesulfonic acid (10 mol %) in water can be carried out in 89–99% yields at 40 °C within 48 h under mechanical stirring.

In 2002, this research team reported dehydration reactions for the synthesis of ethers, thioethers, and dithioacetals [87]. More recently, Shirakawa and Kobayashi reported the use of surfactant-type Brønsted acid for catalytic dehydrative nucleophilic substitutions of benzyl alcohols with various carbon- and heteroatom-centered nucleophiles in water [88]. This catalytic system uses the well-known dodecylbenzenesulfonic acid as a catalyst and can be applied to the stereoselective C-glycosylation of 1-hydroxy sugars in water (Figure 23). These reactions were carried out in 61–96% yields at 40–80 °C within 24–48 h under mechanical stirring.

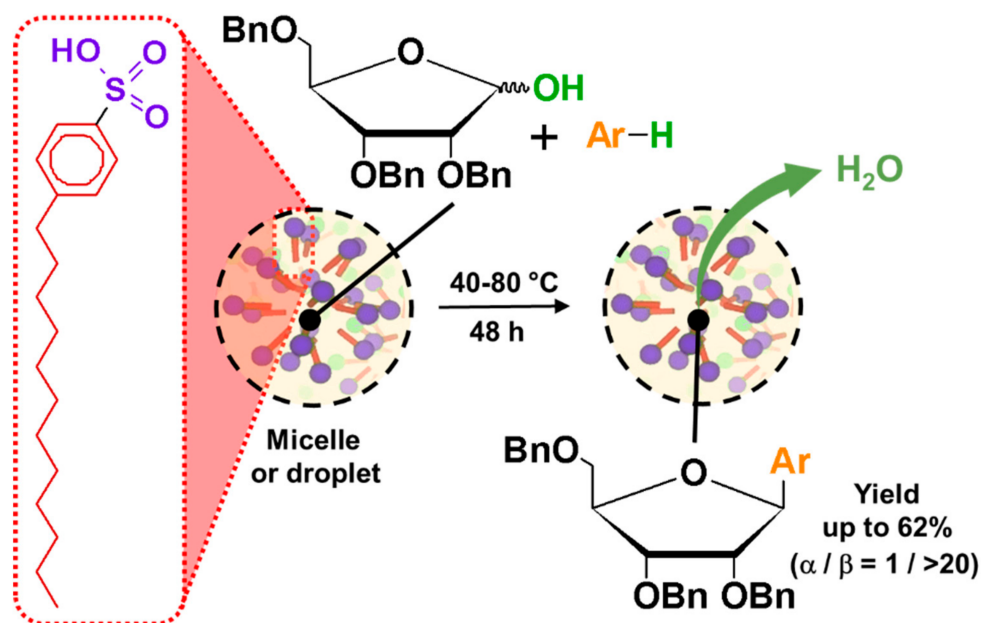


Figure 23. C-Glycosylations of 1-hydroxy sugar in water catalyzed by a Brønsted acid–surfactant, *p*-dodecylbenzenesulfonic acid.

Following these works, this concept was extended to other dehydration reactions using *p*-dodecylbenzenesulfonic acid in aqueous solution. For instance, a typical example has been published by Song et al. in which the synthesis of 12-aryl-8,9,10,12-tetrahydrobenzo[*a*] xanthen-11-ones from aromatic aldehydes, 2-naphthol, and 5,5-dimethyl-1,3-cyclohexanedione (dimedone) was carried out in 76–93% yields at 40–42 °C within 1–2.5 h under ultrasound irradiation instead of classical mechanical stirring [89]. However, it is worth noting that the use of a Brønsted acid–surfactant-combined catalyst is not necessarily required to perform the synthesis of 12-aryl-8,9,10,12-tetrahydrobenzo[*a*] xanthen-11-ones. For instance, the 12-(4-chlorophenyl)-9,9-dimethyl-8,9,10,12-tetrahydrobenzo[*a*] xanthen-11-one can be easily performed at room temperature in the presence of various archetypal cationic surfactants (e.g., cetylpyridinium, methyltriphenylphosphonium, tetradecyltrimethylammonium, cetyltrimethylammonium, or sodium dodecyl sulfate) in an aqueous environment (Figure 24). The authors reported that the best compromise between the reaction time and the product yield was observed with increasing the alkyl chain length of the surfactant up to a C₁₄, after which the reaction yield and reaction time were essentially independent of the surfactant alkyl chain length. The authors supposed that, in this catalytic system, the dehydration rate has only been improved due to the water exclusion outside the hydrophobic core of micelles or emulsion droplets [90].

Some research teams have systematically used ultrasound irradiation instead of mechanical stirring. For instance, in 2012, the condensation of 1,5-diphenyl-1,4-pentadien-3-one with aminoguanidine hydrochloride was easily performed in 84–94% yields within 2–3 h under ultrasound irradiation [91]. In 2015, the same group reported the synthesis of 2,3-disubstituted-2,3-dihydroquinazolin-4(1*H*)-one from one-pot, three-component condensation of isatoic anhydride, aromatic aldehyde, and amine under ultrasound irradiation in 80–92% yields at 40–42 °C within 1–2 h [92]. The same year, Yang et al. investigated the synthesis of 3-hydroxy-5,5-dimethyl-2-[phenyl(phenylthio)methyl]cyclohex-2-enone with aromatic aldehydes, substituted thiophenols, and 5,5-dimethyl-1,3-cyclohexanedione under similar experimental conditions [93]. These reactions were carried out in 20–92% yields at 25 °C within 1–6 h. Numerous catalytic systems based on surfactants are now used to boost multicomponent reactions (e.g., Biginelli [94], Kabachnik–Fields [95], Strecker [96], and Hantzsch [97]). For more information on this topic and for other multicomponent reactions, we advise that the reader refer to the recent review of Ostaszewski and coworkers [98].

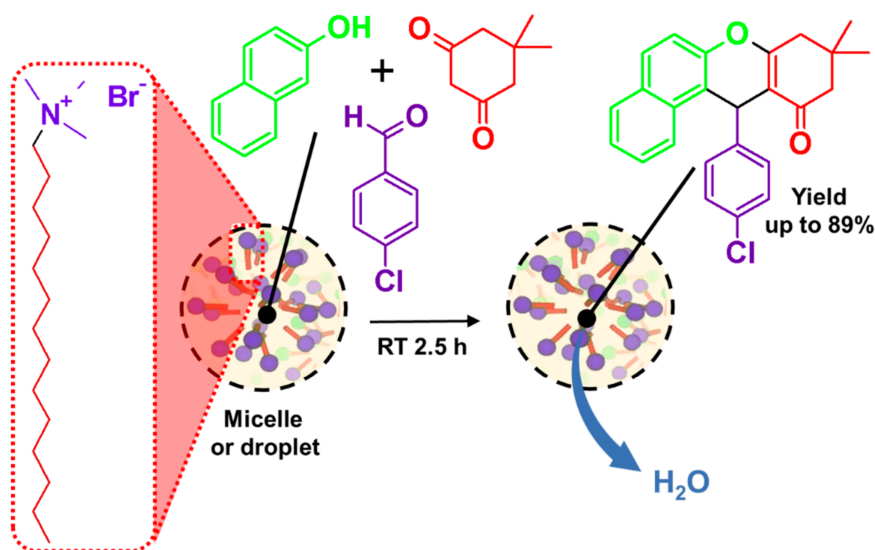


Figure 24. Synthesis of 12-(4-chlorophenyl)-9,9-dimethyl-8,9,10,12-tetrahydrobenzo[a] xanthen-11-one catalyzed by a tetradecyltrimethylammonium bromide surfactant at room temperature.

Due to their clear advantages, including an optimized interfacial area between two immiscible solvents or incompatible molecules and the conversion of a classical stirred batch to the nanoreactor process, these systems have been extended to organometallic catalysts. For instance, Li and co-workers reported the transfer hydrogenation of aldehydes with an amphiphilic polymer-based iridium catalyst, leading to the emulsification of aldehydes and water (Figure 25) [99].

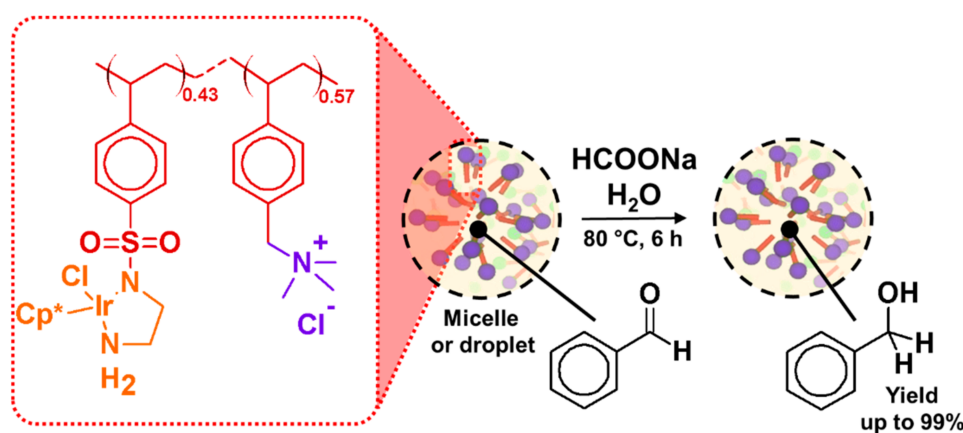


Figure 25. Catalytic hydrogenation of aldehydes using an amphiphilic polymer combined with an iridium organometallic complex.

This smart system greatly improved the reaction rates (up to 93% conversion with the amphiphilic-polymer-based iridium catalyst, whereas the classical Ir complexes only give 8%) as a consequence of the high contact area due to the emulsification and also thanks to the interfacial concentration of reactants around the catalyst.

A very similar strategy uses the stabilization of metallic nanoparticles (NPs) by micelles. For instance, in 2006, Beletskaya and coworkers reported the possibility to stabilize palladium NPs in micelles formed by polystyrene-*co*-poly(ethylene oxide) and cetylpyridinium chloride as surfactants [100] (Figure 26). The activity of this catalytic system was comparable to that of the low-molecular-weight palladium complexes for Heck and heterocyclization reactions. However, the stability of the colloidal palladium system has been improved with very good recyclability thanks to the possibility of the thermomorphous separation of the catalyst and products.

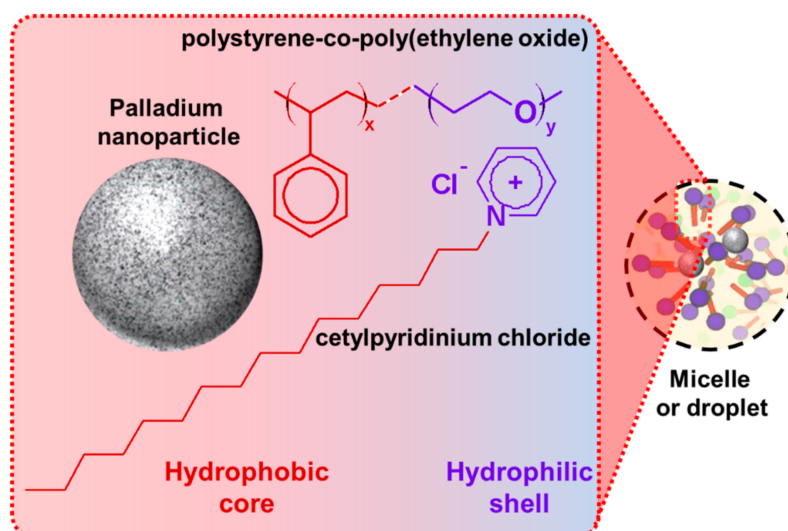


Figure 26. A palladium colloidal system stabilized by a block copolymer and a cationic surfactant.

These biphasic systems can be very useful to obtain domino/cascade ecofriendly processes for chemical syntheses. For instance, McErlean et al. reported, in 2012, a relative interplay between on-water and in-water reactions, where water can serve as a reaction medium, product partitioning, and reaction catalyst depending on the different aqueous solubilities of organic reactants and products, which are shuttled between the two phases of the emulsion [101].

As mixtures of constituents able to interact with each other are dynamic, it is possible to obtain the adaptation of the chemical entities, in response to either internal factors or to external physical stimuli and chemical effectors, through upregulation or downregulation of given members or species by redistribution under thermodynamic control (eventually kinetic) [102]. It is worth noting that colloids, based on molecular surfactants, are able to give commutable systems. The easiest system is obtained from a temperature-sensitive surfactant. For instance, in 2013, Brønsted acid amphiphilic imidazolium salts bearing ethylene oxide (EO) and alkane sulfonic acid residues (Figure 27) were used to esterify the oleic acid with methanol to provide biodiesel [103].



Figure 27. Thermosensitive amphiphilic Brønsted acid imidazolium salts used for the synthesis of biodiesel.

The hydrophilic/lipophilic balance of the surfactant gives it the capacity to generate less stable acid/alcohol emulsions when there is a large number of hydrophilic EO units. However, at a lower number of EO units and/or at high temperatures, the catalyst became lipophilic. Therefore, the control of EO units allows for an emulsification with an optimum catalytic performance for 350 EO. In addition, the produced biodiesel could be separated by a simple decantation and the catalyst could be reused up to 5 times contrary to homogeneous catalytic systems.

In the context of aqueous biphasic hydroformylation (see above), the use of surfactants to generate stable fine emulsions is very exciting to produce a sufficiently large interfacial area to promote mass transfer of the water solubility of olefins. Despite all of the advantages brought about by these systems, the presence of surfactants complicates the phase separation and kinetically stable emulsions

are obtained instead of a biphasic system after cooling down the reaction mixture. In this context, some strategies have been developed to control the emulsification. For instance, in 2009, Schmitzer et al. reported the interfacial Rh/trisulfonated, triphenylphosphine-catalyzed hydroformylation of higher alkenes in emulsion based on a CD/surfactant complex (Figure 28) [28]. The anionic ligands increased the conversion due to Rh localization at the oil droplet surface stabilized by cationic surfactants (i.e., the formation of nanoreactors). However, the combination of cationic surfactants and native α -CD allowed for the fine control of the reaction medium by thermoregulation. Indeed, during the reaction (80 °C), the emulsification, driven by cationic surfactant self-assembly, is allowed due to the dissociation of the CD/surfactant complexes, whereas, at the end of the reaction, α -CDs helped to break the emulsion by the complexation of cationic surfactants, leading to a fast decantation.

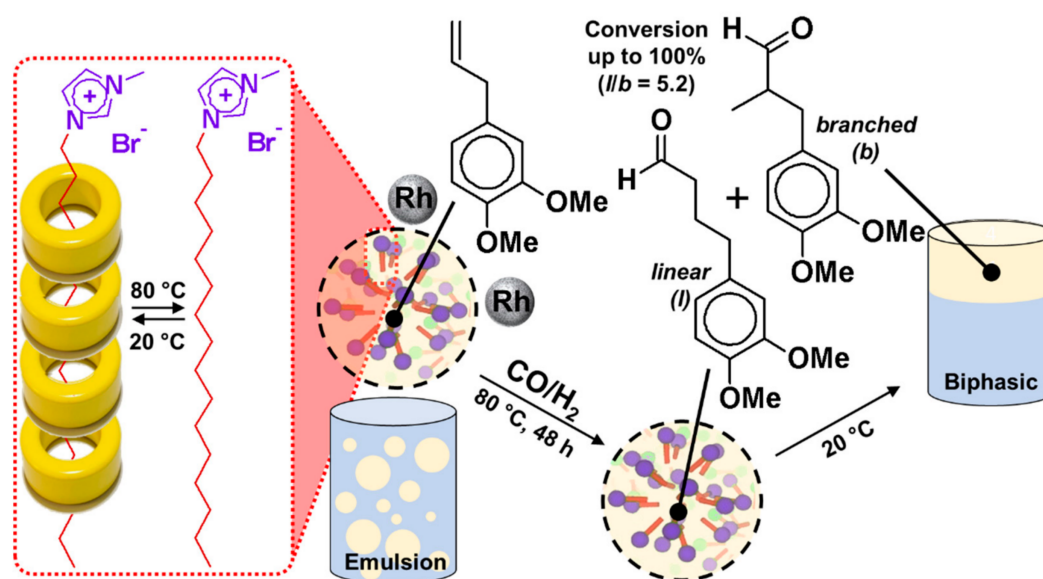


Figure 28. The combination of CD/cationic surfactant for interfacial catalysis in a thermoregulated hydroformylation reaction in an emulsion.

Very similar systems were developed in 2012 by Monflier and co-workers [104]. The authors used a water-soluble phosphine that was able to self-assemble in micelles. In the micellar region, neutral β -CDs formed a complex with the phosphine and destroyed the micelles. In contrast, micelle destabilization was observed with a high concentration of ionic β -CDs. In the Rh-catalyzed hydroformylation reaction of 1-decene, the catalytic performance of such micellar systems was improved without impact of the ionic β -CD on the regioselectivity (i.e., the linear-to-branched ratio). As in the previous case, a beneficial effect on the decantation at the end of the reaction was also reported.

All of these nondiscrete and structurally poorly defined assemblies based on colloidal chemistry (micelles and emulsions) accelerate the reaction rate by the higher concentration of reagents inside the micelles or the emulsion droplets. As a consequence, these procedures are globally simple, mild, efficient, and eco-friendly. Despite all of the advantages brought about by micellar catalysis, these systems are limited to a low reagent loading. Moreover, the presence of surfactants complicates the phase separation and kinetically stable emulsions can be obtained instead of a biphasic system after cooling down the reaction mixture. To solve these drawbacks, some systems, based on switchable media, have been developed; however, their generalization is not easy. Fortunately, molecular surfactants can also provide μ ems with larger aggregate sizes than conventional “swollen micelles” (10–100 versus 5–10 nm) and that allow us, at least in part, to address some of these drawbacks.

3.3. Microemulsions

Unlike classical emulsions, which require an energy input to be produced, microemulsions, abbreviated as μ ems, are spontaneously formed by “solubilizing” water or oil molecules with a mixture of surfactants, co-surfactants, and/or co-solvents [105]. The three basic types of μ ems are direct (O/W), reversed (W/O), and bicontinuous. The Winsor systems are a way to classify the μ ems [106]. There are four types of systems: Winsor I (WI), which is a two-phase system composed of an O/W phase with an organic phase; Winsor II (WII), which is a two-phase system composed of a W/O phase with an aqueous phase; Winsor III (WIII), which is a three-phase system in which an intermediate surfactant-rich phase (a bicontinuous phase) is formed between aqueous and organic phases; and Winsor IV (WIV) can be considered as a single-phase WIII system (Figure 29).

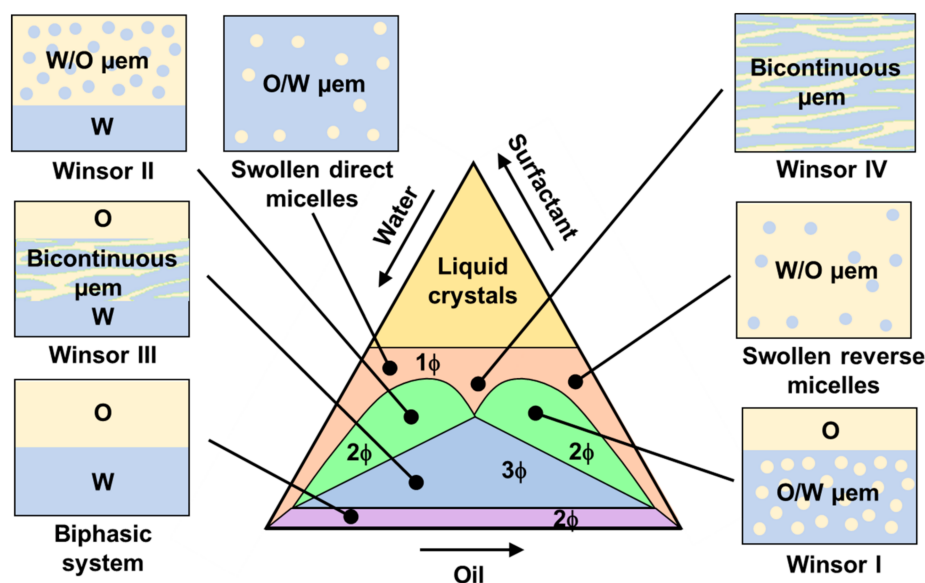


Figure 29. A schematic phase diagram of a surfactant/water/oil ternary system and microemulsion Winsor types. Note that the boundaries are arbitrary and depend on the system chosen.

The WI, WIII, and WIV systems can be very useful to perform catalytic reactions in water/oil systems due to the presence of small nanodomains (i.e., the mass transfer is greatly improved). In addition, their shelf-life and their spontaneous formation are very interesting properties. Unfortunately, these systems require a relatively large amount of surfactant, and the system often needs the addition of cosurfactants (e.g., alcohols). It is worth noting that, for the sake of clarity, only typical systems used for hydroformylation and oxidation are reported in this section.

As previously mentioned, biphasic hydroformylation using water-soluble rhodium catalysts is advantageous in terms of catalyst recovery and product separation. In this context, several elegant approaches have been explored to increase the mass transfer of higher olefins in the aqueous phase. One of these approaches is the use of μ ems stabilized by surfactants. These systems, which are very exciting, produce a sufficiently large interfacial area to promote mass transfer. In contrast to micellar catalysis, μ ems are good platforms on which to increase olefin mass transfer. Unlike emulsions, which require an energy input to be produced, μ ems are spontaneously formed by “solubilizing” oil molecules with one or more surfactant(s) [107]. Consequently, μ ems are thermodynamically stable, in contrast to emulsions, which are kinetically stable. The Winsor IV (WIV) systems can be very useful to dissolve oils due to the presence of small nanodomains (i.e., in these systems, the olefin solubility is greatly enhanced). In order to maximize the separation, the WIII is more relevant because, in this case, the μ em behaves as a third phase located between the oil and water phases. Unfortunately, these systems need a large amount of surfactant. In addition to their properties for catalytic reactions and processes (long shelf-life and their spontaneous formation), μ ems can be easily tuned by the

selection of appropriate surfactants. Indeed, they allow for a better solubilization of hydrophobic reactants or even for the reuse of dissolved catalysts.

Consequently, hydrophobic olefins can be successfully hydroformylated in μem s based on nonionic surfactants with reaction rates higher than in a two-phase system [108–111]. It is worth noting that all of these catalytic systems use alkylpolyglycol ether-type nonionic surfactants, whereas various rhodium complexes, stabilized by water-soluble ligands, can be used, such as SulfoXantPhos ([2,7-bis(SO_3Na)-4,5-bis(diphenylphosphino)-9,9-dimethylxanthene]) or TPPTS (tris-(3-sulfophenyl)-phosphine). Under optimized reaction conditions, very high turnover frequencies and selectivities ($>300\text{ h}^{-1}$ and linear-to-branched aldehydes up to 99/1) were obtained. Moreover, in the majority of cases, the catalyst recovery can be achieved by a simple phase separation followed by ultrafiltration. Recently, the possibility to transfer the hydroformylation of long-chain olefins in μem s at an industrial scale has been studied in miniplants [112–114]. The results prove clearly that μem s can be employed in realistic conditions to perform hydroformylation with easy phase separation (Figure 30). The authors used sulfonated XantPhos as a water-soluble ligand instead of TPPTS. Indeed, this ligand is clearly located in the middle phase (i.e., the μem phase in WIII) to a larger extent. Based on these results, the μem s can be very efficient in the case of hydroformylation. Unfortunately, their phase behavior strongly depends on the composition, temperature, surfactant (e.g., degree of ethoxylation for nonionic surfactants), and surfactant/catalyst interaction [115].

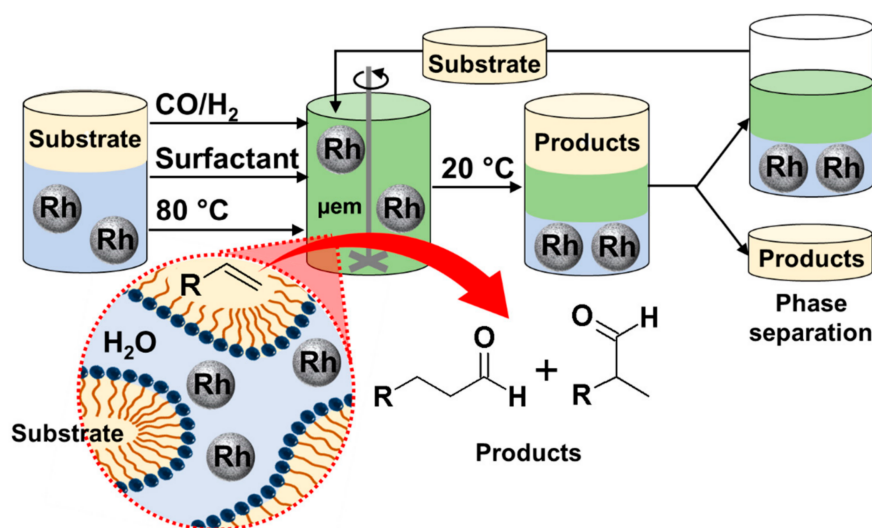


Figure 30. The schematic process for the hydroformylation of long-chain olefins in a microemulsion (μem).

It is worth noting that these kinds of μem can be used for other organometallic reactions [116]. In this study, the authors used cationic (dodecyltrimethylammonium, tetradecyltrimethylammonium and hexadecyltrimethylammonium bromide) and nonionic surfactants (nonylphenylethoxylates, alkylethoxylates, etc.). During the Heck coupling reaction between iodo-benzene and styrene, the obtained reaction medium is a two-phase μem (in the presence of hexadecyltrimethylammonium bromide as a surfactant and 1-propanol as a cosurfactant) due to the stoichiometric amount of the base needed to perform the Heck reaction. In this system, the Heck coupling reaction was successful and about 70% conversion was achieved in 5–6 h with $>75\text{ wt. \%}$ of water. The catalyst can be easily recycled and reused several times with minor catalyst leaching.

Oxidation reactions are widely used for converting organic materials to useful chemicals of a higher oxidation state. In the context of “green” chemistry, catalytic oxidations combined, in particular, with hydrogen peroxide, H_2O_2 , are receiving much attention for liquid-phase catalytic processes. To overcome the incompatibility of the aqueous H_2O_2 solution with the organic substrates, the liquid-liquid multiphase catalysis, which allows for combining efficiency and selectivity with a catalyst and product separation appears to be particularly attractive. One of the elegant strategies consists

of μem systems. A typical example was reported by Holmberg and coworkers in 2001 [117]. The authors reported the oxidation of two aqueous azo dyes (methyl orange and amaranth) catalyzed by manganese porphyrins using H_2O_2 . These reactions have been performed in an oil-in-water μem based on a nonionic surfactant (octaethylene glycol monododecyl ether) using a lipophilic acid as a cocatalyst (benzoic acid or dodecanoic acid) and 4-*tert*-butylpyridine as a base and ligand (Figure 31). The oxidations performed in the water/hexadecane-dichloromethane μem were fast for the two azo dyes and the reaction rate increased with the amount of lipophilic acid added in the catalytic mixture. As expected, the reaction rates in the μem were considerably higher than in a biphasic system (similar conditions but without surfactant). It is worth noting that the addition of anionic surfactants (sodium dodecyl sulfate and tetradecyltrimethylammonium bromide) gave a clear decrease in the reaction rates. The authors proposed that the rate-limiting step is the formation of a metallo-acylperoxy complex in the interfacial layer. This complex oxidizes the azo dye in a subsequent step.

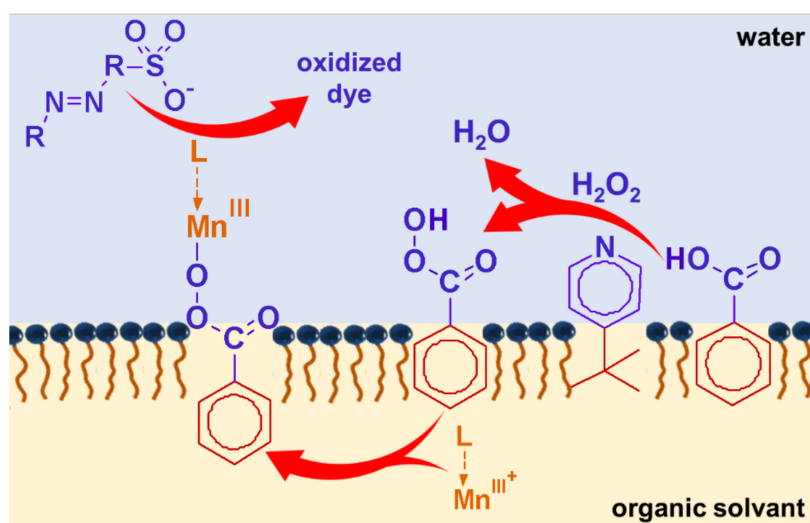


Figure 31. A schematic illustration of a catalytic μem based on octaethylene glycol monododecyl ether, hexadecane, dichloromethane, and water (blue: hydrophilic atoms; red: hydrophobic atoms; orange: manganese porphyrin).

As various catalytic anions can be coupled by electrostatic interactions with cationic surfactants, it is possible to formulate catalytic μems in which the catalyst is in the vicinity of the interfacial layer in order to significantly boost the reaction rates. For instance, classical homogeneous oxidation catalysts, such as molybdate and tungstate anions, can be used to generate singlet oxygen ($^1\text{O}_2$) or peroxometalates in the presence of H_2O_2 and depending on the pH. Obviously, the oxidation of hydrophobic substrates by H_2O_2 occurs under biphasic conditions and the conversion remains weak due to the hydrophilic nature of Na_2MoO_4 or Na_2WO_4 . For the $\text{H}_2\text{O}_2/\text{MoO}_4^{2-}$ system, the singlet oxygen generated in the aqueous phase (100% yield) is deactivated by water before reaching the organic substrate (singlet oxygen lifetime in water $\approx 3 \mu\text{s}$). For Na_2WO_4 , the conversion depends on the solubility of the peroxo species in the organic phase. In this context, cationic surfactants can be used as counterions of the anionic catalyst to promote both mass transfer and the interfacial area. However, to obtain three-liquid-phase μems (Winsor III), with water and an appropriate solvent, it is necessary to design well-balanced surfactants. For example, Aubry and coworkers designed a series of amphiphilic double-tailed quaternary ammonium surfactants coupled with molybdate (Figure 32) [27]. These “Balanced Catalytic Surfactants” were used for the dark singlet [4+2] cycloxygenation of organic substrates. A dimethyldioctylammonium molybdate combination was particularly effective to provide optimal three-liquid-phase μems in the presence of propyl acetate or toluene. The reaction proceeded at competitive rates even with the following advantages: (i) a simple μem composed of

only three components; (ii) low amounts of surfactants; (iii) stability to water dilution; and (iv) fast separation with easy recovery of the product and catalytic surfactant.

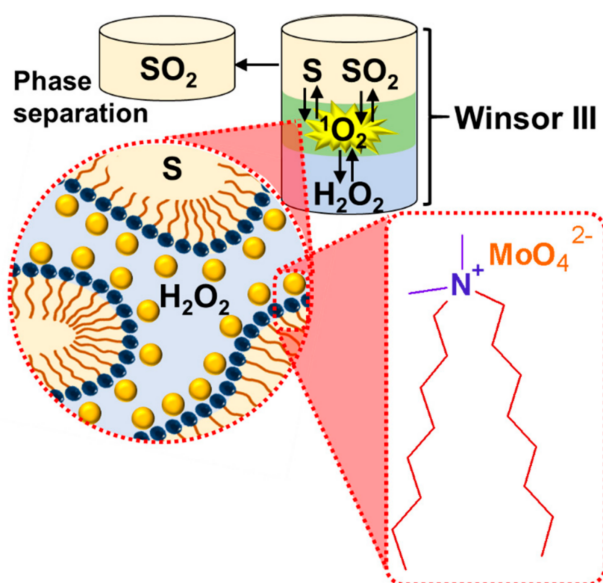


Figure 32. Oxidation in three-liquid-phase microemulsion systems using catalytic surfactants (S: substrate, and SO_2 : oxidized substrate).

Likewise, epoxidation and sulfide oxidation reactions under mild conditions can be performed in three-liquid-phase μems using a dodecyl dimethylammonium tungstate/water/organic solvent and a mixture of a dimethyl dioctylammonium cation combined with dihydrogen phosphate and hydrogen sulfate. Therefore, the epoxidation of olefins with H_2O_2 in a Winsor III μem based on water and toluene can be easily performed at $50\text{ }^\circ\text{C}$ [118]. The authors attributed the high catalytic activities and selectivities to the compartmentalization of reactants and products in this nanostructured medium, leading to very good mass transfer of immiscible components and to the stability of the epoxide suppressing the diol formation via ring opening. It is worth noting that this good epoxide stability was obtained under acidic conditions (dimethyl dioctylammonium dihydrogen phosphate and dimethyl dioctylammonium hydrogen sulfate, pH 2–3). In addition, the combination of these acidic salts allowed for the formation and the stabilization of several oxodiperoxo complexes in the presence of hydrogen peroxide, such as the so-called Venturello species $[\text{PO}_4\{\text{WO}(\text{O}_2)_2\}_4]^{3-}$.

As in the previous cases (catalytic micelles or emulsions), the adaptation of the surfactants or their assemblies in response to either internal or to external stimuli can be used to obtain commutable systems. For instance, in 2015, Nardello-Rataj and coworkers reported on a very simple thermo-responsive one-phase μem for the ene reaction, [4+2] cycloaddition, and sulfide oxidation of organic substrates (Figure 33) [119].

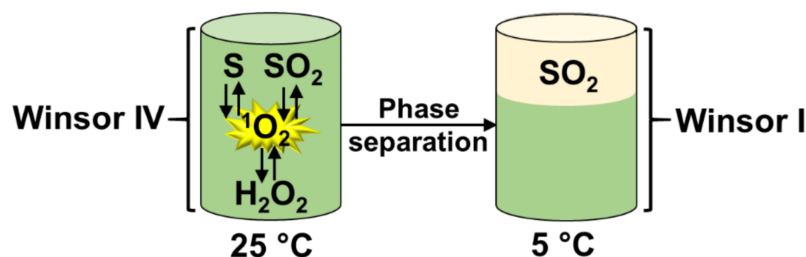


Figure 33. Interfacial catalytic oxidation in thermo-controlled and switchable microemulsions stabilized by bis(dimethyldioctylammonium) molybdate and tetraethylene glycol mono-octyl ether (S: substrate, and SO_2 : oxidized substrate).

This system was prepared by combining bis(dimethyldioctylammonium) molybdate (catalytic surfactant) with the nonionic tetraethylene glycol mono-octyl ether. As these two surfactants strongly interact, a straightforward separation of the catalytic surfactant and products in two distinct phases can be obtained by cooling down the reaction medium. Indeed, the oxidation takes place in a Winsor IV (single-phase Winsor III system), which separates into a Winsor I system (i.e., μem + oil) just by a temperature change thanks to the presence of the thermo-sensitive nonionic surface active agent. These investigated reactions were carried out in 10–92% yields at 19–28 °C within 1–24 h. Unfortunately, this system requires a relatively large amount of surfactants, which is not very relevant in the context of green chemistry.

Finally, it is worth noting that μem systems can also be used to perform bio-catalytic transformations using enzymes [120–122]. One of these publications, published in 1990, reported a coupled substrate coenzyme regenerating cycle using horse liver alcohol dehydrogenase in a water/isooctane or water/heptane μem stabilized by sodium bis-(2-ethylhexyl)sulfosuccinate or pentaethylene glycol dodecyl ether, respectively [123]. This dehydrogenase can oxidize and reduce a wide range of alcohol and ketone substrates, such as cyclohexanol and 3-methylcyclohexanone, using nicotinamide adenine dinucleotide (NAD) as a cofactor, in the following two forms: oxidized and reduced (NAD⁺ and NADH, respectively, see Figure 34). By temperature variation, the μem systems can be shifted to two-phase regions, where an oil-rich phase, containing the product, coexists with a water-rich phase containing surfactant and enzyme. This transition notably facilitates enzyme reuse and product recovery. Indeed, the oil-rich phase was removed and a new batch of fresh organic substrate was added to the water-rich phase. The reaction proceeds without any loss of activity and selectivity after nine consecutive recycles. It is worth noting that the enzyme activity was better in a nonionic than in an ionic surfactant system. However, the authors highlighted two drawbacks: the high surfactant concentration in the oil-rich phase, and the difficulty to separate the μem into two phases at equal volumes of oil and water.

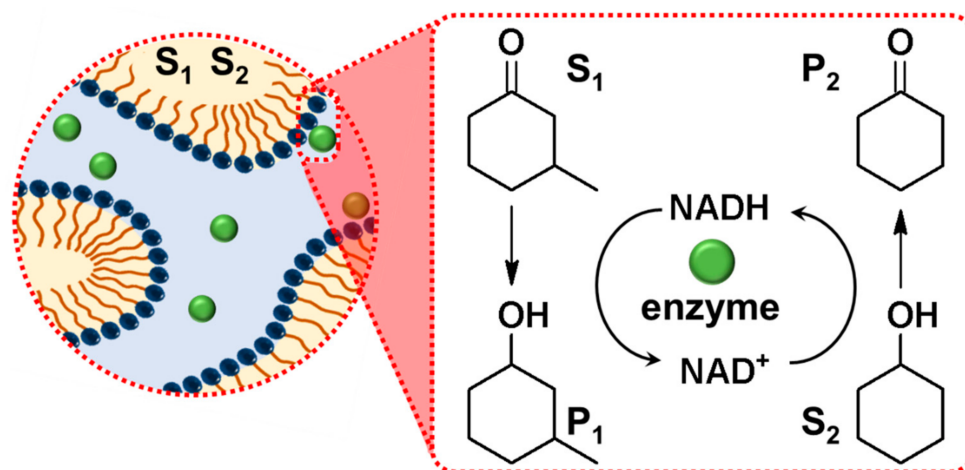


Figure 34. A horse liver alcohol dehydrogenase-catalyzed coupled coenzyme regenerating cycle in a water/isooctane or heptane μem stabilized by sodium bis-(2-ethylhexyl)sulfosuccinate or pentaethylene glycol dodecyl ether, respectively.

It is worth noting that the use of hydrophobic ILs in place of conventional organic solvents can also be applied to obtain μems [124]. For instance, a mixture of water and hydrophobic 1-butyl-3-methylimidazolium hexafluorophosphate results in the formation of a μem in the presence of the nonionic surfactant Triton X-100. In this medium, it is possible to dissolve oxidases, such as lignin peroxidase or laccase [125]. The optimal catalytic activity was obtained when the molar ratio of H₂O to TX-100 was fixed at 8.0 in pH 3.2 buffer for lignin peroxidase and >20 for laccase in pH 4.2 buffer for laccase. In contrast, the two oxidases showed negligible catalytic activity in pure or water-saturated IL due to the strong enzyme denaturation in the IL media. Therefore, the use of the

water/1-butyl-3-methylimidazolium hexafluorophosphate/Triton X-100-structured μem was very successful and led to a significant enhancement of the catalytic activities of both fungal oxidases. In addition, the fluidity is also greatly improved in the μem compared to the IL medium.

The reader who is interested in more details on μem systems for bio-, homogeneous, and heterogeneous catalytic reactions and processes can consult the excellent review of Schwarze and coworkers [126]. Based on all of these investigations, the μems can be very efficient when performing catalytic reactions. However, these systems require a relatively large amount of surfactants, which is not very relevant in terms of sustainable processing. The ideal case would be to achieve biphasic aqueous systems similar to μem systems but without surfactants. Fortunately, contrary to the belief that the surfactant is in every case necessary to stabilize μems through the formation of an interfacial film between the aqueous and oil phases, surfactant-free μems have been easy to obtain since the pioneer works of Barden and coworkers in the late 1970s. Indeed, in 1977, a W/O μem composed of 2-propanol, hexane, and water was reported and constitutes the first example of a surfactant-free multiphase emulsion since no traditional surfactant was involved in this system [127,128].

These systems have attracted much attention, especially in physical chemistry [129]. In this context, Kunz and coworkers studied the μem -like structuring of mixtures of two immiscible solvents with an “amphi-solvent”, which is miscible with both of the two other ones [130–132]. Such a structuring always occurs when the mixture is not too far away from the dephasing boundary [133]. This phenomenon allows for the formation of well-defined μems in the monophasic region. By analogy to classical μems , different microstructures have been identified using various techniques (e.g., conductivity, fluorescence, heat capacity, dynamic light scattering, nuclear magnetic resonance, etc.): direct, inverse, and bicontinuous structures (Figure 35) [134].

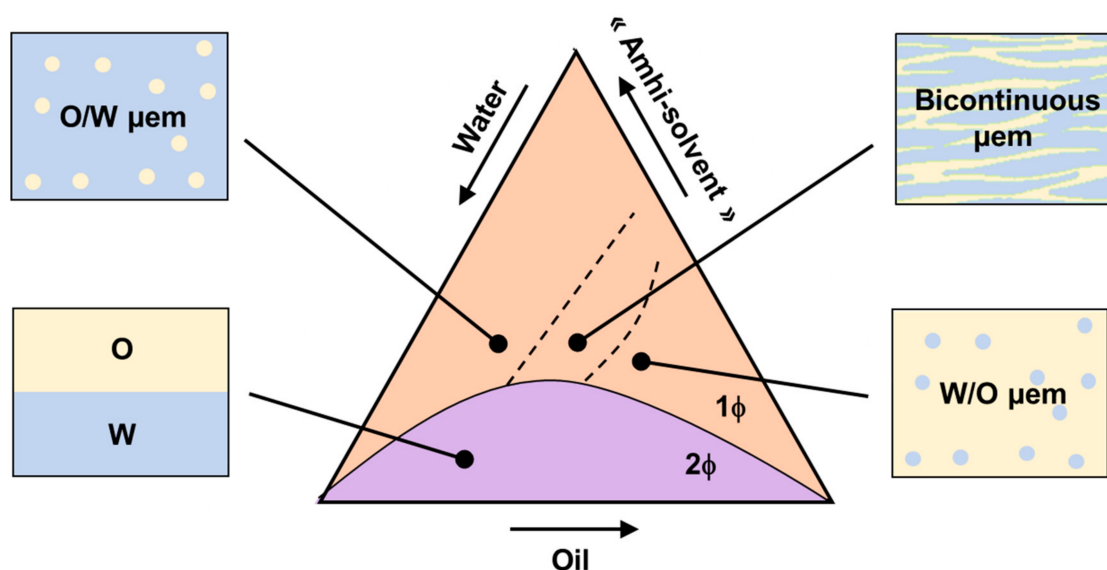


Figure 35. A schematic phase diagram of an “amphi-solvent”/water/oil ternary system and surfactant-free microemulsion types.

However, it is worth noting that the locations of these sub-region boundaries may be significantly different according to the system used and to the environmental factors [135]. In addition, these types of microstructures present distinct microenvironments of varying polarities. From a fundamental point of view, surfactant-free μems have similar properties to classic μems , being stable, optically transparent, and showing microstructures dispersed into a continuous solvent phase [136]. The only condition of this phenomenon is the complete or at least partial miscibility of the “amphi-solvent” with water and oil. Besides their unique physicochemical properties, surfactant-free μems provide new opportunities to create smart processes, especially in the context of green chemistry, as the “amphi-solvents” can be eco-compatible (ethanol, ethyl lactate, γ -valerolactone, etc.) [137,138]. Moreover, it is worth noting

that they also offer the advantage of an easily handled and removable additive instead of hazardous solvents or the usually highly viscous and high-boiling-point classical surfactants. Some typical catalytic systems based on surfactant-free μ ems used for chemical and biochemical transformations are reported below.

As previously mentioned, conventional μ ems are suitable media to perform enzymatically catalyzed reactions due to the large interfacial area, which allows for the enzyme to catalyze reactions involving both hydrophilic and hydrophobic compounds. Nevertheless, large-scale applications of conventional μ ems might be impeded by the difficulty of separating the reaction products from the surfactant without denaturing the enzyme, which should be reused. Since the late 1980s, this kind of μ em was used to perform enzymatic reactions. The majority of ternary systems involved in enzymatic transformations use alcohols as “amphi-solvents”. For instance, *n*-hexane/alcohol/water ternary systems have been used with trypsin [139], cholesterol oxidase [140], mushroom polyphenoloxidase [141], lipase [142–145], horseradish peroxidase [146], and feruloyl esterase [147]. Obviously, it is worth noting that the structure of the ternary surfactant-free μ ems depends on the system’s composition, affecting consequently the catalytic efficiency of the enzyme. Generally, at low water content, the enzyme has low catalytic activity. Indeed, in the water-poor part, weak reverse micelle-like structures are present. Consequently, the enzyme nucleates and the disruption of intra noncovalent interactions leads to the denaturation of enzymes by the organic solvents. In other words, the enzyme lacks its biological activity in the absence of sufficient hydrating water. In contrast, at higher water content, the enzyme exhibits high catalytic activity as it can be in its active conformation due to the existence of a confined water microenvironment stabilized with the propanol molecules that form the interface between the hexane and the water (Figure 36) [148]. For more information on the use of surfactant-free μ ems as reaction media for catalytic transformations using oxidases and lipases, see the recent review of Xenakis and coworkers, which also describes the relationship between the catalytic performance and the system structuration [149].

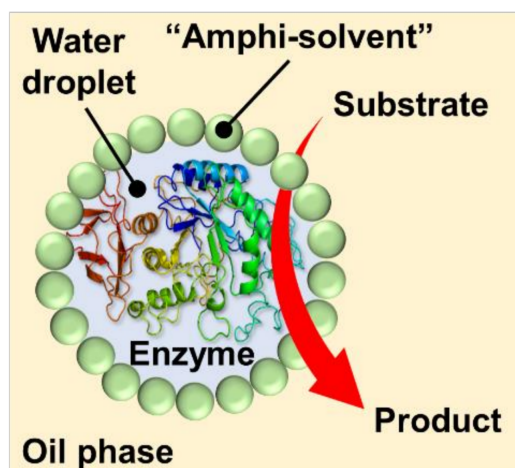


Figure 36. The principle of enzymatic transformations in a W/O surfactant-free microemulsion.

Finally, it is worth noting that Kunz and coworkers investigated, in 2018, the influence of the structuring of two surfactant-free μ em systems, based on water/1-propanol/limonene and water/*tert*-butanol/limonene, on the horseradish peroxidase catalytic activity at various compositions [150]. In order to obtain structural information on the used surfactant-free μ ems, various techniques, such as conductimetry, dynamic light scattering, and small-angle-X-ray scattering, were used. The combination of the data obtained by these techniques and of the enzymatic activities in pure buffer solution and in these two μ em systems led the authors to assert that the ability of “amphi-solvents” (i.e., short-chain alcohols) to form aqueous aggregates in oil has a critical effect on the enzyme activity in these systems. The results proved that 1-propanol molecules give a more

pronounced structuration than the more hydrophobic *tert*-butanol. As the maximum in enzyme activity was obtained for the most pronounced structuring surfactant-free μ ems, where time-stable and sufficiently defined (fluctuations not too fast) W/O μ ems were formed, the authors concluded that these aggregates are able to protect the enzyme from denaturation. Despite some speculation, this effect is due to two mechanisms: (i) the alcohol is pushed more to the interface and into the limonene-rich domain, and (ii) the presence of swollen water-rich aggregates provides sufficient hydration, allowing for the enzymes to reach their active minimum-energy conformation in a straightforward and rapid manner. Due to this hydration shell, water molecules shape a protective and stabilizing shield around the enzyme and protect it against denaturation.

Obviously, the aqueous surfactant-free μ em multiphase systems can also be used as switchable solvents for organometallic catalysis. For instance, in 2016, Pogrzeba and coworkers reported the first applications of these systems as reaction media for a rhodium-catalyzed hydroformylation of 1-dodecene and a Suzuki coupling reaction of 1-chloro-2-nitrobenzene and 4-chlorobenzeneboronic acid [151]. All of the investigated reaction systems were obtained using oil, aqueous catalytic solution, and diethylene glycol butyl ether ($C_4H_9(C_2H_4O)_2OH$, abbreviated as C_4E_2) as a thermosensitive “amphi-solvent”. For each multiphase system, the authors reported the influence of the oil/water ratio, the “amphi-solvent” concentration, the catalyst composition, and the temperature on the phase behavior and on the droplet size distribution. For multiphase systems, based on 1-dodecene (acting both as the reactant and the solvent), the temperature increase allows us to switch from two-phase to three-phase, where the emulsion phase was dispersed inside the continuous phase. Therefore, this system provides the possibility to obtain a smart hydroformylation process based on the concept of temperature-induced phase transition similar to classical μ em systems. For the rhodium-catalyzed hydroformylation of 1-dodecene using a water-soluble SulfoXantPhos ligand, a conversion of 23.4% after 4 h of reaction time (turnover frequency, TOF, = 77.5 h^{-1}) with a linear-to-branched ratio of 99:1 was obtained under mild reaction conditions ($95\text{ }^\circ\text{C}$ and 15 bar of 1:1 mixture of CO and H_2). In addition, the authors mentioned that the reaction seems to take place in the middle phase and that the reaction rate is strongly influenced by the amount of “amphi-solvent” in the system. Finally, the Rhodium–SulfoXantPhos catalyst could be successfully recycled four times, maintaining its very high linear-to-branched ratio. Next, the authors tried to extend the scope of this reaction to the Suzuki coupling reaction catalyzed by palladium using 2'-dicyclohexylphosphino-2,6-dimethoxy-sodium as a ligand. However, in contrast to the hydroformylation reaction, heptane was used as the oil phase. According to the “amphi-solvent” concentration, it is possible to switch from two-phase to three-phase systems. Moreover, the three-phase region is shifted to lower temperatures ($30\text{--}40\text{ }^\circ\text{C}$) with heptane compared to 1-dodecene ($75\text{--}80\text{ }^\circ\text{C}$). Unfortunately, despite the fact that the Suzuki reaction yields up to 90%, the palladium catalyst could not be totally recycled, leading to a decrease in the catalytic activity due to ligand leaching during the separation steps. All of these results demonstrate the potential of surfactant-free multiphase emulsions as switchable reaction media for homogeneous catalysis.

4. Catalytic Systems Based on Extended Supramolecular Networks

Extended supramolecular networks is an area of research devoted to predicting and controlling the packing of building units held together via highly directional and reversible noncovalent interactions to obtain macroscopic assembly or polymeric networks. Unlike conventional bonded systems, these supramolecular networks engage in a variety of noncovalent interactions (hydrogen bonding, π - π stacking, metal coordination, etc.) that define their properties. Owing to the presence of these reversible interactions, extended supramolecular networks exhibit dynamic, reversible, and adaptive properties with potential applications as catalytic systems.

N.B. In this section, some discrete supramolecular networks have also been reported due to their potential application as extended lattices.

4.1. Concept

The engineering of extended supramolecular networks has attracted much attention over the past few decades owing to its potential for the synthesis of new materials. One of the major objectives is the predictable supramolecular synthesis of polymeric molecular networks with prescribed functions from well-designed building blocks. In such an approach, molecular interactions are utilized to assemble supramolecular networks with desired topologies from appropriate molecular subunits. Depending on the strength and the number of interactions, various distinct states of matter can be obtained, such as liquid, solid jelly-like, or solid (Figure 37). It is worth noting that the formation of molecular networks in the crystalline phase generally relies on the molecular tectonics concept, which is defined as the art and science of supramolecular construction using molecular recognition events between complementary tectons (molecules with appropriate binding sites) and their iteration (i.e., a bottom-up synthetic approach) [152–155].

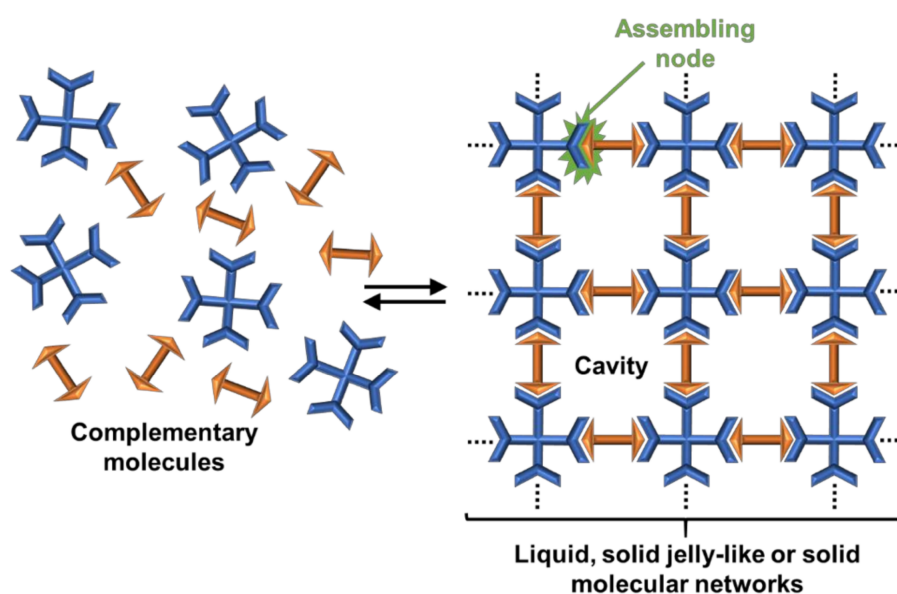


Figure 37. Engineering of extended supramolecular networks from the ordered aggregation of molecules to obtain liquid, solid jelly-like, or solid networks.

In addition to dynamic, reversible, and adaptive properties, these molecular networks can be useful to manage cavities where the guest molecules or catalysts can be accommodated, leading to a particular self-assembly system, named a clathrate, which can be defined as a lattice that traps or contains molecules. These compounds are polymeric and completely envelop the guest molecule. Therefore, clathrates can be seen as inclusion compounds in which the guest molecule is in a cage formed by a lattice of host molecules. These porous networks have numerous applications, such as selective adsorption [156], gas storage [157], single-crystalline nanocomposites [158], novel magnetic materials [159], and, obviously, catalytic systems. Within the cavity environment, the transformation of the substrates by the catalyst enables us to increase the selectivity and/or to accelerate the reaction rate. This section will provide a brief review of some catalytic applications of these molecular networks.

4.2. Organized Liquids

An organized liquid can be defined as a liquid (ideally a solvent) in which the polar or nonpolar constituents are interconnected by way of noncovalent interactions in order to generate more or less complex molecular networks depending on the strength, the number, and the orientation of these interactions. When one substance is dissolved into these organized liquids, a solution is formed. This solvent–solute mixture consists of a single phase from a macroscopic point of view; however, the internal structuration is closer to suspensions, emulsions, and μ ems. Indeed, as these liquids are

organized, it is necessary to keep in mind that the interaction energy between the solvent molecules is greater than that of dissolved substances and solvent molecules. Consequently, solvent molecules are rearranged around the solute, leading to a molecular inclusion of this last (guest) in the solvent “host network”. This rearrangement is mediated by the respective chemical properties of the solvent and solute, such as hydrogen bonding, dipole moment, and polarizability.

A very interesting example comes from the prospect of green chemical solvents at the beginning of the 1990s. Indeed, ILs, defined as special “molten salts” with low melting points (≤ 100 °C, dramatically reduce the use of hazardous and polluting organic solvents [31]. On the last variety of ILs, the 1,3-disubstituted imidazolium salts are the best-studied in terms of physicochemical properties. Their properties can be totally adjusted by the combination of different cations and anions, allowing for the design of solvents for specific applications. For instance, depending on the combination, the polarities can be comparable to DMF or to short chain alcohols with a coordination ability similar to that of dichloromethane. Regarding the anion, imidazolium ILs can be classified into four groups: (i) hygroscopic anions (Cl^- , AlCl_4^-); (ii) hydrophobic anions (CF_3SO_3^- , $(\text{CF}_3\text{SO}_2)_2\text{N}^-$, PF_6^- , and BF_4^-); and (iii) “amphiphilic” anions (alkylsulfates or alkylsulfonates) [33].

In structural aspects, imidazolium ILs may be regarded as supramolecular networks in which the introduction of other molecules occurs with the formation of inclusion-type compounds (clathrates, see above). Indeed, the imidazolium cation can be considered as a “tecton” because it is a three-H-bonds donor by way of the three acidic protons localized on the imidazolium ring and oriented in a divergent fashion (Figure 38). These H-bonds induce structural directionality. Moreover, aromatic stacking can also occur. Therefore, the structuration is dictated by molecular recognition processes between complementary tectons (i.e., between cations and anions via electrostatic forces and H-bonding as well as between cations and cations by way of π -stacking), leading to the formation of three-dimensional (3-D) supramolecular polymeric networks in which the unimeric unit is constituted of one imidazolium cation surrounded by at least three anions and each anion is surrounded by at least three imidazolium cations [33,160]. This model is based on the various X-ray studies reported in the literature. It is worth noting that the structural organization of imidazolium salts in pure liquid phase is due to the unique combination of electrostatic forces, aromatic stacking, and H-bonds. Therefore, the electrostatic forces decrease the dynamic exchange of molecules compared to conventional solvents (e.g., water or ethanol) and facilitate the establishment of secondary interactions (H-bonds and aromatic stacking) [33,161]. The introduction of other molecules and macromolecules in these supramolecular networks occurs with a partial disruption of the H-bonds, leading to liquid nanostructured polar and nonpolar aggregates in which the guest molecules are included in the imidazolium cation/anion network [33,162]. Obviously, these organized solvents, with adaptable properties, present clear advantages for the production of inclusion compounds in which the guest molecule is in a cage formed by a lattice of host molecules. As this phenomenon may involve small molecules, macromolecules, and/or NPs, this lattice of host molecules can be very useful to perform catalytic transformation of included substrates. On this background, numerous organic reactions have been performed in imidazolium ILs; some of them are presented below.

Imidazolium ILs have been studied as a substitute for water in the Diels–Alder reactions, leading to both rate and selectivity improvements compared to classical molecular solvents. Generally, an acceleration of the Diels–Alder reaction was obtained compared to nonpolar organic solvents. Generally, Diels–Alder reactions lead to a mixture of exo and endo products. However, Welton and coworkers observed that the endo- product is preferred in the Diels–Alder reaction of methyl acrylate and cyclopentadiene with imidazolium ILs as solvent due to the H-bond formation in the endo transition state (Figure 39) [163]. On the other hand, if the sonication improves the reaction yields compared to conventional heating, the stereoselectivities are unaffected due to a “cavity effect” [164]. It is worth noting that microwave activation can also be used [165].

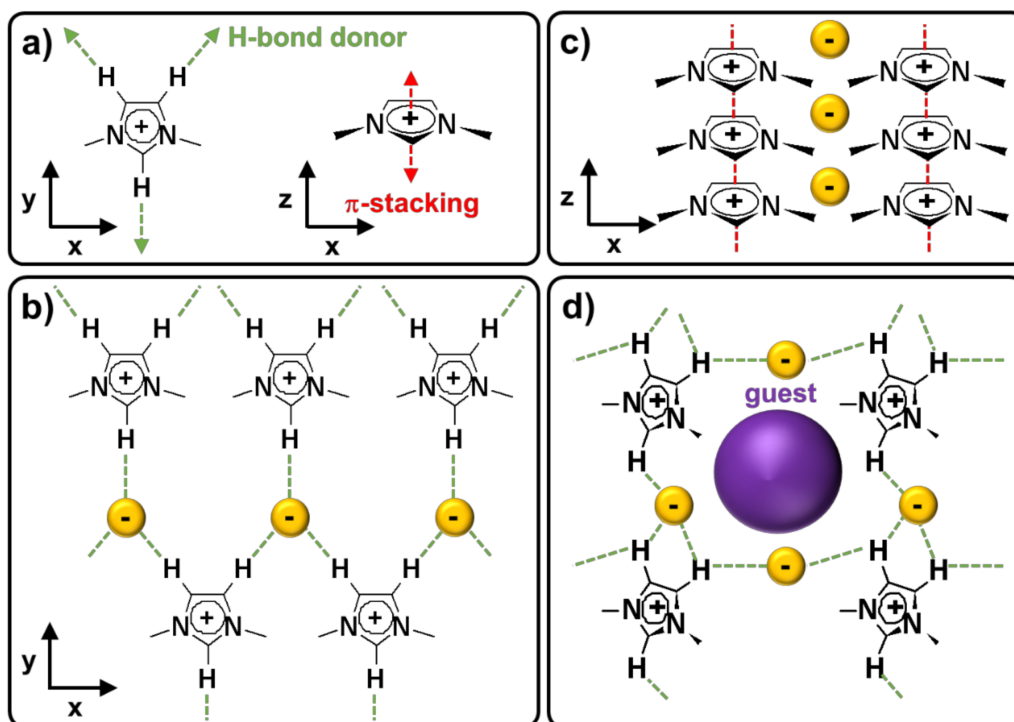


Figure 38. (a) H-bond donors (green) and π -stacking (red) of an imidazolium ring; (b,c) simplified two-dimensional (2-D) and three-dimensional (3-D) organization of the imidazolium salt; (d) the local assembly of the imidazolium ILs around guest molecules.

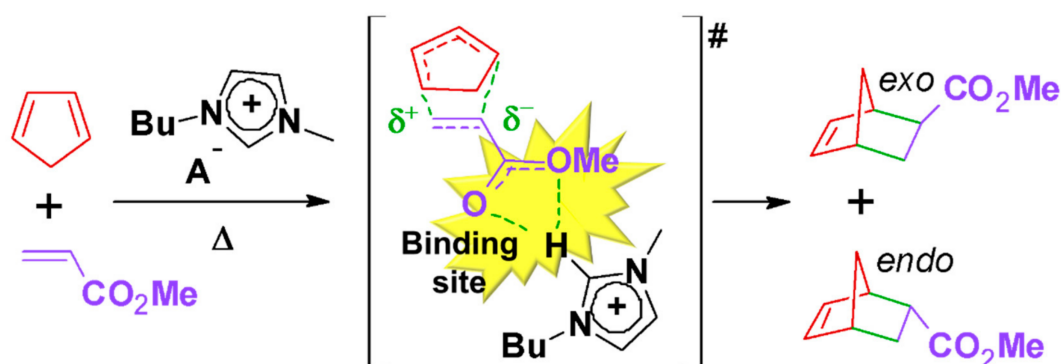


Figure 39. A Diels–Alder reaction of methyl acrylate with cyclopentadiene to give a mixture of endo- and exo-bicyclo-[2.2.1]-hept-5-ene-2-carboxylic acid methyl ester and the activated complex of the reaction ($\text{A} = \text{BF}_4, \text{PF}_6, \text{ClO}_4, \text{TfO}, \text{NTf}_2, \text{CF}_3\text{CO}_2$).

Acetylation reactions can also be performed via ultrasonic irradiation in imidazolium ILs. For instance, in the case of *O*-acetylation of alcohols with acetic anhydride and different esters, the reaction is catalyzed only by the combination of ultrasonic irradiation and the presence of imidazolium ILs, which is supposed to act as a promoter due to the H-bond formation between the most acidic hydrogen of the imidazolium ring with the oxygen of the acetic anhydride, leading to the easy generation of the acetyl required for the reaction (Figure 40) [166]. Other data available in the literature have revealed that the choice of the anion as well as the cation influences the reaction rates because of variation in acidity and polarity by variation in H-bonding networks [167]. In the context of “green” chemistry, it is worth noting that the transesterification reaction for biodiesel production from palm oil can be easily catalyzed by the use of eco-friendly acidic imidazolium ILs (up to 98.93% yield) [168]. Moreover, microwave irradiation accelerates the reaction rate and saves more than 44% energy.

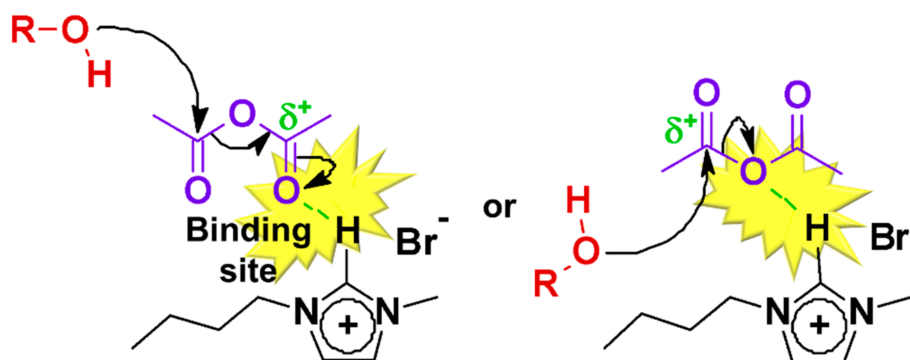


Figure 40. Possible H-bond activation with H-bond formation during O-acetylation of alcohols with acetic anhydride in 1-butyl-3-methylimidazolium bromide under sonication at 30 °C.

Generally, the reaction rate improvement in imidazolium ILs is ascribed to H-bond activation by way of a stabilization of ionic intermediates or transition states in the case of Biginelli [169], Friedel–Crafts [170], Baylis–Hillman [171], etc. reactions. In contrast, the high reaction rate observed during Knoevenagel condensation and Robinson annulation is attributed to the reaction of the imidazolium with the added base to give imidazolidene carbenes, which are supposed to be the active catalysts in the two reactions in addition to providing possible stabilization of transition states [172].

On the other hand, imidazolium ILs can be useful to stabilize NPs. This effect results from the structural organization of ILs, which acts as “entropic driver” that leads to spontaneous, well-defined, and extended ordering of nanoscale structures [173]. Furthermore, the reorganization of the H-bond network and the generation of hydrophobic or hydrophilic regions associated with directional polarizability allow for the stabilization of transition-metal NPs in imidazolium ILs (gold [174], nickel [175], palladium [176], ruthenium [177], etc.). This structural organization is similar to that already observed in the solid, liquid, and gas phase and in solutions of imidazolium salts. This protective layer is probably composed of imidazolium cations and anions aggregated in the vicinity of the NP surface, leading to Coulombic repulsion [178].

These stable metal colloids in imidazolium ILs can be used for different applications, such as catalysis. For instance, Dupont et al. reported that 1-butyl-3-methylimidazolium hexafluorophosphate ILs can be a suitable medium for the preparation and stabilization of iridium NPs [179]. Indeed, the reduction of Ir(I) with H₂ in the IL resulted in the formation of Ir(0) NPs with a mean diameter of 2 nm. In addition, this solvent allowed for the generation of biphasic catalytic systems in the presence of hydrophobic olefins (1-decene, styrene, cyclohexene, methyl methacrylate, and 4-vinylcyclohexene). These biphasic systems were used to perform hydrogenation reactions. Under optimal conditions, the reactions were carried out in 30 min at 75 °C under 4 atm of H₂ with a conversion of 100%. The catalytic activities of iridium NPs dissolved in IL were maintained for at least seven recycles. Another typical example has been published in 2012 by Luska and Moores. The authors studied the stabilization of ruthenium NP catalysts in imidazolium ILs in order to achieve a correlation between the structure of the IL and catalytic properties (such as stability, activity, and recyclability) [180]. As in the previous case, the reduction of Ru(II) with H₂ in 1-butyl-3-methylimidazolium and 1-butyl-2,3-dimethylimidazol-3-ium triflimidate ILs resulted in the formation of Ru(0) NPs. The biphasic hydrogenation reactions were performed with Ru NPs embedded in these ILs using cyclohexene as a model substrate. The presence of an additional H-bond donor by the way of the more acidic proton, H(2), on the 1-butyl-3-methylimidazolium cation confers the lowest ionicity compared to a 1-butyl-2,3-dimethylimidazol-3-ium cation (Figure 41). As 1-butyl-3-methylimidazolium showed better catalyst recyclability than 1-butyl-2,3-dimethylimidazol-3-ium triflimidate, the stabilization of Ru(0) NPs is inversely related to the ionicity. In other words, the formation of ion pairs (or supramolecular aggregates) is the key driving force for the stabilization of NPs.

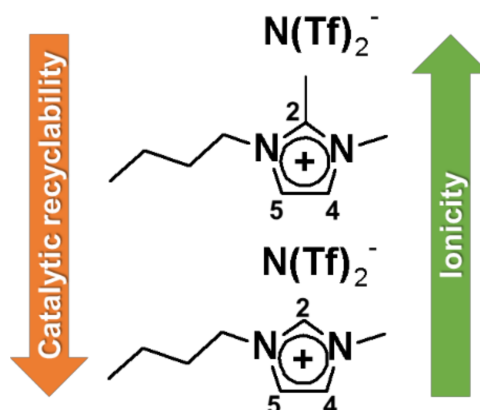


Figure 41. The relationship between imidazolium cations ionicity and ruthenium nanoparticles (NPs) recyclability observed after hydrogenation reactions performed with ruthenium embedded in two imidazolium ILs.

Unfortunately, it is worth noting that the role of metal NPs in imidazolium ILs remains a matter of debate. Indeed, as organometallic species can also be “solubilized” in imidazolium ILs, some results strongly suggest that the metal NPs could only serve as a reservoir of “homogeneous” catalytic active species [181]. Consequently, various research teams investigated their use as a solvent. For instance, Xiao et al. reported the effects of archetypal organic solvent (THF) and imidazolium ILs on the catalytic species during Tsuji–Trost reactions [182]. Generally, for a soft nucleophile, the allylation process involves the following steps: (i) formation of the allylpalladium intermediate, “PdL₂(allyl)”, produced by addition of the allyl acetate substrate to the “PdL₂” key species; and (ii) addition of the nucleophile to the “PdL₂(allyl)” intermediate providing the alkylation product. In THF, the intermediate “PdL₂(allyl)” forms ion pairs with acetate anions, reducing reaction rates since the steric hindrance around palladium does not facilitate the coordination of bulky ligands and makes it less sensitive to the attack of nucleophiles (Figure 42). In contrast, in the polar ionic environment provided by 1-butyl-3-methylimidazolium tetrafluoroborate, the allylpalladium exists as a free cation because of the ease of exchange between the various anions.

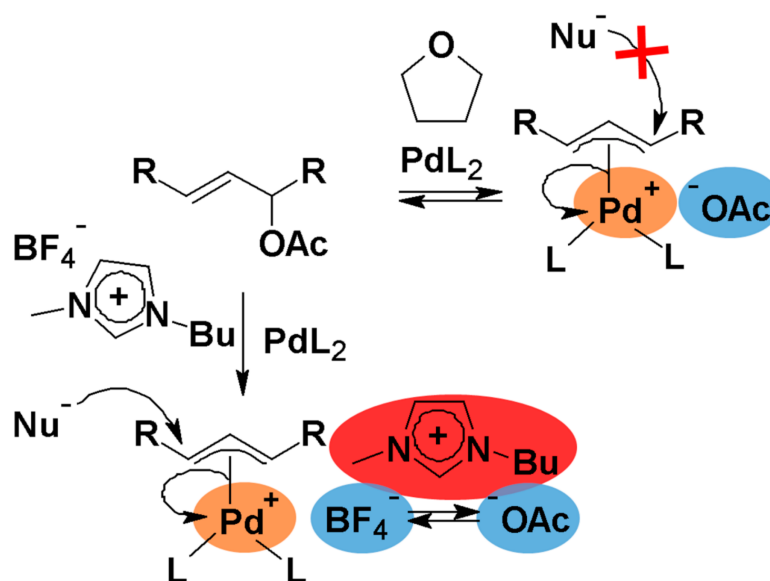


Figure 42. Effects of solvents (THF and 1-butyl-3-methylimidazolium tetrafluoroborate) on the intermediate allylpalladium (PdL₂ = active catalyst, L = phosphine, Nu[−] = soft nucleophile).

In 2007, various imidazolium triflate ILs were applied as solvents in palladium-catalyzed allylic alkylation with high conversions (75% at 50 °C, 12 h) [183]. In these reactions, the requested nucleophile is generated from the deprotonation of diethyl malonate using tetrabutylammonium acetate. At the reaction end, the authors observed the formation of a crystalline solid. The structure has been solved by X-ray diffraction and proves that, during catalysis, anion metathesis between imidazolium triflate and ammonium acetate occurs in order to obtain an ionic co-crystal. The structure is compatible with a partial disruption of the H-bond network, leading to inclusion of tetrabutyl ammonium inside the imidazolium triflate network. Indeed, a cage compound is formed, i.e., a lattice of thiazolium/triflate, connected via H-bonds, that traps and contains the ammonium cation. The possibility to include ammonium cations in a liquid self-assembled network has been later extended to various azolium networks [162,184]. In addition, it is worth noting that the supramolecular structural organization obtained in a solid state is maintained to a great extent in solution. Therefore, during Tsuji–Trost reactions, the tetrabutylammonium cations are supposed to facilitate the organization of the imidazolium ILs.

In 2008, chiral imidazolium ILs (e.g., 1-methyl-3-[(S)-2-methylbutyl]imidazolium triflate) were used to demonstrate the potential of imidazolium to transfer chiral information during the biphasic hydroformylation of styrene (water/IL), in which small enantiomeric excesses (up to 12%) were obtained with the use of chiral imidazolium ILs [30]. Based on NMR experiments (^{31}P NMR titrations and 2-D T-ROESY), the authors proved the “inclusion” of various phosphine ligands (e.g., triphenylphosphine, monosulfonated triphenylphosphine, and trisulfonated triphenylphosphine) inside the host imidazolium network via electrostatic forces for anionic phosphine and π -stacking interactions for the neutral phosphine. The complementary 2-D NMR experiments confirm the π -stacking interactions between the cationic imidazolium and the phenyl ring (Figure 43). The authors note that these stacking interactions have already been postulated by Wipff et al. using a molecular dynamics simulation [185]. It should be noted that π -stacking interactions are also very likely with styrene.

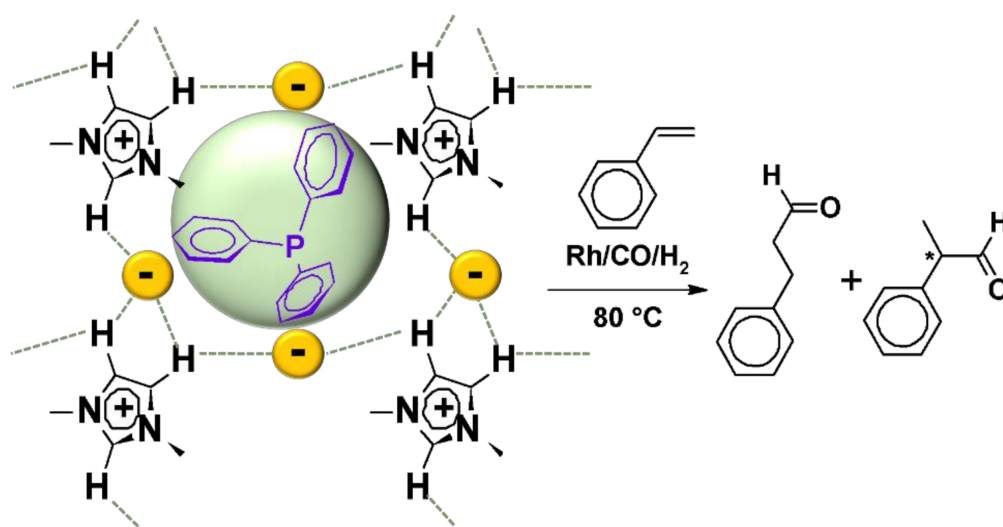


Figure 43. The inclusion of a triphenylphosphine ligand in the 1-methyl-3-[(S)-2-methylbutyl]imidazolium triflate lattice and its application in the biphasic hydroformylation of styrene (water/IL).

All of these studies support the idea that supramolecular assistance by self-organized solvents as well as peristatic chirality are phenomena of general importance for chemical transformations. However, it is worth noting that imidazolium ILs can catalyze transformations under metal-free conditions. For instance, 1-alkyl-3-methylimidazolium ILs can be used in the catalytic formylation of amines with carbon dioxide and phenylsilane at room temperature [186]. The formylation of amines

operates in excellent yields under a metal-free condition. The imidazolium has a dual role: (i) activation of the Si-H bond of phenylsilane for its reaction with CO₂ to form the formoxysilane intermediate; and (ii) activation of the amine through a H-bond.

4.3. Supramolecular Physical Gels

By definition, gels consist of a solid 3-D network that spans the volume of a liquid medium and ensnares it. This internal network is principally the result of physical bonds (physical gels) or chemical bonds (chemical gels). Physical gels formed by low-molecular-weight organic compounds by the sole action of noncovalent intermolecular interactions (electrostatic, solvophobic, H-bonding, π -stacking, van der Waals, metal coordination, etc.) are named supramolecular gels (Figure 44) [187].

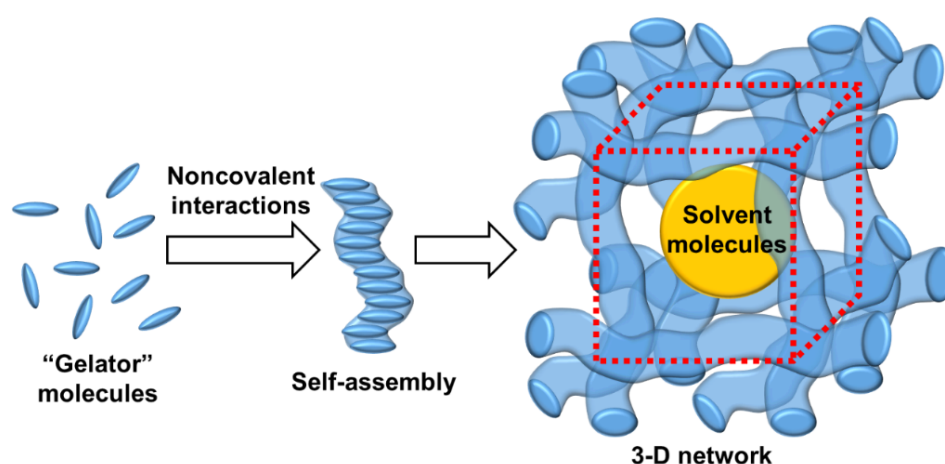


Figure 44. The formation of supramolecular gels.

As supramolecular gels (physical gels), characterized by dynamic cross-links that are constantly created and broken, allow us to switch from the solid state to liquid state as a function of various environmental factors, they constitute an important class of materials with many applications. Indeed, supramolecular gels can be obtained from very simple molecules that are capable of hierarchically self-assembling into a 3-D network that immobilizes a solvent, such as oil or water, to form organogels or hydrogels, respectively. Although slower than in homogeneous systems, the porous network of a gel allows for the diffusion of solutions containing different components [188]. It is worth noting that other molecules can be entrapped in the gel during the gelation process (in-situ loading) except if they modify the gelator self-assembly mechanism. Generally, small molecules that are not interacting with the gel network remain unaffected as in a pure solvent [189]. In addition, the gelation can be controllable by the introduction of appropriate stimuable groups in the "gelator" structure. Therefore, it is possible to switch from gel to sol and vice versa [190]. This reversibility and sensitivity for stimuli make them very appealing for catalytic applications because their activity can be conveniently adjusted. For the sake of clarity, only some selected typical examples are reported in this section to highlight the various possibilities to obtain catalytic transformations using supramolecular gels. For complementary information on this topic, we advise the reader to refer to the very recent review of Tu and coworkers [191].

In 2007, Xu and coworkers combined supramolecular-hydrogel-encapsulated hemin as an artificial enzyme to mimic peroxidase with high catalytic activity in organic media [192]. For instance, in toluene, hemin chloride encapsulated in such a hydrogel achieves about 60 % nascent catalytic activity of horseradish peroxidase. Moreover, the catalytic activity of encapsulated hemin chloride is 387.1 times greater than that of the control experiments (hemin alone). Although the effect of mass transfer at the oil/water interface in the supramolecular hydrogel provides a certain enhancement, the high catalytic activities of the artificial peroxidases in toluene, compared to the hemin chloride alone, are mainly due

to the incorporation of the hemin into the nanofibers of gelators. One year later, the same research team improved this catalytic system to obtain catalytic activity of up to 90% of the nascent activity of horseradish peroxidase in toluene (Figure 45) [193].

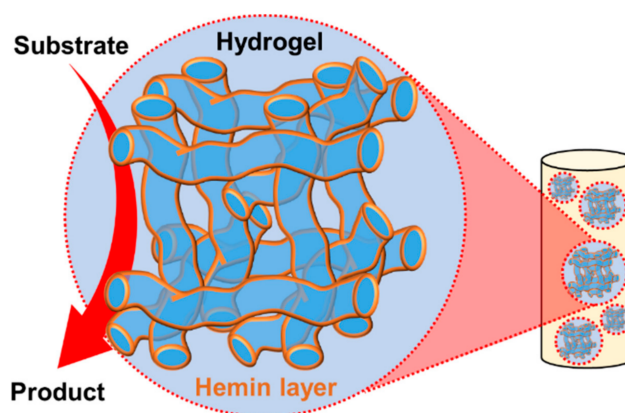


Figure 45. The principle of supramolecular-hydrogel-encapsulated hemin as an artificial peroxidase.

In addition, the authors reported that the catalytic activities can be easily modulated by the variation of the distal substituents above the coordinated-metal centers of the heme model compounds. This strategy constitutes a new and useful approach to the development of biomimetic catalyst supramolecular hydrogels as a structural component of artificial enzymes.

However, organogels can also be useful to catalyze several transformations. For instance, as L-proline acts as an organocatalyst in numerous asymmetric reactions, Miravet and coworkers used series of organogels based on an L-proline fragment in the bola-amphiphilic backbone of L-valine [194]. The H-bonds between the amides residues allowed for the formation of supramolecular gels. The resulting gels showed a basicity increase compared to solution, which allowed the authors to perform base-catalyzed aldol racemization in the gel phase due to its high basicity in combination with enantioselective catalysts for the aldol reaction in solution (Figure 46).

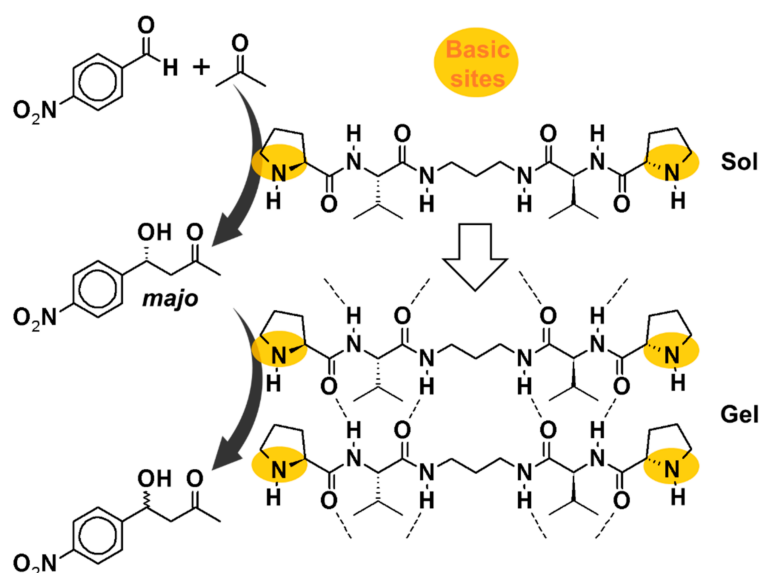


Figure 46. An aldol reaction between acetone and 4-nitrobenzaldehyde catalyzed by an L-proline derivative in acetonitrile solution and racemization in a supramolecular organogel.

Another strategy is to use organogels as a platform to provide new catalysts. For instance, in 2016, Moretto and coworkers developed a terminally protected dipeptide gelator (Boc-L-Cys(Me)-L-

Leu-OMe), which could associate with multiwall carbon nanotubes (MWCNTs) and fullerene (C_{60}) in a hybrid gelator–MWCNTs– C_{60} organogel (Figure 47) [195].

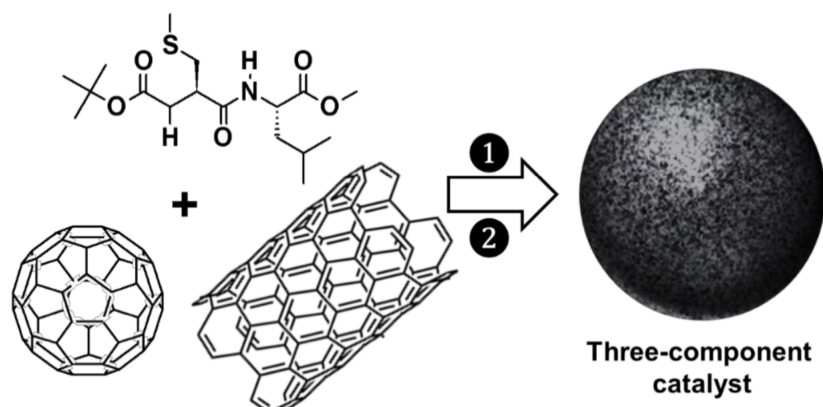


Figure 47. The self-assembly of a terminally protected hydrophobic dipeptide (Boc-L-Cys(Me)-L-Leu-OMe) with carbon-based materials (carbon nanotubes and fullerene C_{60}) to obtain a ternary catalyst (1: formation of organogel, and 2: vacuum drying).

This organogel can easily be transformed into a very robust and water-insoluble solid material using high-vacuum drying. It is worth noting that the C_{60} entities were well-dispersed over the entire matrix. This three-component material can be used as a catalyst for the reduction of water-soluble azo compounds in the presence of $NaBH_4$ and UV irradiation and for the transformation of benzoic acid in benzyl alcohol mediated by $NaBH_4$. The results showed higher activity for both reduction reactions compared to C_{60} alone.

On the other hand, as it is known that metal catalysts with high activity can easily form metal complexes. The introduction of metal centers into gelator molecules leads to metallogels with potential applications as novel catalysts. Two strategies can be used to prepare metallogels: (i) direct incorporation; and (ii) post-modification. It is evident that direct incorporation leads to the coordination of metal ions with various organic ligands, which plays a crucial role in the formation of metallogels.

The first strategy can be illustrated by the work of Xu and co-workers [196]. The authors used Pd(II)-coordination metallogels to catalyze a Suzuki–Miyaura coupling (Figure 48). The metallogels, which were based on Pd(II), were obtained after direct incorporation of a palladium salt (i.e., $Pd(\text{cycloocta-1,5-diene})(NO_3)_2$) and a C_3 -symmetric multidentate pyridine-based tripodal ligand (i.e., 4,4',4''-(1,3,5-triazine-2,4,6-triyl)tris(*N*-(pyridin-3-ylmethyl)benzamide) in $CH_3OH/CHCl_3$ solution. Various spectroscopy experiments (e.g., FT-IR and NMR) showed that H-bonding, π -stacking, as well as coordination bonding are involved in the gel formation. According to the Pd/ligand ratio, the morphologies of these metallogels ranged from spheres (1/4 equiv. Pd) to fibers (1 equiv. Pd). The best catalytic activity in the Suzuki–Miyaura coupling reaction was obtained with the fibrous networked gels compared to the spherical gel. It is worth noting that the catalytic performance remained unchanged upon recycling. Compared with the wet gel, the xerogel retained its catalytic activity even after recycling five times, without a significant loss of catalytic efficiency.

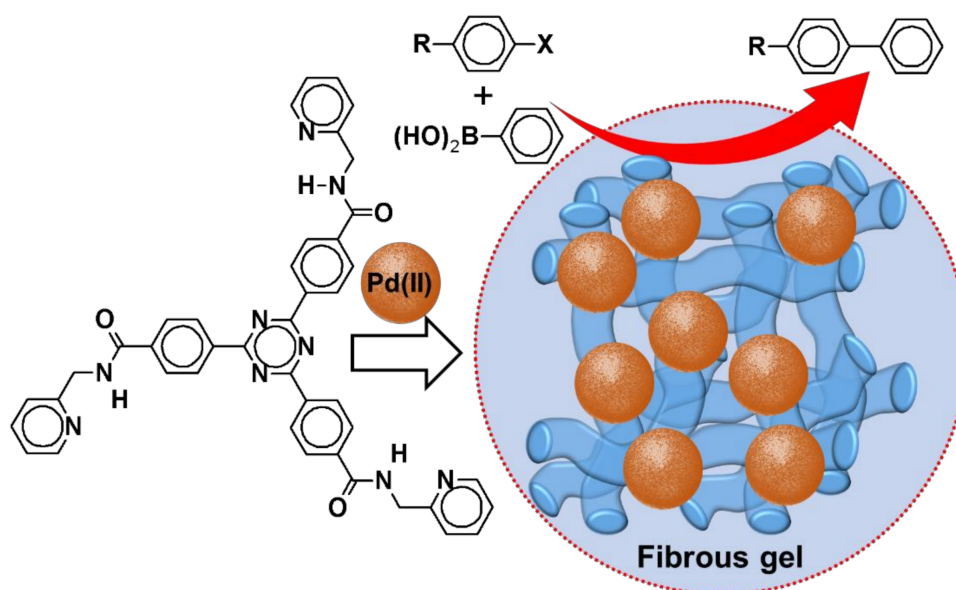


Figure 48. A metallogel formed from the self-assembly of a palladium salt and a C_3 -symmetric multidentate pyridine-based tripodal ligand in $\text{CH}_3\text{OH}/\text{CHCl}_3$ solution and a Suzuki–Miyaura coupling using the fibrous gel.

The works of Liu et al. provide an excellent illustration of the second strategy [197]. As it is known that the bola-amphiphilic L-glutamic acid derivatives, such as *N,N'*-hexadecanedioyl-di-L-glutamic acid (L-HDGA) and 1,4-dodecyloxy-bis(4-benzoyl-L-glutamic acid) (L-BECA), can be self-assembled into helical nanotubes leading to supramolecular gels [198], the authors assumed that $\text{Cu}(\text{II})$ cations could help to stabilize these nanostructures, thus facilitating access to metallogels. Surprisingly, the gel based on L-BECA was destroyed immediately after the introduction of Cu^{2+} and nanofiber structures were obtained. In contrast, for L-HDGA, the gel was kept after the addition of Cu^{2+} and chiral nanotube structures were observed. However, the diameter of the metallogel nanotubes was greater than that observed in the organogel due to a transition from a single-layer nanotube to a multilayer nanotube (the thickness of the tubular wall was about 10 nm) during post-modification. In this paper, the authors, for the first time, used this metallogel to catalyze asymmetric a Diels–Alder cycloaddition of (*E*)-3-phenyl-1-(pyridin-2-yl)prop-2-en-1-one (aza-chalcone) with cyclopentadiene. The results clearly show that the L-HDGA/ Cu^{2+} nanotube showed good reaction rates with efficient enantiomeric selectivity (an *ee* up to 51%). The authors suggested that the perfect alignment of Cu^{2+} on the surface of the chiral nanotube structures provided a stereochemically favored environment with a high density of catalytic sites. Under such conditions, the aza-chalcone can be anchored on the nanotube surfaces, leading to an accessible and a tunable approach to the cyclopentadiene (Figure 49). Consequently, this supramolecular chiral catalyst gives high activity and enantioselectivity. This work opens a new way to perform efficient chiral catalysis via metallogels.

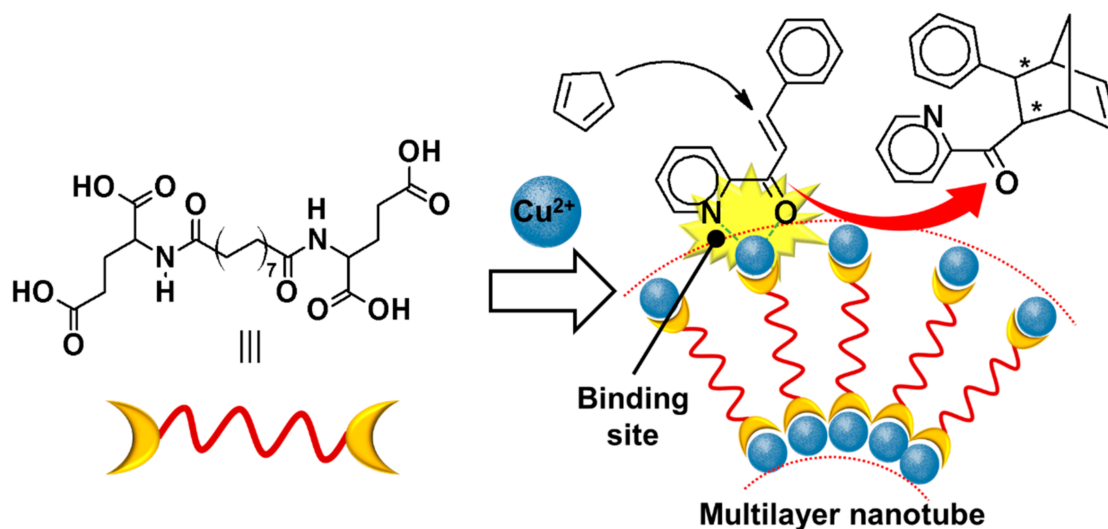


Figure 49. A metallogel *N,N'*-hexadecanedioyl-di-L-glutamic acid/Cu(II)-catalyzed asymmetric Diels–Alder cycloaddition of aza-chalcone with cyclopentadiene.

4.4. Discrete and Infinite Porous Metal–Organic Networks

Developed at an extraordinary pace over the past two decades, metal–organic frameworks (MOFs) are obtained by the self-assembly of organic linkers and inorganic connectors of metal ions and/or clusters [199]. MOFs not only enrich the domain of porous materials, but also lead to a number of applications, including heterogeneous catalysis with the possible inclusion of guest substrates or other active species (Figure 50).

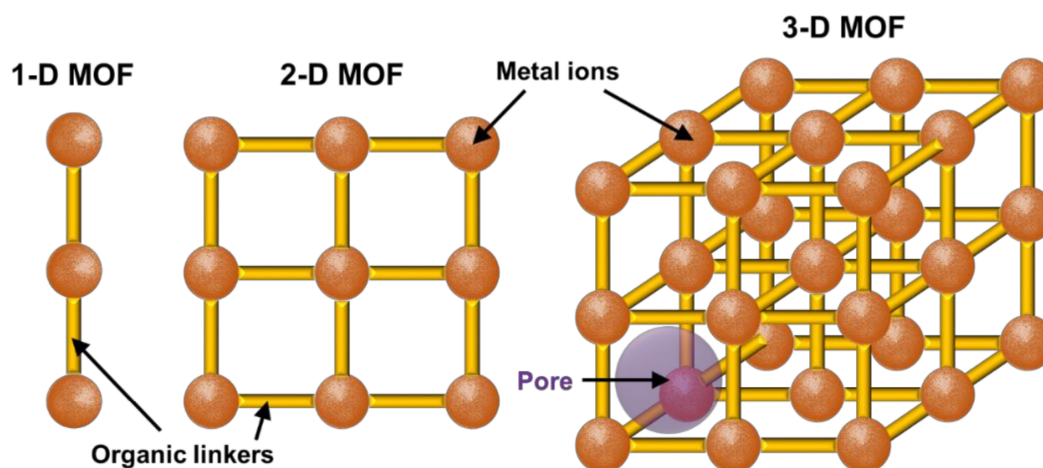


Figure 50. The basic building units of one-, two-, and three-dimensional metal–organic frameworks (MOFs).

In the formation of MOFs, the organic linkers must meet certain requirements to form coordination bonds. They must be: (i) multidentate with at least two donor atoms (N-, O-, or S-); and (ii) anionic or neutral. For instance, the linkers commonly used in the MOFs are 4,4'-bipyridine, piperazine, polycarboxylates, porphyrins, and metalloporphyrins. The two last ones have received great attention in building porous porphyrinic framework materials with catalytic functionalities due to the possible modulation of catalytic-active metal sites and their adaptation to the peripheral environment [200,201]. In this general context, one of the most active and important areas of chemical research is probably the self-assembly of modular components into well-defined supramolecular nanostructures. The molecular recognition events involved in the formation of these architectures can range from weak to fairly

strong, the most common of these interactions being H-bonding, aromatic stacking, and metal–ligand bond formation. The use of transition metals in coordination-directed self-assembly has been an especially active area. The resultant metal–organic coordination networks can be finite or infinite [202]. As liquid-phase and solid-phase ordered porous architecture materials have been widely used in catalysis, we report here some catalytic MOFs. However, as numerous reviews are available in the literature, we will present only some of the very recent examples [203–205].

N.B. In this subsection, some discrete supramolecular networks have also been reported due to their suitability with the concepts mentioned above and their potential application as extended lattices.

A typical example of post functionalization of a supramolecular MOF by the inclusion of an active guest species was reported, in 2016, by Wang and coworkers in order to obtain homogeneous and heterogeneous systems with photocatalytic activity for H₂ production [206]. The authors described a self-assembly strategy for the generation of the first homogeneous supramolecular MOF in water at room temperature based on hexaarmed tris(bipyridine)ruthenium(II) (i.e., a hexaarmed [Ru(bpy)₃]²⁺) precursor and a synthetic host (cucurbit[8]uril, CB[8]), which is able to form complexes with various positively charged molecules (Figure 51) [207,208].

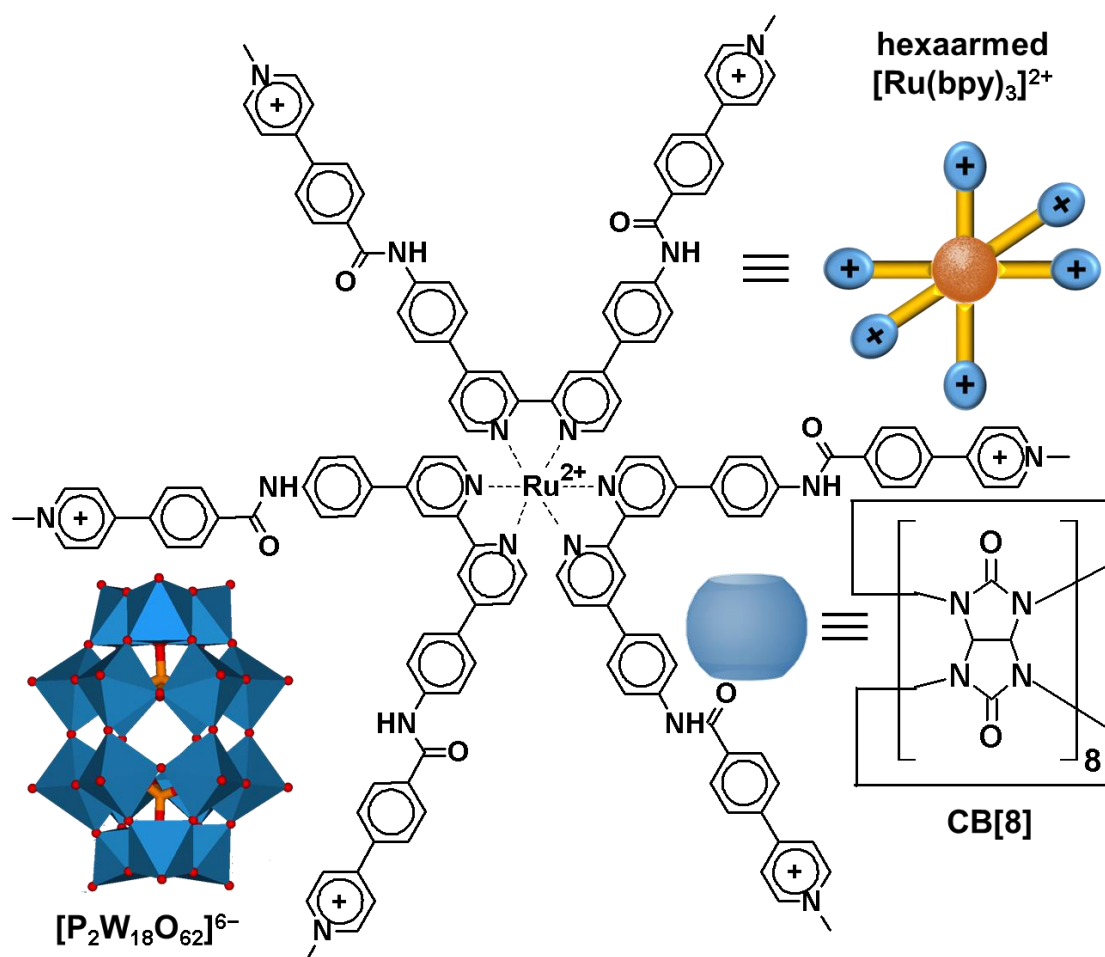


Figure 51. The structure of hexaarmed [Ru(bpy)₃]²⁺, CB[8], and a redox-active [P₂W₁₈O₆₂]⁶⁻ unit.

A comparison between TEM, small-angle X-ray scattering (SAXS), and diffraction experiments suggests that a cubic transition-metal-cored supramolecular organic framework was obtained in solution as well as in a solid-state. Moreover, this supramolecular MOF was able to encapsulate anionic polyoxometalates, such as redox-active [P₂W₁₈O₆₂]⁶⁻, in a one-cage-one-guest manner to give hybrid assemblies (Figure 52). Such hybrids enable fast multi-electron injection from photosensitive [Ru(bpy)₃]²⁺ units to redox-active [P₂W₁₈O₆₂]⁶⁻ units using 500 nm of light irradiation, leading to

efficient photo-driven H_2 production in an acidic aqueous solution ($pH = 1.8$) using methanol as the sacrificial electron donor (homogeneous system). However, heterogeneous photo-driven H_2 production was also possible in organic media as the hybrid microcrystals were insoluble in an acetonitrile and *N,N*-dimethylformamide mixture (3:7). Finally, it is worth noting that, for both the homogeneous and heterogeneous systems, $[P_2W_{18}O_{62}]^{6-}$ units did not escape from the supramolecular MOF to the solution after irradiation.

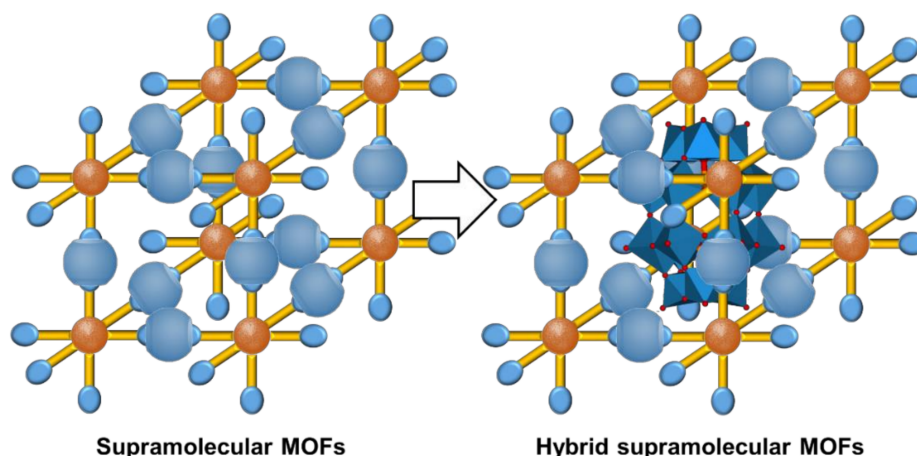


Figure 52. The formation of a hybrid assembly obtained after $[P_2W_{18}O_{62}]^{6-}$ encapsulation inside the cavities of supramolecular metal–organic frameworks.

On the other hand, the inclusion of guest substrates inside the cavities of the supramolecular MOF can also be very useful in catalysis. Recently, Gupta and Mandal reported the one-pot self-assembly of three components: (i) a metal precursor (Mn, Co, Ni, Zn, or Cd); (ii) a tridentate polypyridyl ligand, such as *N,N'*-bis(2-pyridylmethyl)-*tert*-butylamine; and (iii) a bent dicarboxylic acid, such as 4,4'-(dimethylsilanediyl)bis-benzoic acid or 4,4'-oxybis-benzoic acid (Figure 53) [209].

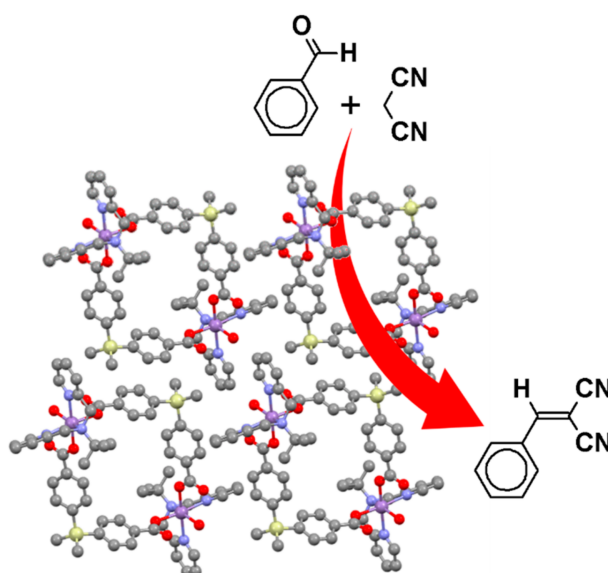


Figure 53. Catalytic Knoevenagel condensation between malononitrile and benzaldehyde catalyzed by discrete $[2+2+2]$ molecular squares in a water environment (see CCDC reference number 1,835,561).

Under ambient conditions, this condensation resulted in the formation of a series of discrete $[2+2+2]$ molecular squares. It is worth noting that the metal centers present some coordinated water molecules. As the self-assembly of $[2+2+2]$ molecular squares was only driven by metal–ligand

bonds (i.e., coordination), the chemical and thermal stabilities were established by powder X-ray diffraction and a thermogravimetric analysis, respectively. These results have demonstrated a relatively high chemical stability against various conventional solvents (water, MeOH, EtOH, CH₃CN, CH₂Cl₂, acetone, THF, and DMF) as well as heating (up to 200 °C). The presence of water molecules coordinated with metal centers could be applied for Knoevenagel reactions of malononitrile with various aldehydes via an efficient Lewis acid catalysis. These reactions were carried out in > 98% conversion in 100 min with a 2 mol % catalyst in a water environment. The proposed mechanism involves host–guest interactions between the porous networks and the substrates via aromatic stacking.

Chiral MOFs can also be used to perform catalytic asymmetric reactions. One of the very recent example uses homochiral MOFs as recyclable heterogeneous catalysts for an asymmetric ring-opening reaction of meso-epoxides with aromatic amines [210]. For instance, a homochiral MOF was obtained by treating (*R*)-2,2'-dihydroxy-1,1'-binaphthalene-5,5'-dicarboxylic acid (a ligand) with Cu(NO₃)₂ (a metal precursor) and gave excellent results in the asymmetric ring-opening of cyclohexene oxide with several aromatic amines (*N*-methyl aniline, *N*-methyl-*p*-toluidine, *N*-methyl-*p*-anisidine, and *N*-methyl-*p*-chloroaniline). Indeed, the reactions furnished the various desired β-amino alcohols in good yields (85–94%) with excellent enantioselectivities (92–95%) Furthermore, other homochiral MOFs based on (*R*)-2,2'-dihydroxy-1,1'-binaphthyl-4,4'-di(4-benzoic acid) and (*R*)-2,2'-diethoxy-1,1'-binaphthyl-4,4'-di(5-isophthalic acid), combined with Cu(II) or Zn(II), also catalyzed asymmetric ring-opening reactions of *cis*-stilbene oxide with 1-naphthylamine in high yield and enantioselectivity: up to 95% and 97%, respectively (Figure 54). It is worth noting that control experiments with asymmetric ring-opening reactions clearly proved that the enantioselectivity observed within the MOF may be attributed to the restricted movement of the substrates in combination with a multiple chiral induction in the confined system. Finally, the reusability of the MOF catalysts were also investigated by the authors. Their results proved the high recoverability and recyclability of MOFs with a clear retention of their performance.

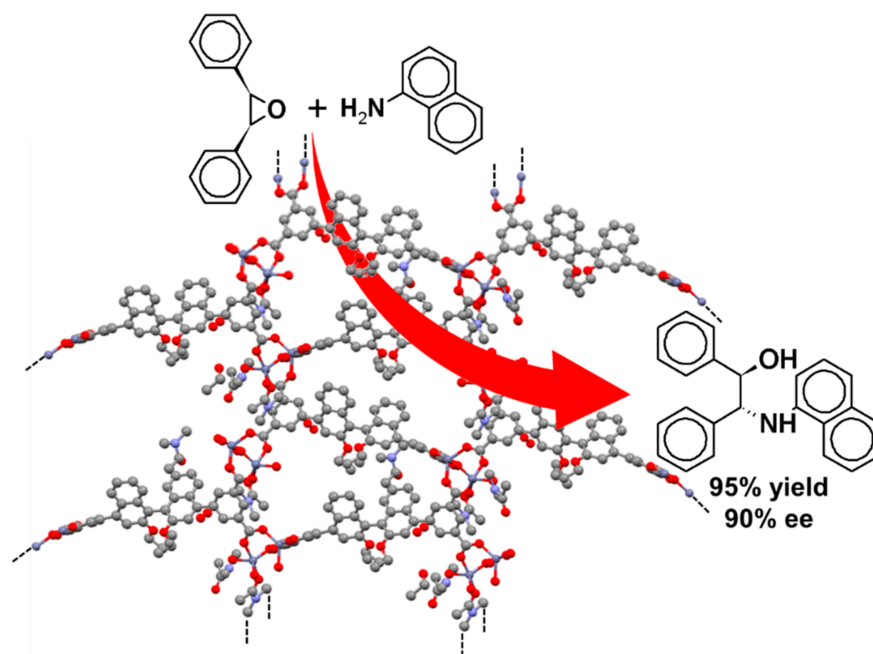


Figure 54. A homochiral MOF obtained by treating (*R*)-2,2'-dihydroxy-1,1'-binaphthyl-4,4'-di(5-isophthalic acid) with Zn(NO₃)₂·6H₂O and an asymmetric ring-opening reaction of *cis*-stilbene oxide with 1-naphthylamine (see CCDC reference number 1,832,085).

However, it is worth noting that the porosity of supramolecular porous metal–organic coordination complexes can be also used as a protective layer in the context of enzyme immobilization.

Indeed, depending on the size of the pores, the substrate can diffuse but not the enzyme. Moreover, immobilized enzymes on solid supports constitute a useful approach to facilitate the recycling operations. Unfortunately, these immobilized enzymes remain accessible, resulting in leaching processes and/or inactivation caused by denaturing stresses and a hazardous external environment. To solve this issue, Jia and coworkers proposed to use a novel shielding strategy for enzymes, leading to hybrid organic/inorganic nanobiocatalysts. Indeed, the authors used the self-assembly of a supramolecular metal–organic coordination complex, made from tannic acid and Fe(III) cations, at the surface of Fe₃O₄/silica core-shell NPs that embedded catalase [211]. This supramolecular metal–organic coordination complex allowed the authors to obtain a mesoporous nanocoating at the surface of immobilized catalase on the NPs, protecting this enzyme from biological, thermal, and chemical degradation (Figure 55). As expected, the immobilized catalase exhibited improved stability towards heat, denaturants, and proteolytic agents compared to the free enzyme or to the immobilized catalase without the protective nanocoating. The reutilizing catalytic activity of the immobilized enzyme was also improved. Indeed, the immobilized catalase with the protective nanocoating showed more than 50% of residual activity after nine cycles in comparison with an unprotected immobilized enzyme, which preserved only 20% of the activity.

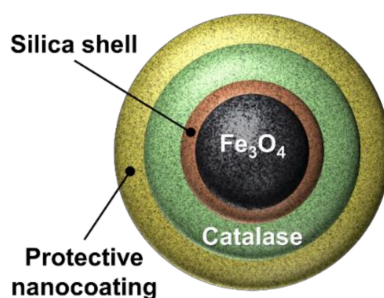


Figure 55. An immobilized enzyme at the surface of magnetic Fe₃O₄@silica core-shell nanoparticles (NPs) with a protective nanocoating.

5. Catalytic Systems Based on “Colloidal Tectonics”

Following the “colloidal tectonics” approach, inspired by “molecular tectonics”, the design and bottom-up edification of self-assembled colloidal NPs with controlled sequences can be achieved by the complementarity between two or more molecules (i.e., tectonic subunits). These NPs emerge as a smart solution to build a variety of supracolloidal systems (e.g., Pickering emulsions and colloidal suspensions). As a consequence, these colloidal or supracolloidal systems can be very useful to obtain catalysts or catalytic systems with tunable properties that are highly compatible with the “green chemistry” concept.

5.1. Concept

From a historical point of view, the phenomenon that NPs can be easily obtained from the self-assembly of molecules was firstly observed in 2012 [212]. Following this work, new research in the area gathered a rapid pace with the appearance of the “colloidal tectonics” concept in 2018 [34]. This concept is defined as the art and science of the supramolecular formation of colloidal or supracolloidal structures using complementary tectons (molecular building blocks).

Some biological examples of the spontaneous bottom-up formation of colloidal structures using tectonic subunits (i.e., “colloidal tectonics”) can be found in nature. For instance, the four phosphoproteins present in milk (α_{S1} , α_{S2} , β , and κ -caseins) are known to form casein micelles, which are large spherical water-insoluble aggregates (a size from 20 to 600 nm in diameter) composed of several thousand associated casein subunits [213]. The hydrophobic interactions between the caseins is the essential driving force. However, the growth is inhibited by electrostatic and steric repulsions, leading to porous colloidal NPs constituted of hydrophilic and hydrophobic regions in

which water molecules can be accommodated [214]. In addition, these NPs are able to stabilize Pickering emulsions in water/oil biphasic systems [215]. These emulsions are supracolloids, since their formations and stabilities depend not only on the particle size but also on particle–particle, particle–water, and particle–oil interactions.

To obtain the spontaneous formation of colloidal or supracolloidal structures using tectonic subunits, it is necessary to keep in mind that the total interaction energy is the sum of hydrophobic attractions, steric repulsions, and electrostatic repulsions (or attractions). As a consequence, to achieve colloidal structures stabilized by hydrophobic/hydrophilic intermolecular forces, it is necessary to use tectons (building blocks) with a precise and scalable algorithm [34]. From a theoretical point of view, in water/oil biphasic systems, these colloidal systems result from the following sequential recognition events: (i) the self-assembly between the “polar” and “apolar” tectons using complementary binding sites (e.g., electrostatic forces and host–guest interactions) leads to the formation of discrete elementary clusters; (ii) the solvophobic effect tends to aggregate the elementary clusters at the water/oil interface upon the exclusion of water and oil molecules (i.e., nucleation); (iii) the pseudo-crystallization progresses by an increase in supersaturation caused by the interfacial accumulation of clusters, leading to the formation of colloidal NPs; (iv) the tecton transfer rates across the liquid/solid/liquid interface decrease with the NPs’ emergence, which increases the interfacial rigidity and/or some defects appear in the NPs’ organization, limiting their growth; and (v) the packing of NPs allows for the formation of superstructures named supracolloidal assemblies: Pickering emulsions, colloidal crystals, colloidosomes, etc. (Figure 56). It is worth noting that that number of tecton–tecton, cluster–cluster, and NP–NP interactions must be higher than the number of tecton–solvent, cluster–solvent, and NP–solvent interactions [34].

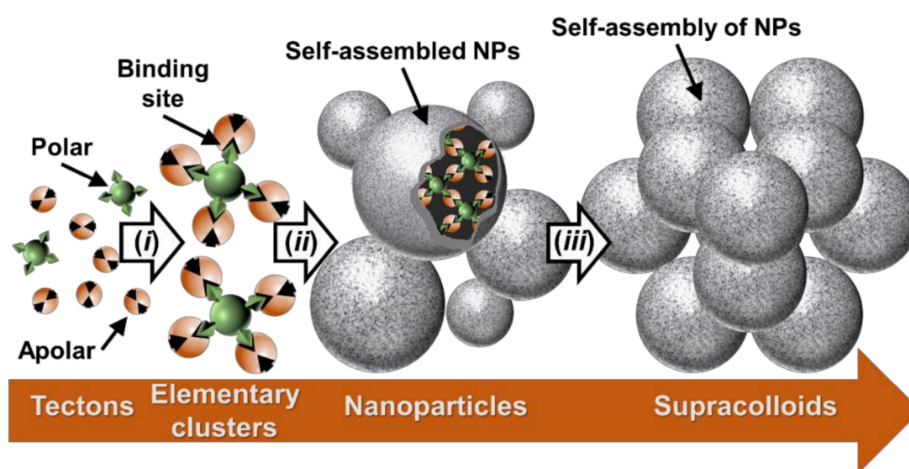


Figure 56. The hierarchical formation of supramolecular colloidal systems based on the “colloidal tectonics” approach: (i) self-assembly between tectons; (ii) nucleation and growth; and (iii) packing of NPs.

Finally, it is worth noting that “colloidal tectonics” can be related to phase-boundary catalysis, as these two systems use catalytic NPs lying in the boundary between an aqueous and an organic phase. Consequently, these two concepts combine the advantages of interfacial catalytic processes: high activity and selectivity, easy phase separation, and recyclability of the catalyst [216–221]. However, some fundamental differences must be emphasized: on the catalyst’s preparation and on the system’s flexibility. Indeed, synthetic steps are required to obtain phase-boundary catalysts (e.g., usually chemically modified zeolites), whereas the “colloidal tectonics” approach uses only self-assembly processes [222]. Moreover noncovalent functional systems, contrary to phase-boundary catalysis, can be robust yet adaptive and self-healing. Therefore, noncovalent colloidal systems represent a versatile, multifunctional, and environmentally friendly alternative to conventional covalent systems.

5.2. Sol Systems

Colloidal solution suspensions of very small particles in a continuous liquid medium are named sols. Sols are generally quite stable; however, some of them require the presence of dispersing agents to improve their stabilities. “Colloidal tectonics”, which enables the smart design of self-assembled NPs with switchable amphiphilic properties, can be very useful to obtain sol catalytic processes.

In 2012, Nardello-Rataj and coworkers, following this background, published the first self-assembled NPs. These NPs were obtained after ionic metathesis between anionic polyoxometalates (POMs, $\text{PW}_{12}\text{O}_{40}^{3-}$, “polar” tectons) and cationic surfactants (dodecyltrimethylammonium hydroxide, “apolar” tectons) [212]. In aqueous solution, the dodecyltrimethylammonium/ $\text{PW}_{12}\text{O}_{40}$ uncharged combination (discrete elementary clusters) was easily formed after an acid–base reaction between the “polar” and “apolar” tectons using electrostatic forces. The elementary clusters tend to aggregate in water upon the hydrophobic effect, leading to the exclusion of water molecules. (i.e., nucleation). This pseudo-crystallization (i.e., growth) leads to the formation of colloidal NPs in order to decrease the hydrophobic/water contact [223]. From the combined effects of hydrophobic, van der Waals, electrostatic, and steric forces, the tectons are arranged in order to obtain parallel inorganic planes of unconnected POMs separated by interdigitated cationic surfactant chains. This organization is typical of ionic surfactants in a solid-state. However, during the growth process, some defects may appear in the lamellar packing and may lead to the appearance of surface charges that would limit the particle growth, leading to well-defined monodisperse spherical NPs. The self-assembled internal structure results in a porous particles in which small organic molecules can be accommodated [223]. This property is essential in order to obtain stable sols without the presence of dispersing agents.

In 2014, these NPs were used to perform olefin epoxidation in eco-friendly solvents, such as cyclopentyl methyl ether, 2-methyl tetrahydrofuran, methyl acetate, and glycerol triacetate (Figure 57) [224].

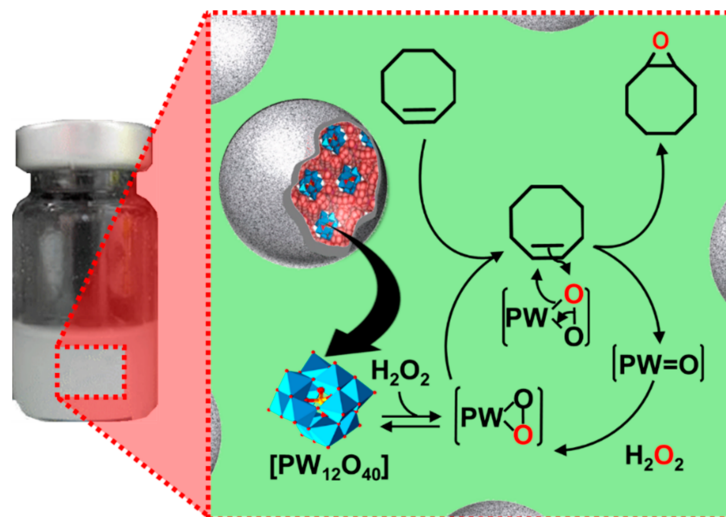


Figure 57. The mechanism of olefin epoxidation inside a colloidal solution suspension (sol) of dodecyltrimethylammonium/ $\text{PW}_{12}\text{O}_{40}$ NPs in a continuous aqueous medium.

With these solvents, the epoxidation of cyclooctene proceeds at competitive rates (initial turnover frequency, TOF_0 , $>260 \text{ h}^{-1}$), good yields ($>95\%$), and high selectivity ($>99\%$). As the catalytic activities are directly correlated to the dispersion stability in a given solvent, the better the stability, the higher the activity. Moreover, the self-assembled NPs are much more active than the native POM. This effect can be clearly related to the high concentration of catalyst species inside the amphiphilic NPs lying in the boundary between the aqueous and the solid phase. In addition, the accommodation of substrates inside the porous NPs is also a key factor to explain the great stability of these sol reaction media

as well as the competitive rates. The recyclability of the systems was demonstrated: the catalytic activity and selectivity of the recovered catalyst were identical after at least five consecutive recyclings. In addition, the scope of substrates has been successfully extended to cyclohexene, 1-octene, limonene, 3-carene, α -pinene, β -pinene, and neryl acetate. It is worth noting that excellent epoxide selectivities were obtained in each case. Therefore, this catalytic system offers an eco-friendly solution with the advantages of homogeneous and heterogeneous catalysis.

5.3. Pickering Emulsions

On the other hand, nano-sized colloidal NPs are also able to stabilize Pickering emulsions [224–226]. Unlike molecular surfactants, these NPs do not need to be amphiphilic, and only a partial wettability of the NPs is required to allow for the strong anchoring of NPs at the oil/water interface [227]. In order to characterize the wetting, the three-phase contact angle of NPs to the interface, θ (measured through the aqueous phase), can be used to predict and explain the type of emulsions (i.e., oil-in-water, O/W, or water-in-oil, W/O). Following the empirical Finkle's rule, hydrophilic NPs ($\theta < 90^\circ$) stabilize O/W emulsions, while the opposite applies for NPs that have been more wetted by oil than water ($\theta > 90^\circ$, see Figure 58) [228].

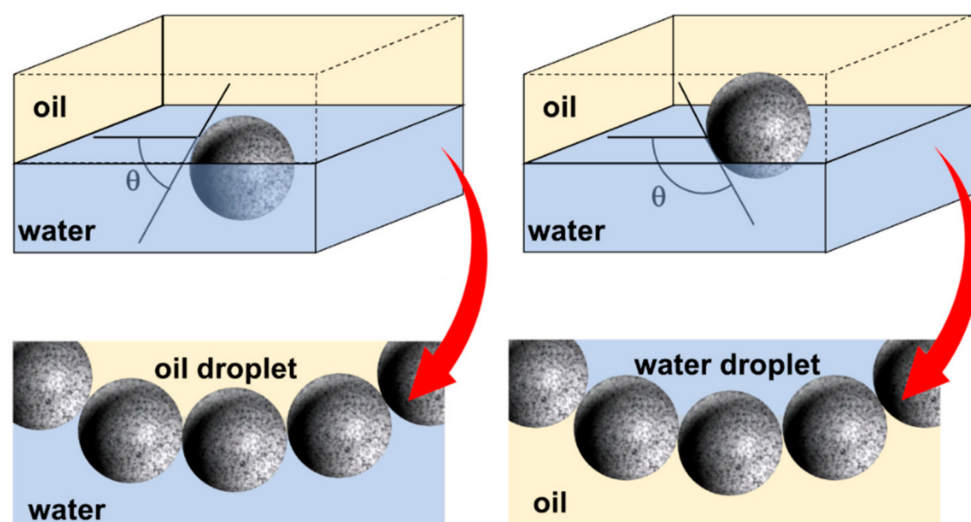


Figure 58. The three-phase contact angle, θ , and its relation to the type of Pickering emulsion.

It is worth noting that the transition from the O/W to the W/O emulsion type occurs at $\theta = 90^\circ$. As consequence, at this peculiar value, the NPs are not able to stabilize emulsions and only a “bipolar”-like behavior is observed [229]. However, when θ tends to 90° , desorption energies of NPs can easily reach several thousands of $k_B T$, contrary to a molecular surfactant, where this energy is of the order of $k_B T$. Consequently, molecular emulsifiers are in dynamic equilibrium between the interface and the bulk, whereas NPs are “irreversibly” anchored at the interface (except with the use of extrinsic forces). Therefore, the surface coating by NPs acts against coalescence by the formation of an egg shell (i.e., a rigid layer that separates the two phases) [227]. Unfortunately, if the surface coverage (τ , proportion of oil-water interface covered by the NPs) is partial, the droplets coalesce until a compact monolayer is obtained. This limited coalescence is observed immediately after emulsification and stopped when the droplet interface becomes densely coated with NPs (Figure 59).

However, the emulsion destabilization can be produced “on demand” with the use of appropriate external stimuli (e.g., centrifugation, dilution, pH, or temperature variation) [230]. Therefore, these Pickering emulsions are good platforms on which to perform catalytic transformations due to: (i) the presence of immiscible NPs optionally with catalytic activities; (ii) the improvement of mass transfer, which can be ascribed to a huge interfacial contact; and (iii) the easy separation of the reaction products, facilitating the catalyst’s recovery.

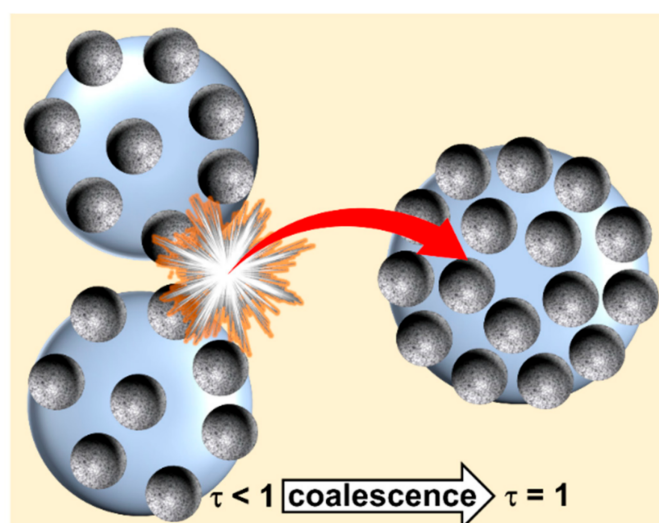


Figure 59. A schematic representation of the limited-coalescence process in a W/O Pickering emulsion.

The previously described dodecyltrimethylammonium/ $\text{PW}_{12}\text{O}_{40}$ NPs (see Section 5.2) can also be used as surface-active building blocks for the preparation of water-in-toluene Pickering emulsions that consist of egg-like shell interfaces of NPs. As the penetration of toluene molecules inside the NPs results in the release of some alkyl chains, the interlocking of NPs occurs, leading to very stable emulsions [212, 231]. These catalytic emulsions can be applied to perform various olefin epoxidations (e.g., cyclooctene, cyclohexene, and limonene) using hydrogen peroxide as an oxidant, under mild conditions ($65\text{ }^{\circ}\text{C}$), and without stirring (except during the emulsification, see Figure 60) [212]. For instance, the catalytic oxidation of cyclooctene, at competitive rates ($\text{TOF}_0 = 32\text{ h}^{-1}$) and high selectivity ($>99\%$), can be successfully performed in these emulsions. In addition, the direct ionic metathesis between $\text{PW}_{12}\text{O}_{40}^{3-}$ and a dodecyltrimethylammonium cation (molar ratio 3:1) in the catalytic medium provides lower catalytic performance than the system made with the prepared NPs ($\text{TOF}_0 \approx 10\text{ h}^{-1}$, $\text{Conv.} \approx 35\%$). This behavior can be ascribed to the in-situ generation of NPs providing a very unstable emulsion with some water in excess due to a partial ionic exchange, leading to a mixture of various species with different interfacial activities that contribute to the appearance of defects in the lamellar packing that limit the NP growth and lead to inefficient catalytic systems. Consequently, the correlation between the catalytic performance and the structuration of the biphasic medium (i.e., emulsion) results clearly from a Pickering interfacial catalysis. Moreover, it is relevant to note that quantitative epoxidation could be achieved with easy product and catalyst separation for the other investigated substrates.

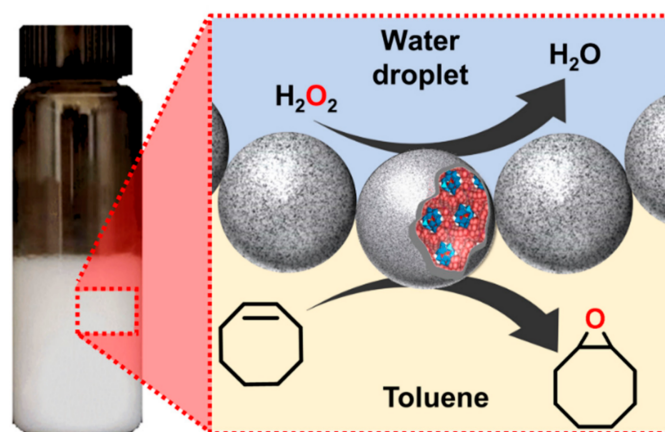


Figure 60. A schematic representation of cyclooctene epoxidation in a water-in-toluene Pickering emulsion stabilized with an amphiphilic dodecyltrimethylammonium/ $\text{PW}_{12}\text{O}_{40}$ NP catalyst.

In 2013, our group reported on the catalytic applications of oil-in-water Pickering emulsions stabilized by the in-situ formation of spherical NPs that adsorb onto the interface between the two phases [232]. The following ordered sequential mechanism occurs: (i) the formation of surface-active inclusion complexes via host-guest interactions between the tectons (CDs and oil molecules, respectively); (ii) the interfacial dehydration of CD/oil inclusion complexes allows for their aggregation (i.e., nucleation); (iii) the pseudo-crystal growth via supersaturation caused by the interfacial accumulation of CD/oil inclusion complexes, leading to the formation of NPs; and (iv) the decrease of CD and oil transfer rates across the interface due to the NPs' emergence leading to growth limitation. It is worth noting that these NPs have a pseudo-spherical shape in order to decrease the hydrophobic/water contact. The great advantages of these emulsions lie in the extemporaneous formation and self-assembly of CD/oil insoluble complexes at the water/oil interface. This system has been used for the oxidation of various substrates (e.g., olefins, organosulfurs, and alcohols) using a $\text{PW}_{12}\text{O}_{40}^{3-}$ anion as a water-soluble catalyst and H_2O_2 as an oxidant (Figure 61). Our first proposal is that the anionic catalyst lies in the aqueous phase, contrary to the Pickering catalytic systems based on amphiphilic dodecyltrimethylammonium/ $\text{PW}_{12}\text{O}_{40}$ NPs (see above). However, our recent investigations prove that the $\text{PW}_{12}\text{O}_{40}^{3-}$ anions have a propensity to adsorb on electrically neutral surfaces of CD/oil NPs due to their large, sticky, polarizable, and salting-in nature, leading to supramolecular hybrid core-shell CD/oil@ $\text{PW}_{12}\text{O}_{40}$ NPs via the “colloidal tectonics” approach [233]. These Pickering emulsions, based on hybrid NPs, behave as a highly efficient reaction medium. For instance, the epoxidation of cyclooctene in the water/heptane biphasic system proceeds at a competitive rate (370 h^{-1}), good yield (>99% in 30 min), and high selectivity (>99%). Under similar conditions, the catalytic activity based on amphiphilic dodecyltrimethylammonium/ $\text{PW}_{12}\text{O}_{40}$ NPs exhibits a weaker efficacy ($\text{TOF}_0 = 32 \text{ h}^{-1}$, see above) for the epoxidation of cyclooctene. This excellent catalytic activity, extended to various substrates, is now totally ascribed to the strong propensity of $\text{PW}_{12}\text{O}_{40}^{3-}$ anions to adsorb on CD/oil NP surfaces as well as to the promoted interfacial contact between the substrate and the catalyst. In addition, these catalytic systems allow for the straightforward separation of the phases by centrifugation or by heating and can be used without any organic solvent for liquid substrates.

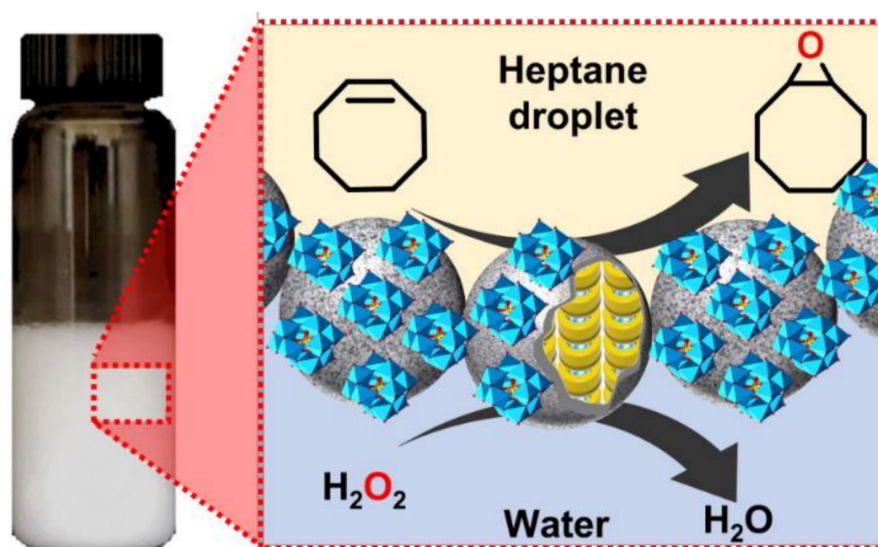


Figure 61. A schematic representation of cyclooctene epoxidation in a heptane-in-water Pickering emulsion stabilized with an amphiphilic hybrid core-shell CD/oil@ $\text{PW}_{12}\text{O}_{40}$ NP catalyst.

Also, in 2013, Hapiot et al. published a similar approach based on the formation of inclusion complexes between native α -CD and high-molecular-weight polyethylene glycol (PEG 20,000 or 35,000 g/mol), leading to the formation of hydrogels [234]. Indeed, in aqueous solution, α -CD/PEG

nanocrystallites, formed by the columnar CD domains, act as physical cross-links alongside the not-included polymer chains. In the presence of oil, these hydrogels provide a good platform on which to obtain oil-in-water Pickering-like emulsions that are particularly useful to the Rh-catalyzed hydroformylation of higher olefins due to the improvement of the contact between the organic substrate and the water-soluble catalyst (Figure 62). The catalytic performance was drastically enhanced in comparison to neat biphasic conditions or in the sole presence of α -CD or PEG. Indeed, control experiments show very little conversion of 1-decene in the presence of α -CD because of the precipitation of an α -CD/1-decene inclusion complex ($\approx 5\%$). Similarly, the use of PEG as a sole additive also leads to a very low conversion of 1-decene ($\approx 20\%$). In contrast, the conversion of 1-decene was 16-fold higher than that observed in neat water. In addition, the linear-to-branched aldehydes ratio was constant, proving that the equilibrium between the catalytic species has not been significantly modified and that the mass-transfer improvement was only due to the contact area increase between the olefins and the water-soluble catalyst. In contrast to the amphiphilic hybrid core-shell CD/oil@PW₁₂O₄₀ NPs (see above), which behave concomitantly as emulsifiers and interfacial catalysts, the present system constitutes the simplest approach in which a homogeneous catalyst (Rh combined with a water-soluble ligand: trisulfonated triphenylphosphine, TPPTS) is combined with Pickering emulsifiers (α -CD/PEG nanocrystallites).

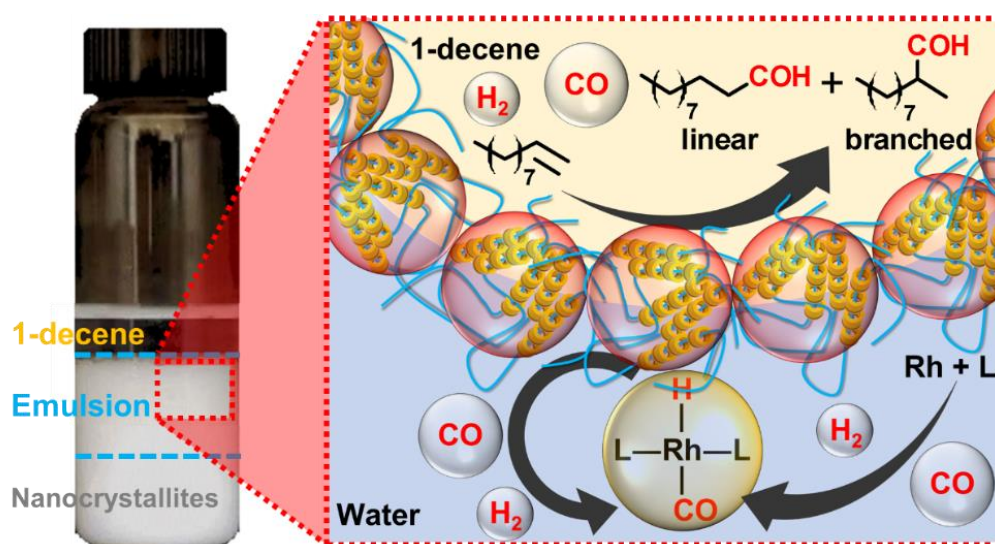


Figure 62. A schematic representation of the Rh-catalyzed hydroformylation of 1-decene in a 1-decene-in-water Pickering emulsion stabilized with α -CD/PEG nanocrystallites (L = TPPTS).

In 2014, the same research team reported the effect of additives on the catalytic performance of the previous Pickering emulsion based on α -CD/PEG20000 nanocrystallites adsorbed at the water/oil interface [235]. Indeed, the authors mentioned that the presence of randomly methylated β -CD positively affected the catalytic activity as well as the chemoselectivity of the hydroformylation reaction of highly hydrophobic olefins. However, an excess of RAME- β -CD resulted in the absence of Pickering emulsion, leading to lower catalytic performance. This behavior is related to the formation of a more fluid Pickering emulsion because the RAME- β -CD prevents the accumulation of α -CD/PEG nanocrystallites at the oil droplet surface. Under such conditions, the mass transfer between the hydrophobic substrate and the water-soluble catalyst is greatly improved. It is worth noting that RAME- β -CD can also act as a supramolecular carrier able to transport the olefins. In 2017, an advanced catalytic system was proposed [236]. This system used poloxamines (Tetronics[®]) instead of PEG. Consequently, the biphasic rhodium-catalyzed hydroformylation of olefins resulted in a thermo-responsive system in the presence of α -CD. However, the catalytic performances was greatly affected by the nature of the used Tetraonic[®]. For instance, the systems that use the reverse-sequential

Tetronic[®] 90R4 were more effective than those containing the conventional sequential Tetronic[®] 701. This behavior is due to the Tetronic[®] structures. Indeed, Tetronics[®] 90R4 is a reversed poloxamine in which ethylene oxide (EO) blocks are directly attached to the central diamino core while the propylene oxide (PO) blocks are at the periphery. As PO blocks act as “stoppers”, the α -CD/Tetronics[®] 90R4 nanocrystallites are more stable to heating. The opposite holds for the conventional sequential Tetronic[®] 701, where the α -CDs can be easily removed upon heating. As hydroformylation is performed at 80 °C and as the catalytic activities depend on the formation of polypseudorotaxane nanocrystallites, resulting in a Pickering-like emulsion, the stability of these emulsions is greater with α -CD/Tetronics[®] 90R4 than with α -CD/Tetronics[®] 701. It is worth noting that the catalytic performance remains unchanged upon recycling.

In 2019, “colloidal tectonics” were used for tandem synergistic Pickering interfacial catalysis. Indeed, two surface-active NPs containing both recognition and catalytic sites have been reported to control the formation and the properties of Pickering emulsions, such as stability (Figure 63). This new catalytic system used a combination of amphiphilic dodecyltrimethylammonium/ $PW_{12}O_{40}$ and silica NPs functionalized with sulfonic acids and alkyl groups [237]. The interfacial self-assembly occurred thanks to the penetration of the alkyl chains of modified silica NPs into the amphiphilic self-assembled dodecyltrimethylammonium/ $PW_{12}O_{40}$ NPs, which possess a supramolecular porous structure constituted of polar and apolar regions. Consequently, in the presence of a water/oil biphasic system, both NPs are interlocked, leading to elastic “springs” in the interfacial layer that condition the droplet size and the emulsion stability. These very stable water-in-oil Pickering emulsions were used as a non-nitric acid route for adipic acid synthesis (precursor of Nylon 6,6) from the one-pot oxidative cleavage of epoxycyclohexane with aqueous hydrogen peroxide. The catalytic performance was significantly boosted due to the interfacial co-adsorption of both NPs catalyzing the hydrolysis and oxidation steps implied in this transformation. Under optimal conditions (80 °C, 500 rpm, 12 h), this system combines the benefits of supramolecular chemistry (flexible, versatile, and highly dynamic self-assembly systems) with those of homogeneous (high activity and selectivity) and heterogeneous (simple phase separation and catalyst reuse) catalyses.

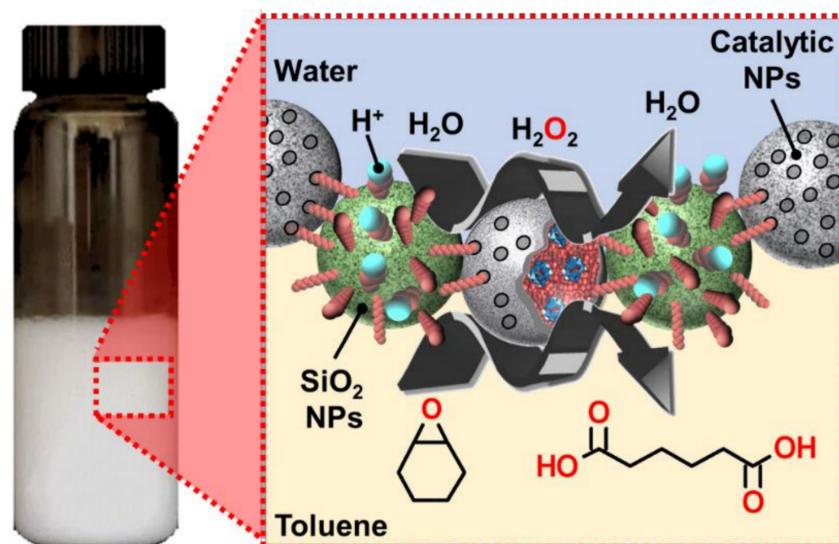


Figure 63. A schematic representation of Pickering oxidative cleavage of epoxycyclohexane in a water-in-toluene Pickering emulsion stabilized with amphiphilic dodecyltrimethylammonium/ $PW_{12}O_{40}$ and modified silica NPs.

6. Conclusions

This review proposes an overview of the main cutting-edge strategies involving supramolecular chemistry and self-organization in catalysis via the formation of new self-assembled catalytic entities

and/or systems. Indeed, supramolecular chemistry is one of the most important and interdisciplinary topical fields of contemporary chemistry. This field has been rapidly growing during the past few decades, making possible the production of infinite numbers of molecular assemblies by exploiting intermolecular forces and electrostatic or hydrogen bonding. Presently, one of the major interest areas with these molecular assemblies is shifting from structure to function. Ever since the pioneer works of Cram and coworkers in the 1970s, and the discovery by Corey et al. in 1989 of oxazaborolidine catalysts, referred to as “chemzymes” due to the binding between the catalyst and substrate, the holy grail has been to achieve the “syntheses” of various supramolecular systems with a catalytic function. The extension of this concept to numerous molecular associations with infinite numbers of molecules allowed us to switch from discrete species in solution to complex materials with regular internal structures by the way of the molecular tectonics concept. Indeed, the supramolecular assemblies may vary from nano- to microscales (i.e., from discrete to extended systems). More recently, the “colloidal tectonics” approach has made it possible to build various self-assembled colloidal systems from the packing of molecules and to create an exciting environment for research at the junction between molecular and colloidal sciences. As the number of supramolecular systems is limited, perhaps, only by our imagination, these methodologies, by their power over the expressions of matter, provide, at least partially, an invitation to be creative and innovative to solve current and future problems. Chemistry has expanded from molecular to supramolecular chemistry and now moves towards adaptive chemistry by way of constitutional dynamic chemistry. Indeed, the adaptation of molecular assemblies, in response to external agents, to switching processes, to morphological changes or shape switching, to phase change, and to an interface opens the way to smart systems with potential application in catalysis. Consequently, supramolecular chemistry and self-organization constitute an infinite playground for tomorrow’s catalytic systems, from an academic and industrial point of view, contributing without doubt to the invention of new chemistry and to the protection and preservation of our planet in the future.

Author Contributions: All authors contributed equally to this work and approved the final version of the manuscript.

Funding: This research received no external funding.

Acknowledgments: This review is dedicated to André Mortreux (Université de Lille, France) to honor his outstanding contributions to homogeneous catalysis both in terms of academic research and teaching.

Conflicts of Interest: There are no conflicts to declare.

References

1. James, T.D. Specialty grand challenges in supramolecular chemistry. *Front. Chem.* **2017**, *5*, 83. [[CrossRef](#)] [[PubMed](#)]
2. Rest, C.; Mayoral, J.M.; Fernández, G. Aqueous self-sorting in extended supramolecular aggregates. *Int. J. Mol. Sci.* **2013**, *14*, 1541–1565. [[CrossRef](#)] [[PubMed](#)]
3. Amabilino, D.B.; Smith, D.K.; Steed, J.W. Supramolecular materials. *Chem. Soc. Rev.* **2017**, *46*, 2404–2420. [[CrossRef](#)] [[PubMed](#)]
4. Ma, X.; Zhao, Y. Biomedical applications of supramolecular systems based on host–guest interactions. *Chem. Rev.* **2015**, *115*, 7794–7839. [[CrossRef](#)] [[PubMed](#)]
5. Leclercq, L. Interactions between cyclodextrins and cellular components: Towards greener medical applications? *Beilstein J. Org. Chem.* **2016**, *12*, 2644–2662. [[CrossRef](#)] [[PubMed](#)]
6. Cui, H.; Xu, B. Supramolecular medicine. *Chem. Soc. Rev.* **2017**, *46*, 6430–6432. [[CrossRef](#)] [[PubMed](#)]
7. Amin, M.C.; Ahmad, N.; Pandey, M.; Abeer, M.M.; Mohamad, N. Recent advances in the role of supramolecular hydrogels in drug delivery. *Expert Opin. Drug. Deliv.* **2015**, *12*, 1149–1161. [[CrossRef](#)] [[PubMed](#)]
8. Webber, M.J.; Langer, R. Drug delivery by supramolecular design. *Chem. Soc. Rev.* **2017**, *46*, 6600–6620. [[CrossRef](#)]

9. Andréasson, J.; Pischel, U. Storage and processing of information using molecules: The all-photonic approach with simple and multi-photochromic switches. *Isr. J. Chem.* **2013**, *53*, 236–246. [[CrossRef](#)]
10. Lehn, J.-M. Supramolecular chemistry: Receptors, catalysts, and carriers. *Science* **1985**, *227*, 849–856. [[CrossRef](#)]
11. Vriezema, D.M.; Comellas Aragonés, M.; Elemans, J.A.A.W.; Cornelissen, J.J.L.M.; Rowan, A.E.; Nolte, R.J.M. Self-assembled nanoreactors. *Chem. Rev.* **2005**, *105*, 1445–1489. [[CrossRef](#)] [[PubMed](#)]
12. Badi, N.; Guégan, P.; Legrand, F.-X.; Leclercq, L.; Tilloy, S.; Monflier, E. β -Cyclodextrins modified by alkyl and poly(ethylene oxide) chains: A novel class of mass transfer additives for aqueous organometallic catalysis. *J. Mol. Catal. A* **2010**, *318*, 8–14. [[CrossRef](#)]
13. Ballester, P.; Vidal-Ferrana, A. *Supramolecular Catalysis*; van Leeuwen, P.W., Ed.; Wiley-VCH: Weinheim, Germany, 2008; pp. 1–27.
14. Raynal, M.; Ballester, P.; Vidal-Ferrana, A.; van Leeuwen, P.W. Supramolecular catalysis. Part 1: Non-covalent interactions as a tool for building and modifying homogeneous catalysts. *Chem. Soc. Rev.* **2014**, *43*, 1660–1733. [[CrossRef](#)] [[PubMed](#)]
15. Pauling, L. Molecular Architecture and Biological Reactions. *Chem. Eng. News* **1946**, *24*, 1375–1377. [[CrossRef](#)]
16. Meeuwissen, J.; Reek, J.N.H. Supramolecular catalysis beyond enzyme mimics. *Nat. Chem.* **2010**, *2*, 615–621. [[CrossRef](#)] [[PubMed](#)]
17. Chao, Y.; Cram, D.J. Catalysis and chiral recognition through designed complexation of transition states in transacylations of amino ester salts. *J. Am. Chem. Soc.* **1976**, *98*, 1015–1017. [[CrossRef](#)]
18. Breslow, R. Biomimetic chemistry and artificial enzymes: Catalysis by design. *Acc. Chem. Res.* **1995**, *28*, 146–153. [[CrossRef](#)]
19. Kirby, A.J. Enzyme Mechanisms, Models, and Mimics. *Angew. Chem. Int. Ed.* **1996**, *35*, 706–724. [[CrossRef](#)]
20. Rebek, J., Jr.; Wyler, R.; de Mendoza, J. A synthetic cavity assembles through self-complementary hydrogen bonds. *Angew. Chem. Int. Ed.* **1993**, *32*, 1699–1701. [[CrossRef](#)]
21. Rebek, J., Jr.; Kang, J. Acceleration of a Diels–Alder reaction by a self-assembled molecular capsule. *Nature* **1997**, *385*, 50–52. [[CrossRef](#)]
22. Bai, C.C.; Tian, B.R.; Zhao, T.; Huang, Q.; Wang, Z.Z. Cyclodextrin-catalyzed organic synthesis: Reactions, mechanisms, and applications. *Molecules* **2017**, *22*, 1475. [[CrossRef](#)] [[PubMed](#)]
23. Hapiot, F.; Tilloy, S.; Monflier, E. Cyclodextrins as supramolecular hosts for organometallic complexes. *Chem. Rev.* **2006**, *106*, 767–781. [[CrossRef](#)] [[PubMed](#)]
24. Catti, L.; Zhang, Q.; Tiefenbacher, K. Advantages of catalysis in self-assembled molecular capsules. *Chem. Eur. J.* **2016**, *22*, 9060–9066. [[CrossRef](#)]
25. Rico-Lattes, I.; Perez, E.; Franceschi-Messant, S.; Lattes, A. Organized molecular systems as reaction media. *C. R. Chim.* **2011**, *14*, 700–715. [[CrossRef](#)]
26. La Sorella, G.; Strukul, G.; Scarso, A. Recent advances in catalysis in micellar media. *Green Chem.* **2015**, *17*, 644–683. [[CrossRef](#)]
27. Nardello-Rataj, V.; Caron, L.; Borde, C.; Aubry, J.-M. Oxidation in three-liquid-phase microemulsion systems using “balanced catalytic surfactants”. *J. Am. Chem. Soc.* **2008**, *130*, 14914–14915. [[CrossRef](#)] [[PubMed](#)]
28. Leclercq, L.; Lacour, M.; Sanon, S.H.; Schmitzer, A.R. Thermoregulated microemulsions by cyclodextrin sequestration: A new approach to efficient catalyst recovery. *Chem. Eur. J.* **2009**, *15*, 6327–6331. [[CrossRef](#)] [[PubMed](#)]
29. Miravet, J.F.; Escuder, D. Pyridine-functionalised ambidextrous gelators: Towards catalytic gels. *Chem. Commun.* **2005**, 5796–5798. [[CrossRef](#)] [[PubMed](#)]
30. Leclercq, L.; Suisse, I.; Agbossou-Niedercorn, F. Biphasic hydroformylation in ionic liquids: Interaction between phosphane ligands and imidazolium triflate, toward an asymmetric process. *Chem. Commun.* **2008**, 311–313. [[CrossRef](#)]
31. Leclercq, L.; Schmitzer, A.R. Supramolecular effects involving the incorporation of guest substrates in imidazolium ionic liquid networks: Recent advances and future developments. *Supramol. Chem.* **2009**, *21*, 245–263. [[CrossRef](#)]
32. Rodríguez-Llansola, F.; Miravet, J.F.; Beatriu Escuder, B. Supramolecular catalysis with extended aggregates and gels: Inversion of stereoselectivity caused by self-assembly. *Chem. Eur. J.* **2010**, *16*, 8480–8486. [[CrossRef](#)] [[PubMed](#)]

33. Dupont, J. On the solid, liquid and solution structural organization of imidazolium ionic liquids. *J. Braz. Chem. Soc.* **2004**, *15*, 341–350. [[CrossRef](#)]
34. Leclercq, L. Get beyond limits: From colloidal tectonics concept to the engineering of eco-friendly catalytic systems. *Front. Chem.* **2018**, *6*, 168. [[CrossRef](#)] [[PubMed](#)]
35. Pera-Titus, M.; Leclercq, L.; Clacens, J.-M.; De Campo, F.; Nardello-Rataj, V. Pickering interfacial catalysis for biphasic systems: From emulsion design to green reactions. *Angew. Chem. Int. Ed.* **2015**, *54*, 2006–2021. [[CrossRef](#)] [[PubMed](#)]
36. Corey, E.J.; Link, J.O. A new chiral catalyst for the enantioselective synthesis of secondary alcohols and deuterated primary alcohols by carbonyl reduction. *Tetrahedron Lett.* **1989**, *30*, 6275–6278. [[CrossRef](#)]
37. Waldrop, M.M. “Chemzymes” mimic biology in miniature. *Science* **1989**, *245*, 354–355. [[CrossRef](#)] [[PubMed](#)]
38. Bjerre, J.; Rousseau, C.; Marinescu, L.; Bols, M. Artificial enzymes, “Chemzymes”: Current state and perspectives. *Appl. Microbiol. Biotechnol.* **2008**, *81*, 1–11. [[CrossRef](#)]
39. Noujeim, N.; Leclercq, L.; Schmitzer, A.R. Imidazolium cations in organic chemistry: From chemzymes to supramolecular building blocs. *Curr. Org. Chem.* **2010**, *14*, 1500–1516. [[CrossRef](#)]
40. Szejtli, J. Introduction and general overview of cyclodextrin chemistry. *Chem. Rev.* **1998**, *98*, 1743–1754. [[CrossRef](#)]
41. Hussain, M.A.; Ashraf, M.U.; Muhammad, G.; Tahir, M.N.; Bukhari, S.N.A. Calixarene: A versatile material for drug design and applications. *Curr. Pharm. Des.* **2017**, *23*, 2377–2388. [[CrossRef](#)]
42. Steed, J.W. First- and second-sphere coordination chemistry of alkali metal crown ether complexes. *Coord. Chem. Rev.* **2001**, *215*, 171–221. [[CrossRef](#)]
43. Hilvert, D.; Breslow, R. Functionalized cyclodextrins as holoenzyme mimics of thiamine-dependent enzymes. *Bioorg. Chem.* **1984**, *12*, 206–220. [[CrossRef](#)]
44. Breslow, R.; Kool, E.T. A γ -cyclodextrin thiazolium salt holoenzyme mimic for the benzoin condensation. *Tetrahedron Lett.* **1988**, *29*, 1635–1638. [[CrossRef](#)]
45. Zhao, H.; Foss, F.W., Jr.; Breslow, R. Artificial enzymes with thiazolium and imidazolium coenzyme mimics. *J. Am. Chem. Soc.* **2008**, *130*, 12590–12591. [[CrossRef](#)] [[PubMed](#)]
46. Breslow, R.; Anslyn, E. Proton inventory of a bifunctional ribonuclease model. *J. Am. Chem. Soc.* **1989**, *111*, 8931–8932. [[CrossRef](#)]
47. Breslow, R.; Graff, A. Geometry of enolization using a bifunctional cyclodextrin-based catalyst. *J. Am. Chem. Soc.* **1993**, *115*, 10988–10989. [[CrossRef](#)]
48. Desper, J.M.; Breslow, R. Catalysis of an intramolecular aldol condensation by imidazole-bearing cyclodextrins. *J. Am. Chem. Soc.* **1994**, *116*, 12081–12082. [[CrossRef](#)]
49. Breslow, R.; Schmuck, C. Goodness of fit in complexes between substrates and ribonuclease mimics: Effects on binding, catalytic rate constants, and regiochemistry. *J. Am. Chem. Soc.* **1996**, *118*, 6601–6605. [[CrossRef](#)]
50. Breslow, R.; Desper, J.; Huang, Y. A selective intramolecular aldol condensation directed by a bifunctional enzyme mimic. *Tetrahedron Lett.* **1996**, *37*, 2541–2544. [[CrossRef](#)]
51. Ortega-Caballero, F.; Rousseau, C.; Christensen, B.; Petersen, T.E.; Bols, M. Remarkable supramolecular catalysis of glycoside hydrolysis by a cyclodextrin cyanohydrin. *J. Am. Chem. Soc.* **2005**, *127*, 3238–3239. [[CrossRef](#)]
52. Galia, A.; Scialdone, O.; Spanò, T.; Grazia Valenti, M.; Grignard, B.; Lecomte, P.; Monflier, E.; Tilloy, S.; Rousseau, C. Ring opening polymerization of ϵ -caprolactone in the presence of wet β -cyclodextrin: Effect of the operative pressure and of water molecules in the β -cyclodextrin cavity. *RSC Adv.* **2016**, *6*, 90290–90299. [[CrossRef](#)]
53. Molenveld, P.; Engbersen, J.F.J.; Kooijman, H.; Spek, A.L.; Reinhoudt, D.N. Efficient catalytic phosphate diester cleavage by the synergetic action of two Cu(II) centers in a dinuclear cis-diaqua Cu(II) calix[4]arene enzyme model. *J. Am. Chem. Soc.* **1998**, *120*, 6726–6737. [[CrossRef](#)]
54. Dospil, G.; Schatz, J. Synthesis and characterization of imidazole-substituted calix[4]arenes as simple enzyme-mimics with acyltransferase activity. *Tetrahedron Lett.* **2001**, *42*, 7837–7840. [[CrossRef](#)]
55. Cacciapaglia, R.; Di Stefano, S.; Kelderman, E.; Mandolini, L. Supramolecular catalysis of ester and amide cleavage by a dinuclear barium(II) complex. *Angew. Chem. Int. Ed.* **1999**, *38*, 348–351. [[CrossRef](#)]
56. Mortreux, A.; Petit, F. *Industrial Applications of Homogeneous Catalysis*; D. Reidel Publishing Compagny: Dordrecht, The Netherlands, 1988.
57. Cornils, B.; Herrmann, W.A. *Aqueous-Phase Organometallic Catalysis*; Wiley-VCH: Weinheim, Germany, 2004.

58. Monflier, E.; Fremy, G.; Castanet, Y.; Mortreux, A. Molecular recognition between chemically modified β -cyclodextrin and dec-1-ene: New prospects for biphasic hydroformylation of water-insoluble olefins. *Angew. Chem. Int. Ed.* **1995**, *34*, 2269–2271. [[CrossRef](#)]
59. Mathivet, T.; Méliet, C.; Castanet, Y.; Mortreux, A.; Caron, L.; Tilloy, S.; Monflier, E. Rhodium catalyzed hydroformylation of water insoluble olefins in the presence of chemically modified β -cyclodextrins: Evidence for ligand-cyclodextrin interactions and effect of various parameters on the activity and the aldehydes selectivity. *J. Mol. Catal. A* **2001**, *176*, 105–116. [[CrossRef](#)]
60. Leclercq, L.; Sauthier, M.; Castanet, Y.; Mortreux, A.; Bricout, H.; Monflier, E. Two-phase hydroformylation of higher olefins using randomly methylated α -cyclodextrin as mass transfer promoter: A smart solution for preserving the intrinsic properties of the rhodium/trisulfonated triphenylphosphine catalytic system. *Adv. Synth. Catal.* **2005**, *347*, 55–59. [[CrossRef](#)]
61. Sueur, B.; Leclercq, L.; Sauthier, M.; Castanet, Y.; Mortreux, A.; Bricout, H.; Tilloy, S.; Monflier, E. Rhodium complexes non-covalently bound to cyclodextrins: Novel water-soluble supramolecular catalysts for the biphasic hydroformylation of higher olefins. *Chem. Eur. J.* **2005**, *11*, 6228–6236. [[CrossRef](#)]
62. Leclercq, L.; Schmitzer, A.R. Assembly of tunable supramolecular organometallic catalysts with cyclodextrins. *Organometallics* **2010**, *29*, 3442–3449. [[CrossRef](#)]
63. Blaszkiewicz, C.; Bricout, H.; Léonard, E.; Len, C.; Landy, D.; Cézard, C.; Djedaïni-Pilard, F.; Monflier, E.; Tilloy, S. A cyclodextrin dimer as supramolecular reaction platform for aqueous organometallic catalysis. *Chem. Commun.* **2013**, *49*, 6989–6991. [[CrossRef](#)]
64. Machut-Binkowski, C.; Legrand, F.-X.; Azaroual, N.; Tilloy, S.; Monflier, E. New phosphane based on a β -cyclodextrin exhibiting a solvent-tunable conformation and its catalytic properties. *Chem. Eur. J.* **2010**, *16*, 10195–10201. [[CrossRef](#)] [[PubMed](#)]
65. Ngan Tran, D.; Legrand, F.-X.; Menuel, S.; Bricout, H.; Tilloy, S.; Monflier, E. Cyclodextrin-phosphane possessing a guest-tunable conformation for aqueous rhodium-catalyzed hydroformylation. *Chem. Commun.* **2012**, *48*, 753–755. [[CrossRef](#)] [[PubMed](#)]
66. Leblond, J.; Potier, J.; Menuel, S.; Bricout, H.; Machut-Binkowski, C.; Landy, D.; Tilloy, S.; Monflier, E.; Hapiot, F. Water-soluble phosphane-substituted cyclodextrin as an effective bifunctional additive in hydroformylation of higher olefins. *Catal. Sci. Technol.* **2017**, *7*, 3823–3830. [[CrossRef](#)]
67. Tung Wong, Y.; Yang, C.; Ying, K.-C.; Jia, G. Synthesis of a Novel β -cyclodextrin-functionalized diphosphine ligand and its catalytic properties for asymmetric hydrogenation. *Organometallics* **2002**, *21*, 1782–1787. [[CrossRef](#)]
68. Potier, J.; Menuel, S.; Rousseau, J.; Tumkevicius, S.; Hapiot, F.; Monflier, E. Multifunctional cyclodextrin-based *N,N*-bidentate ligands for aqueous Heck arylation. *Appl. Catal. A* **2014**, *479*, 1–8. [[CrossRef](#)]
69. Legrand, F.-X.; Ménand, M.; Sollogoub, M.; Tilloy, S.; Monflier, E. An *N*-heterocyclic carbene ligand based on a β -cyclodextrin-imidazolium salt: Synthesis, characterization of organometallic complexes and Suzuki coupling. *New J. Chem.* **2011**, *35*, 2061–2065. [[CrossRef](#)]
70. Hapiot, F.; Monflier, E. Unconventional approaches involving cyclodextrin-based, self-assembly-driven processes for the conversion of organic substrates in aqueous biphasic catalysis. *Catalysts* **2017**, *7*, 173. [[CrossRef](#)]
71. Jouffroy, M.; Armspach, D.; Matt, D. Cyclodextrin and phosphorus(III): A versatile combination for coordination chemistry and catalysis. *Dalton Trans.* **2015**, *44*, 12942–12969. [[CrossRef](#)]
72. Hapiot, F.; Bricout, H.; Tilloy, S.; Monflier, E. Functionalized cyclodextrins as first and second coordination sphere ligands for aqueous organometallic catalysis. *Eur. J. Inorg. Chem.* **2012**, *10*, 1571–1578. [[CrossRef](#)]
73. Bricout, H.; Hapiot, F.; Ponchel, A.; Tilloy, S.; Monflier, E. Chemically modified cyclodextrins: an attractive class of supramolecular hosts for the development of aqueous biphasic catalytic processes. *Sustainability* **2009**, *1*, 924–945. [[CrossRef](#)]
74. Yang, L.; Mashooq, K.; Park, S.-Y. Liquid crystal droplets functionalized with charged surfactant and polyelectrolyte for non-specific protein detection. *RSC Adv.* **2015**, *5*, 97264–97271. [[CrossRef](#)]
75. Creighton, M.A.; Zhu, W.; van Krieken, F.; Petteruti, R.A.; Gao, H.; Hurt, R.H. Three-dimensional graphene-based microbarriers for controlling release and reactivity in colloidal liquid phases. *ACS Nano* **2016**, *10*, 2268–2276. [[CrossRef](#)] [[PubMed](#)]
76. Kim, J.-W.; Lee, D.; Shum, H.C.; Weitz, D.A. Colloid surfactants for emulsion stabilization. *Adv. Mater.* **2008**, *20*, 3239–3243. [[CrossRef](#)]

77. Israelachvili, J.N. *Intermolecular and Surface Forces*; Academic Press: New York, NY, USA, 2011.
78. Israelachvili, J.N.; Mitchell, D.J.; Ninham, B.W. Theory of self-assembly of hydrocarbon amphiphiles into micelles and bilayers. *J. Chem. Soc. Faraday Trans.* **1976**, *72*, 1525–1568. [[CrossRef](#)]
79. Malcolmson, C.; Lawrence, M.J. A comparison of the incorporation of model steroids into non-ionic micellar and microemulsion systems. *J. Pharm. Pharmacol.* **1993**, *45*, 141–143. [[CrossRef](#)] [[PubMed](#)]
80. Kobayashi, S.; Wakabayashi, T.; Nagayama, S.; Oyamada, H. Lewis acid catalysis in micellar systems. Sc(OTf)₃-catalyzed aqueous aldol reactions of silyl enol ethers with aldehydes in the presence of a surfactant. *Tetrahedron Lett.* **1997**, *38*, 4559–4562. [[CrossRef](#)]
81. Kobayashi, S.; Wakabayashi, T. Scandium trisdodecylsulfate (STDS). A new type of lewis acid that forms stable dispersion systems with organic substrates in water and accelerates aldol reactions much faster in water than in organic solvents. *Tetrahedron Lett.* **1998**, *39*, 5389–5392. [[CrossRef](#)]
82. Manabe, K.; Mori, Y.; Kobayashi, S. A Brønsted acid-surfactant-combined catalyst for Mannich-type reactions of aldehydes, amines, and silyl enolates in water. *Synlett* **1999**, 1401–1402. [[CrossRef](#)]
83. Manabe, K.; Mori, Y.; Kobayashi, S. Mannich-type reactions of aldehydes, amines, and ketones in a colloidal dispersion system created by a Brønsted acid–surfactant-combined catalyst in water. *Org. Lett.* **1999**, *1*, 1965–1967. [[CrossRef](#)]
84. Otto, S.; Engberts, J.B.F.N.; Kwak, J.C.T. Million-fold acceleration of a Diels–Alder reaction due to combined Lewis acid and micellar catalysis in water. *J. Am. Chem. Soc.* **1998**, *120*, 9517–9525. [[CrossRef](#)]
85. Manabe, K.; Mori, Y.; Kobayashi, S. Three-component carbon–carbon bond-forming reactions catalyzed by a Brønsted acid–surfactant-combined catalyst in water. *Tetrahedron* **2001**, *57*, 2537–2544. [[CrossRef](#)]
86. Manabe, K.; Sun, X.-M.; Kobayashi, S. Dehydration reactions in water. Surfactant-type Brønsted acid-catalyzed direct esterification of carboxylic acids with alcohols in an emulsion system. *J. Am. Chem. Soc.* **2001**, *123*, 10101–10102. [[CrossRef](#)] [[PubMed](#)]
87. Manabe, K.; Iimura, S.; Sun, X.-M.; Kobayashi, S. Dehydration reactions in water. Brønsted acid–surfactant-combined catalyst for ester, ether, thioether, and dithioacetal formation in water. *J. Am. Chem. Soc.* **2002**, *124*, 11971–11978. [[CrossRef](#)] [[PubMed](#)]
88. Shirakawa, S.; Kobayashi, S. Surfactant-type Brønsted acid catalyzed dehydrative nucleophilic substitutions of alcohols in water. *Org. Lett.* **2007**, *9*, 311–314. [[CrossRef](#)] [[PubMed](#)]
89. Li, J.-T.; Li, Y.-W.; Song, Y.-L. Efficient synthesis of 12-aryl-8,9,10,12-tetrahydrobenzo[a]xanthen-11-one derivatives catalyzed by *p*-dodecylbenzenesulfonic acid in aqueous media under ultrasound irradiation. *Synth. Commun.* **2012**, *42*, 2161–2170. [[CrossRef](#)]
90. Shinde, P.V.; Kategaonkar, A.H.; Shingate, B.B.; Shingare, M.S. Surfactant catalyzed convenient and greener synthesis of tetrahydrobenzo[a]xanthen-11-ones at ambient temperature. *Beilstein J. Org. Chem.* **2011**, *7*, 53–58. [[CrossRef](#)] [[PubMed](#)]
91. Li, J.-T.; Du, C.; Xu, X.-Y.; Chen, G.-F. Synthesis of 2-(1,5-diaryl-1,4-pentadien-3-ylidene)-hydrazinecarboximidamide hydrochloride catalyzed by *p*-dodecylbenzenesulfonic acid in aqueous media under ultrasound irradiation. *Ultrason. Sonochem.* **2012**, *19*, 1033–1038. [[CrossRef](#)]
92. Chen, B.-H.; Li, J.-T.; Chen, G.H. Efficient synthesis of 2,3-disubstituted-2,3-dihydroquinazolin-4(1H)-ones catalyzed by dodecylbenzenesulfonic acid in aqueous media under ultrasound irradiation. *Ultrason. Sonochem.* **2015**, *23*, 59–65. [[CrossRef](#)]
93. Song, Y.-L.; Dong, Y.-F.; Wu, F.; Yang, T.; Yang, G.-L. One-pot three-component synthesis of 3-hydroxy-5,5-dimethyl-2-[phenyl(phenylthio)methyl]cyclohex-2-enone derivatives under ultrasound. *Ultrason. Sonochem.* **2015**, *22*, 119–124. [[CrossRef](#)]
94. Suzuki, I.; Suzumura, Y.; Takeda, K. Metal triflimide as a Lewis acid catalyst for Biginelli reactions in water. *Tetrahedron Lett.* **2006**, *47*, 7861–7864. [[CrossRef](#)]
95. Genet, J.P.; Yziel, J.; Port, M.; Touzin, A.M.; Roland, S.; Thorimbert, S.; Tanier, S. A practical synthesis of α -aminophosphonic acids. *Tetrahedron Lett.* **1992**, *33*, 77–80. [[CrossRef](#)]
96. Shekouhy, M. Sulfuric acid-modified PEG-6000 (PEG-OSO₃H): An efficient Brønsted acid-surfactant combined catalyst for the one-pot three component synthesis of α -aminonitriles in water. *Catal. Sci. Technol.* **2012**, *2*, 1010–1020. [[CrossRef](#)]
97. Kumar, A.; Maurya, R.A. Efficient Synthesis of Hantzsch Esters and Polyhydroquinoline Derivatives in Aqueous Micelles. *Synlett* **2008**. [[CrossRef](#)]

98. Paprocki, D.; Madej, A.; Koszelewski, D.; Brodzka, A.; Ostaszewski, R. Multicomponent Reactions Accelerated by Aqueous Micelles. *Front. Chem.* **2018**, *6*, 502. [[CrossRef](#)] [[PubMed](#)]
99. Li, J.; Zhang, Y.; Han, D.; Jia, G.; Gao, J.; Zhong, L.; Li, C. Transfer hydrogenation of aldehydes on amphiphilic catalyst assembled at the interface of emulsion droplets. *Green Chem.* **2008**, *10*, 608–611. [[CrossRef](#)]
100. Beletskaya, I.P.; Kashin, A.N.; Litvinov, A.E.; Tyurin, V.S.; Valetsky, P.M.; van Koten, G. Palladium colloid stabilized by block copolymer micelles as an efficient catalyst for reactions of C–C and C–heteroatom bond formation. *Organometallics* **2006**, *25*, 154–158. [[CrossRef](#)]
101. Norcott, P.; Spielman, C.; McErlean, C.S.P. An in-water, on-water domino process for synthesis. *Green Chem.* **2012**, *14*, 605–609. [[CrossRef](#)]
102. Lehn, J.-M. Perspectives in Chemistry: Aspects of Adaptive Chemistry and Materials. *Angew. Chem. Int. Ed.* **2015**, *54*, 3276–3289. [[CrossRef](#)]
103. Wu, Q.; Wan, H.; Li, H.; Song, H.; Chu, T. Bifunctional temperature-sensitive amphiphilic acidic ionic liquids for preparation of biodiesel. *Catal. Today* **2013**, *200*, 74–79. [[CrossRef](#)]
104. Ferreira, M.; Bricout, H.; Azaroual, N.; Landy, D.; Tilloy, S.; Hapiot, F.; Monflier, E. Cyclodextrin/amphiphilic phosphane mixed systems and their applications in aqueous organometallic catalysis. *Adv. Synth. Catal.* **2012**, *354*, 1337–1346. [[CrossRef](#)]
105. McClements, D.J. Nanoemulsions versus microemulsions: Terminology, differences, and similarities. *Soft Matter* **2012**, *8*, 1719–1729. [[CrossRef](#)]
106. Winsor, P.A. Hydrotropy, solubilisation and related emulsification processes. *Trans. Faraday Soc.* **1948**, *44*, 376–398. [[CrossRef](#)]
107. Kahlweit, M.; Strey, R. Phase behavior of ternary systems of the type H₂O-oil-nonionic amphiphile (microemulsions). *Angew. Chem. Int. Ed.* **1985**, *24*, 654–668. [[CrossRef](#)]
108. Haumann, M.; Koch, H.; Hugo, P.; Schomäcker, R. Hydroformylation of 1-dodecene using Rh-TPPTS in a microemulsion. *Appl. Catal. A* **2002**, *225*, 239–249. [[CrossRef](#)]
109. Haumann, M.; Yildiz, H.; Koch, H.; Schomäcker, R. Hydroformylation of 7-tetradecene using Rh-TPPTS in a microemulsion. *Appl. Catal. A* **2002**, *236*, 173–178. [[CrossRef](#)]
110. Yildiz Ünveren, H.H.; Schomäcker, R. Rhodium catalyzed hydroformylation of 1-octene in microemulsion: Comparison with various catalytic systems. *Catal. Lett.* **2006**, *110*, 195–201. [[CrossRef](#)]
111. Hamerla, T.; Rost, A.; Kasaka, Y.; Schomäcker, R. Hydroformylation of 1-dodecene with water-soluble rhodium catalysts with bidentate ligands in multiphase systems. *Chem. Cat. Chem.* **2013**, *5*, 1854–1862. [[CrossRef](#)]
112. Müller, M.; Kasaka, Y.; Müller, D.; Schomäcker, R.; Wozny, G. Process design for the separation of three liquid phases for a continuous hydroformylation process in a miniplant scale. *Ind. Eng. Chem. Res.* **2013**, *53*, 7259–7264. [[CrossRef](#)]
113. Illner, M.; Müller, D.; Esche, E.; Pogrzeba, T.; Schmidt, M.; Schomäcker, R.; Wozny, G.; Repke, J.-U. Hydroformylation in microemulsions: Proof of concept in a miniplant. *Ind. Eng. Chem. Res.* **2016**, *55*, 8616–8626. [[CrossRef](#)]
114. Pogrzeba, T.; Illner, M.; Schmidt, M.; Repke, J.-U.; Schomäcker, R. Microemulsion systems as switchable reaction media for the catalytic upgrading of long-chain alkenes. *Chem. Ing. Tech.* **2017**, *89*, 459–463. [[CrossRef](#)]
115. Pogrzeba, T.; Schmidt, M.; Milojevic, N.; Urban, C.; Illner, M.; Repke, J.-U.; Schomäcker, R. Understanding the role of nonionic surfactants during catalysis in microemulsion systems on the example of rhodium-catalyzed hydroformylation. *Ind. Eng. Chem. Res.* **2017**, *56*, 9934–9941. [[CrossRef](#)]
116. Kasaka, Y.; Bibouche, B.; Volovych, I.; Schwarze, M.; Schomäcker, R. Investigation of phase behaviour of selected chemical reaction mixtures in microemulsions for technical applications. *Colloids Surf. A* **2016**, *494*, 49–58. [[CrossRef](#)]
117. Häger, M.; Holmberg, K.; d’ARocha Gonsalves, A.M.; Serra, A.C. Oxidation of azo dyes in oil-in-water microemulsions catalyzed by metalloporphyrins in presence of lipophilic acids. *Colloids Surf. A* **2001**, *183*–185, 247–257. [[CrossRef](#)]
118. Fressancourt-Collinet, M.; Hong, B.; Leclercq, L.; Alsters, P.L.; Aubry, J.-M.; Nardello-Rataj, V. Acidic three-liquid-phase microemulsion systems based on balanced catalytic surfactant for epoxidation and sulfide oxidation under mild conditions. *Adv. Synth. Catal.* **2013**, *355*, 409–420. [[CrossRef](#)]

119. Hong, B.; Leclercq, L.; Collinet-Fressancourt, M.; Lai, J.; Bauduin, P.; Aubry, J.-M.; Nardello-Rataj, V. Synergy between bis(dimethyldioctylammonium) molybdate and tetraethylene glycol mono-octyl ether: A winning combination for interfacial catalysis in thermo-controlled and switchable microemulsions. *J. Mol. Catal. A* **2015**, *397*, 142–149. [[CrossRef](#)]
120. Hedström, G.; Slotte, J.P.; Molander, O.; Rosenholm, J.B. Enzyme-catalyzed oxidation of cholesterol in physically characterized water-in-oil microemulsions. *Biotechnol. Bioeng.* **1992**, *39*, 218–224. [[CrossRef](#)]
121. Lee, K.M.; Biellmann, J.-F. Cholesterol oxidase in microemulsion: Enzymatic activity on a substrate of low water solubility and inactivation by hydrogen peroxide. *Bioorganic Chem.* **1986**, *14*, 262–273. [[CrossRef](#)]
122. Piazza, G.J. Lipoyxygenase catalyzed hydroperoxide formation in microemulsions containing nonionic surfactant. *Biotechnol. Lett.* **1992**, *14*, 1153–1158. [[CrossRef](#)]
123. Larsson, K.M.; Adlercreutz, P.; Mattiasson, B.; Olsson, U. Enzymatic catalysis in microemulsions: Enzyme reuse and product recovery. *Biotechnol. Bioeng.* **1990**, *36*, 135–141. [[CrossRef](#)]
124. Kuchlyan, J.; Kundu, N.; Sarkar, N. Ionic liquids in microemulsions: Formulation and characterization. *Curr. Opin. Colloid Interface Sci.* **2016**, *25*, 27–38. [[CrossRef](#)]
125. Zhou, G.-P.; Zhang, Y.; Huang, X.-R.; Shi, C.-H.; Liu, W.-F.; Li, Y.-Z.; Qu, Y.-B.; Gao, P.-J. Catalytic activities of fungal oxidases in hydrophobic ionic liquid 1-butyl-3-methylimidazolium hexafluorophosphate-based microemulsion. *Colloids Surf. B* **2008**, *66*, 146–149. [[CrossRef](#)]
126. Schwarze, M.; Pogrzeba, T.; Volovych, I.; Schomäcker, R. Microemulsion systems for catalytic reactions and processes. *Catal. Sci. Technol.* **2015**, *5*, 24–33. [[CrossRef](#)]
127. Smith, G.D.; Donelan, C.E.; Barden, R.E. Oil-continuous microemulsions composed of hexane, water, and 2-propanol. *J. Colloid Interface Sci.* **1977**, *60*, 488–496. [[CrossRef](#)]
128. Kelsner, B.A.; Varie, D.; Barden, R.E.; Holt, S.L. Detergentless water/oil microemulsions composed of hexane, water, and 2-propanol. 2. Nuclear magnetic resonance studies, effect of added sodium chloride. *J. Phys. Chem.* **1979**, *83*, 1276–1280. [[CrossRef](#)]
129. Hou, W.; Xu, J. Surfactant-free microemulsions. *Curr. Opin. Colloid Interface Sci.* **2016**, *25*, 67–74. [[CrossRef](#)]
130. Klossek, M.; Touraud, D.; Zemb, T.; Kunz, W. Structure and solubility in surfactant-free microemulsions. *ChemPhysChem* **2012**, *13*, 4116–4119. [[CrossRef](#)]
131. Marcus, J.; Klossek, M.; Touraud, D.; Kunz, W. Nano-droplets formation in fragrance tinctures. *Flavour Frag. J.* **2013**, *28*, 294–299. [[CrossRef](#)]
132. Diat, O.; Klossek, M.; Touraud, D.; Deme, B.; Grillo, I.; Kunz, W.; Zemb, T. Octanol-rich and water-rich domains in dynamic equilibrium in the pre-ouzo region of ternary systems containing a hydrotrope. *J. Appl. Crystallogr.* **2013**, *46*, 1665–1669. [[CrossRef](#)]
133. Zemb, T.N.; Klossek, M.; Lopian, T.; Marcus, J.; Schöetl, S.; Horinek, D.; Prevost, S.F.; Touraud, D.; Diat, O.; Marčelja, S.; et al. How to explain microemulsions formed by solvent mixtures without conventional surfactants. *Proc. Natl. Acad. Sci. USA* **2016**, *113*, 4260–4265. [[CrossRef](#)]
134. Knickerbocker, B.M.; Pesheck, C.V.; Davis, H.T.; Scriven, L.E. Patterns of three-liquid-phase behavior illustrated by alcohol-hydrocarbon-water-salt mixtures. *J. Phys. Chem.* **1982**, *86*, 393–400. [[CrossRef](#)]
135. Marcus, J.; Touraud, D.; Prévost, S.; Diat, O.; Zemb, T.; Kunz, W. Influence of additives on the structure of surfactant-free microemulsions. *Phys. Chem. Chem. Phys.* **2015**, *17*, 32528–32538. [[CrossRef](#)]
136. Marcus, J.; Müller, M.; Nistler, J.; Touraud, D.; Kunz, W. Nano-droplet formation in water/ethanol or isopropanol/mosquito repellent formulations. *Colloids Surf. A* **2014**, *458*, 3–9. [[CrossRef](#)]
137. Klossek, M.L.; Touraud, D.; Kuntz, W. Eco-solvents–cluster-formation, surfactant less microemulsions and facilitated hydrotropy. *Phys. Chem. Chem. Phys.* **2013**, *15*, 10971–10977. [[CrossRef](#)]
138. Fischer, V.; Marcus, J.; Touraud, D.; Diat, O.; Kunz, K. Toward surfactant-free and water-free microemulsions. *J. Colloid Int. Sci.* **2015**, *453*, 186–193. [[CrossRef](#)]
139. Khmelnitsky, Y.L.; Zharinova, I.N.; Berezin, I.V.; Levashov, A.V.; Martinek, K. Detergentless microemulsions. A new microheterogeneous medium for enzymatic reactions. *Ann. N.Y. Acad. Sci.* **1987**, *501*, 161–164. [[CrossRef](#)]
140. Khmelnitsky, Y.L.; Hilhorst, R.; Veeger, C. Detergentless microemulsions as media for enzymatic reactions. Cholesterol oxidation catalyzed by cholesterol oxidase. *Eur. J. Biochem.* **1988**, *176*, 265–271. [[CrossRef](#)]
141. Vulfson, E.N.; Ahmed, G.; Gill, I.; Kozlov, I.A.; Goodenough, P.W.; Law, B.A. Alterations in the catalytic properties of polyphenoloxidase in detergentless microemulsions and ternary water–organic solvent mixtures. *Biotechnol. Lett.* **1991**, *13*, 91–96. [[CrossRef](#)]

142. O'Connor, C.J.; Aggett, A.; Williams, D.R.; Stanley, R.A. Candida cylindracea lipase-catalysed hydrolysis of methyl palmitate in detergentless microemulsion and paraffin/water biphasic media. *Aust. J. Chem.* **1991**, *44*, 53–60. [[CrossRef](#)]
143. Zoumpantioti, M.; Karali, M.; Xenakis, A.; Stamatis, H. Lipase biocatalytic processes in surfactant-free microemulsion-like ternary systems and related organogels. *Enzyme Microb. Technol.* **2006**, *39*, 531–539. [[CrossRef](#)]
144. Zoumpantioti, M.; Merianou, E.; Karandreas, T.; Stamatis, H.; Xenakis, A. Esterification of phenolic acids catalyzed by lipases immobilized in organogels. *Biotechnol. Lett.* **2010**, *32*, 1457–1462. [[CrossRef](#)]
145. O'Connor, C.J.; Cleverly, D.R. Bile salt stimulated human milk lipase catalyzed ester hydrolysis in detergentless microemulsion media. *Biocatal. Biotransform.* **1995**, *12*, 193–204. [[CrossRef](#)]
146. Shin, M.J.; Park, J.Y.; Park, K.; Song, S.H.; Yoo, Y.J. Novel sol–gel immobilization of horseradish peroxidase employing a detergentless micro-emulsion system. *Biotechnol. Bioprocess. Eng.* **2007**, *12*, 640–645. [[CrossRef](#)]
147. Topakas, E.; Stamatis, H.; Biely, P.; Kekos, D.; Macris, B.J.; Christakopoulos, P. Purification and characterization of a feruloyl esterase from *Fusarium oxysporum* catalyzing esterification of phenolic acids in ternary water–organic solvent mixtures. *J. Biotechnol.* **2003**, *102*, 33–44. [[CrossRef](#)]
148. Zoumpantioti, M.; Stamatis, H.; Papadimitriou, V.; Xenakis, A. Spectroscopic and catalytic studies of lipases in ternary hexane–1-propanol–water surfactantless microemulsion systems. *Colloids Surf B* **2006**, *47*, 1–9. [[CrossRef](#)]
149. Xenakis, A.; Zoumpantioti, M.; Stamatis, H. Enzymatic reactions in structured surfactant-free microemulsions. *Curr. Opin. Colloid Interface Sci.* **2016**, *22*, 41–45. [[CrossRef](#)]
150. Krickl, S.; Touraud, T.; Bauduin, P.; Zinn, T.; Kunz, W. Enzyme activity of horseradish peroxidase in surfactant-free microemulsions. *J. Colloid Int. Sci.* **2018**, *516*, 466–475. [[CrossRef](#)]
151. Pogrzeba, T.; Schmidt, M.; Hohl, L.; Weber, A.; Buchner, G.; Schulz, J.; Schwarze, M.; Kraume, M.; Schomäcker, R. Catalytic reactions in aqueous surfactant-free multiphase emulsions. *Ind. Eng. Chem. Res.* **2016**, *55*, 12765–12775. [[CrossRef](#)]
152. Simard, M.; Su, D.; Wuest, J.D. Use of hydrogen bonds to control molecular aggregation. Self-assembly of three-dimensional networks with large chambers. *J. Am. Chem. Soc.* **1991**, *113*, 4696–4698. [[CrossRef](#)]
153. Su, D.; Wang, X.; Simard, M.; Wuest, J.D. Molecular tectonics. *Supramol. Chem.* **1995**, *6*, 171–178. [[CrossRef](#)]
154. Hosseini, M.W. Reflection on molecular tectonics. *CrystEngComm* **2004**, *6*, 318–322. [[CrossRef](#)]
155. Hosseini, M.W. Molecular tectonics: From simple tectons to complex molecular networks. *Acc. Chem. Res.* **2005**, *38*, 313–323. [[CrossRef](#)] [[PubMed](#)]
156. Kosal, M.E.; Chou, J.-H.; Wilson, S.R.; Suslick, K.S. A functional zeolite analogue assembled from metalloporphyrins. *Nat. Mater.* **2002**, *1*, 118–121. [[CrossRef](#)] [[PubMed](#)]
157. Noro, S.-I.; Kitagawa, S.; Kondo, M.; Seki, K. A new, methane adsorbent, porous coordination polymer $[(\text{CuSiF}_6(4,4'\text{-bipyridine})_2)_n]$. *Angew. Chem. Int. Ed.* **2000**, *39*, 2081–2084. [[CrossRef](#)]
158. Zheng, N.; Bu, X.; Feng, P. Self-assembly of novel dye molecules and $[\text{Cd}_8(\text{SPH})_{12}]^{4+}$ cubic clusters into three-dimensional photoluminescent superlattice. *J. Am. Chem. Soc.* **2002**, *124*, 9688–9689. [[CrossRef](#)] [[PubMed](#)]
159. Entley, W.R.; Girolami, G.S. High-temperature molecular magnets based on cyanovanadate building blocks: Spontaneous magnetization at 230 K. *Science* **1995**, *268*, 397–400. [[CrossRef](#)] [[PubMed](#)]
160. Dupont, J.; Suarez, P.A.Z.; de Souza, R.F.; Burrow, R.A.; Kintzinger, J.P. C–H– π interactions in 1-*n*-butyl-3-methylimidazolium tetraphenylborate molten salt: Solid and solution structures. *Chem. Eur. J.* **2000**, *6*, 2377–2381. [[CrossRef](#)]
161. Shimizu, K.; Tariq, M.; Freitas, A.A.; Páduac, A.A.H.; Lopes, J.N.C. Self-organization in ionic liquids: From bulk to interfaces and films. *J. Braz. Chem. Soc.* **2016**, *27*, 349–362. [[CrossRef](#)]
162. Leclercq, L.; Suisse, I.; Roussel, P.; Agbossou-Niedercorn, F. Inclusion of tetrabutylammonium cations in a chiral thiazolium/triflate network: Solid state and solution structural investigation. *J. Mol. Struct.* **2012**, *1010*, 152–157. [[CrossRef](#)]
163. Aggarwal, A.; Llewellyn Lancaster, N.; Sethia, A.R.; Welton, T. The role of hydrogen bonding in controlling the selectivity of Diels–Alder reactions in room-temperature ionic liquids. *Green Chem.* **2002**, *4*, 517–520. [[CrossRef](#)]

164. Bravo, J.L.; López, I.; Cintas, P.; Silvero, G.; Arévalo, M.J. Sonochemical cycloadditions in ionic liquids. Lessons from model cases involving common dienes and carbonyl dienophiles. *Ultrason. Sonochem.* **2006**, *13*, 408–414. [[CrossRef](#)]
165. Bica, K.; Gmeiner, G.; Reichel, C.; Lendl, B.; Gaertner, P. Microwave-assisted synthesis of camphor-derived chiral imidazolium ionic liquids and their application in diastereoselective Diels-Alder reaction. *Synthesis* **2007**, 1333–1338. [[CrossRef](#)]
166. Gholap, A.R.; Venkatesan, K.; Daniel, T.; Lahoti, R.J.; Srinivasan, K.V. Ultrasound promoted acetylation of alcohols in room temperature ionic liquid under ambient conditions. *Green Chemistry* **2003**, *5*, 693–696. [[CrossRef](#)]
167. Fraga-Dubreuil, J.; Bourahla, K.; Rahmouni, M.; Bazureau, J.-P.; Hamelin, J. Catalysed esterifications in room temperature ionic liquids with acidic counteranion as recyclable reaction media. *Catal. Commun.* **2002**, *3*, 185–190. [[CrossRef](#)]
168. Ding, H.; Ye, W.; Wang, Y.; Wang, X.; Lia, L.; Liu, D.; Guid, J.; Song, C.; Ji, N. Process intensification of transesterification for biodiesel production from palm oil: Microwave irradiation on transesterification reaction catalyzed by acidic imidazolium ionic liquids. *Energy* **2018**, *144*, 957–967. [[CrossRef](#)]
169. Gholap, A.R.; Venkatesan, K.; Daniel, T.; Lahoti, R.J.; Srinivasan, K.V. Ionic liquid promoted novel and efficient one pot synthesis of 3,4-dihydropyrimidin-2-(1H)-ones at ambient temperature under ultrasound irradiation. *Green Chem.* **2004**, *6*, 147–150. [[CrossRef](#)]
170. Avent, A.G.; Chaloner, P.A.; Day, M.P.; Seddon, K.R.; Welton, T. Evidence for hydrogen bonding in solutions of 1-ethyl-3-methylimidazolium halides, and its implications for room-temperature halogenoaluminate(III) ionic liquids. *J. Chem. Soc. Dalton Trans.* **1994**, 3405–3413. [[CrossRef](#)]
171. Santos, L.S.; Neto, B.A.D.; Consorti, C.S.; Pavam, C.H.; Almeida, W.P.; Coelho, F.; Dupont, J.; Eberlin, M.N. The role of ionic liquids in co-catalysis of Baylis-Hillman reaction: Interception of supramolecular species via electrospray ionization mass spectrometry. *J. Phys. Org. Chem.* **2006**, *19*, 731–736. [[CrossRef](#)]
172. Morrison, D.W.; Forbesa, D.C.; Davis, J.H., Jr. Base-promoted reactions in ionic liquid solvents. The Knoevenagel and Robinson annulation reactions. *Tetrahedron Lett.* **2001**, *42*, 6053–6055. [[CrossRef](#)]
173. Antonietti, M.; Kuang, D.B.; Smarsly, B.; Yong, Z. Ionic liquids for the convenient synthesis of functional nanoparticles and other inorganic nanostructures. *Angew. Chem. Int. Ed.* **2004**, *43*, 4988–4992. [[CrossRef](#)]
174. Dash, P.; Miller, S.M.; Scott, R.W.J. Stabilizing nanoparticle catalysts in imidazolium-based ionic liquids: A comparative study. *J. Mol. Catal. A* **2010**, *329*, 86–95. [[CrossRef](#)]
175. Migowski, P.; Machado, G.; Teixeira, S.R.; Alves, M.C.; Morais, J.; Traverse, A.; Dupont, J. Synthesis and characterization of nickel nanoparticles dispersed in imidazolium ionic liquids. *Phys. Chem. Chem. Phys.* **2007**, *9*, 4814–4821. [[CrossRef](#)] [[PubMed](#)]
176. Calò, V.; Nacci, A.; Monopoli, A.; Detomaso, A.; Iliade, P. Pd nanoparticle catalyzed Heck arylation of 1,2-disubstituted alkenes in ionic liquids. Study on factors affecting the regioselectivity of the coupling process. *Organometallics* **2003**, *22*, 4193–4197. [[CrossRef](#)]
177. Gutel, T.; Garcia-Anton, J.; Pelzer, K.; Philippot, K.; Santini, C.C.; Chauvin, Y.; Chaudret, B.; Basset, J.-M. Influence of the self-organization of ionic liquids on the size of ruthenium nanoparticles: Effect of the temperature and stirring. *J. Mat. Chem.* **2007**, 3290–3292. [[CrossRef](#)]
178. Machado, G.; Scholten, J.D.; Vargas, T. d.; Teixeira, S.R.; Ronchi, L.H.; Dupont, J. Structural aspects of transition-metal nanoparticles in imidazolium ionic liquids. *Int. J. Nanotech.* **2007**, *4*, 541–563. [[CrossRef](#)]
179. Dupont, J.; Fonseca, G.S.; Umpierre, A.P.; Fichtner, P.F.P.; Teixeira, S.R. Transition-metal nanoparticles in imidazolium ionic liquids: recyclable catalysts for biphasic hydrogenation reactions. *J. Am. Chem. Soc.* **2002**, *124*, 4228–4229. [[CrossRef](#)] [[PubMed](#)]
180. Luska, K.L.; Moores, A. Ruthenium nanoparticle catalysts stabilized in phosphonium and imidazolium ionic liquids: Dependence of catalyst stability and activity on the ionicity of the ionic liquid. *Green Chem.* **2012**, *14*, 1736–1742. [[CrossRef](#)]
181. Cassol, C.C.; Umpierre, A.P.; Machado, G.; Wolke, S.I.; Dupont, J. The role of Pd nanoparticles in ionic liquid in the Heck reaction. *J. Am. Chem. Soc.* **2005**, *127*, 3298–3299. [[CrossRef](#)]
182. Ross, J.; Chen, W.; Xu, L.; Xiao, J. Ligand Effects in palladium-catalyzed allylic alkylation in ionic liquids. *Organometallics* **2001**, *20*, 138–142. [[CrossRef](#)]

183. Leclercq, L.; Suisse, I.; Nowogrocki, G.; Agbossou-Niedercorn, F. Halide-free highly-pure imidazolium triflate ionic liquids: Preparation and use in palladium-catalysed allylic alkylation. *Green Chem.* **2007**, *9*, 1097–1103. [[CrossRef](#)]
184. Leclercq, L.; Suisse, I.; Agbossou-Niedercorn, F. On the solid state inclusion of tetrabutylammonium cation in the imidazolium/trifluoromethanesulfonate H-bonds network observed in ionic co-crystals. *J. Mol. Struct.* **2008**, *892*, 433–437. [[CrossRef](#)]
185. Sieffert, N.; Wipff, G. Rhodium-catalyzed hydroformylation of 1-hexene in an ionic liquid: A molecular dynamics study of the hexene/[BMI][PF₆] interface. *J. Phys. Chem. B* **2007**, *111*, 4951–4962. [[CrossRef](#)] [[PubMed](#)]
186. Hao, L.; Zhao, Y.; Yu, B.; Yang, Z.; Zhang, H.; Han, B.; Gao, X.; Liu, Z. Imidazolium-based ionic liquids catalyzed formylation of amines using carbon dioxide and phenylsilane at room temperature. *ACS Catal.* **2015**, *5*, 4989–4993. [[CrossRef](#)]
187. Terech, P.; Weiss, R.G. Low molecular mass gelators of organic liquids and the properties of their gels. *Chem. Rev.* **1997**, *97*, 3133–3160. [[CrossRef](#)] [[PubMed](#)]
188. Escuder, B.; Rodríguez-Llansola, F.; Miravet, J.F. Supramolecular gels as active media for organic reactions and catalysis. *New J. Chem.* **2010**, *34*, 1044–1054. [[CrossRef](#)]
189. Escuder, B.; Llusar, M.; Miravet, J.F. Insight on the NMR study of supramolecular gels and its application to monitor molecular recognition on self-assembled fibers. *J. Org. Chem.* **2006**, *71*, 7747–7752. [[CrossRef](#)]
190. Yuan, T.; Sun, Z.; Mu, A.U.; Zeng, M.; Kalin, A.J.; Cheng, Z.; Olson, M.A.; Fang, L. Assembly and chiral memory effects of dynamic macroscopic supramolecular helices. *Chem. Eur. J.* **2018**, *24*, 16553–16557. [[CrossRef](#)] [[PubMed](#)]
191. Fang, W.; Zhang, Y.; Wu, J.; Liu, C.; Zhu, H.; Tu, T. Recent advances in supramolecular gels and catalysis. *Chem. Asian J.* **2018**, *13*, 712–729. [[CrossRef](#)]
192. Wang, Q.; Yang, Z.; Zhang, X.; Xiao, X.; Chang, C.K.; Xu, B. A Supramolecular-hydrogel-encapsulated hemin as an artificial enzyme to mimic peroxidase. *Angew. Chem. Int. Ed.* **2007**, *46*, 4285–4289. [[CrossRef](#)]
193. Wang, Q.; Yang, Z.; Ma, M.; Chang, C.K.; Xu, B. High catalytic activities of artificial peroxidases based on supramolecular hydrogels that contain heme models. *Chem. Eur. J.* **2008**, *14*, 5073–5078. [[CrossRef](#)]
194. Rodríguez-Llansola, F.; Escuder, B.; Miravet, J.F. Remarkable increase in basicity associated with supramolecular gelation. *Org. Biomol. Chem.* **2009**, *7*, 3091–3094. [[CrossRef](#)]
195. Mazzier, D.; Carraro, F.; Crisma, M.; Rancan, M.; Toniolo, C.; Moretto, A. A terminally protected dipeptide: From crystal structure and self-assembly, through co-assembly with carbon-based materials, to a ternary catalyst for reduction chemistry in water. *Soft Matter* **2016**, *12*, 238–245. [[CrossRef](#)] [[PubMed](#)]
196. Liu, Y.-R.; He, L.; Zhang, J.; Wang, X.; Su, C.-Y. Evolution of spherical assemblies to fibrous networked Pd(II) metallogels from a pyridine-based tripodal ligand and their catalytic property. *Chem. Mater.* **2009**, *21*, 557–563. [[CrossRef](#)]
197. Jin, Q.; Zhang, L.; Cao, H.; Wang, T.; Zhu, X.; Jiang, J.; Liu, M. Self-assembly of copper(II) ion-mediated nanotube and its supramolecular chiral catalytic behavior. *Langmuir* **2011**, *27*, 13847–13853. [[CrossRef](#)] [[PubMed](#)]
198. Jiang, J.; Wang, T.; Liu, M. Creating chirality in the inner walls of silica nanotubes through a hydrogel template: Chiral transcription and chiroptical switch. *Chem. Commun.* **2010**, *46*, 7178–7180. [[CrossRef](#)]
199. Zhou, H.-C.; Long, J.R.; Yaghi, O.M. Introduction to metal-organic frameworks. *Chem. Rev.* **2012**, *112*, 673–1268. [[CrossRef](#)] [[PubMed](#)]
200. Zhao, M.; Ou, S.; Wu, C.-D. Porous metal-organic frameworks for heterogeneous biomimetic catalysis. *Acc. Chem. Res.* **2014**, *47*, 1199–1207. [[CrossRef](#)] [[PubMed](#)]
201. Drake, T.; Ji, P.; Lin, W. Site Isolation in metal-organic frameworks enables novel transition metal catalysis. *Acc. Chem. Res.* **2018**, *51*, 2129–2138. [[CrossRef](#)]
202. Guillerme, V.; Kim, D.; Eubank, J.F.; Luebke, R.; Liu, X.; Adil, K.; Soo Lah, M.; Eddaoudi, M. A supermolecular building approach for the design and construction of metal-organic frameworks. *Chem. Soc. Rev.* **2014**, *43*, 6141–6172. [[CrossRef](#)]
203. Oh, M.; Carpenter, G.B.; Sweigart, D.A. Supramolecular Metal-organometallic coordination networks based on quinonoid π -complexes. *Acc. Chem. Res.* **2004**, *37*, 1–11. [[CrossRef](#)]
204. Liu, J.; Chen, L.; Cui, H.; Zhang, J.; Zhang, L.; Su, C.-Y. Applications of metal-organic frameworks in heterogeneous supramolecular catalysis. *Chem. Soc. Rev.* **2014**, *43*, 6011–6061. [[CrossRef](#)]

205. Chughtai, A.H.; Ahmad, N.; Younus, H.A.; Laypkov, A.; Verpoort, F. Metal-organic frameworks: Versatile heterogeneous catalysts for efficient catalytic organic transformations. *Chem. Soc. Rev.* **2015**, *44*, 6804–6849. [[CrossRef](#)] [[PubMed](#)]
206. Tian, J.; Xu, Z.-Y.; Zhang, D.-W.; Wang, H.; Xie, S.-H.; Xu, D.-W.; Ren, Y.-H.; Wang, H.; Liu, Y.; Li, Z.-T. Supramolecular metal-organic frameworks that display high homogeneous and heterogeneous photocatalytic activity for H₂ production. *Nat. Commun.* **2016**, *7*, 11580. [[CrossRef](#)] [[PubMed](#)]
207. Lagona, J.; Mukhopadhyay, P.; Chakrabarti, S.; Isaacs, L. The cucurbit[n]uril family. *Angew. Chem. Int. Ed.* **2005**, *44*, 4844–4870. [[CrossRef](#)] [[PubMed](#)]
208. Lee, J.W.; Samal, S.; Selvapalam, N.; Kim, H.-J.; Kim, K. Cucurbituril homologues and derivatives: new opportunities in supramolecular chemistry. *Acc. Chem. Res.* **2003**, *36*, 621–630. [[CrossRef](#)]
209. Gupta, V.; Mandal, S.K. Coordination driven self-assembly of [2 + 2 + 2] molecular squares: Synthesis, crystal structures, catalytic and luminescence properties. *Dalton Trans.* **2018**, *47*, 9742–9754. [[CrossRef](#)] [[PubMed](#)]
210. Tanaka, K.; Kinoshita, M.; Kayahara, J.; Uebayashi, Y.; Nakaji, K.; Morawiak, M.; Urbanczyk-Lipkowska, Z. Asymmetric ring-opening reaction of *meso*-epoxides with aromatic amines using homochiral metal-organic frameworks as recyclable heterogeneous catalysts. *RSC Adv.* **2018**, *8*, 28139–28146. [[CrossRef](#)]
211. Cui, J.; Ren, S.; Lin, T.; Feng, Y.; Jia, S. Shielding effects of Fe³⁺-tannic acid nano-coatings for immobilized enzyme on magnetic Fe₃O₄@silica core shell nanosphere. *Chem. Eng. J.* **2018**, *343*, 629–637. [[CrossRef](#)]
212. Leclercq, L.; Mouret, A.; Proust, A.; Schmitt, V.; Bauduin, P.; Aubry, J.-M.; Nardello-Rataj, V. Pickering emulsion stabilized by catalytic polyoxometalate nanoparticles: A new effective medium for oxidation reactions. *Chem. Eur. J.* **2012**, *18*, 14352–14358. [[CrossRef](#)]
213. Horne, D.S. Casein structure, self-assembly and gelation. *Curr. Opin. Coll. Interface Sci.* **2002**, *7*, 456–461. [[CrossRef](#)]
214. McMahon, D.J.; Oommen, B.S. Casein micelle structure, functions, and interactions. In *Advanced Dairy Chemistry*; McSweeney, P., Fox, P., Eds.; Springer: New York, NY, USA, 2013; pp. 185–209.
215. Dickinson, E. Food emulsions and foams: Stabilization by particles. *Curr. Opin. Colloid Interface Sci.* **2010**, *15*, 40–49. [[CrossRef](#)]
216. Nur, H.; Ikeda, S.; Ohtani, B. Phase-boundary catalysis: A new approach in alkene epoxidation with hydrogen peroxide by zeolite loaded with alkylsilane-covered titanium oxide. *Chem. Commun.* **2000**, 2235–2236. [[CrossRef](#)]
217. Nur, H.; Ikeda, S.; Ohtani, B. Phase-boundary catalysis of alkene epoxidation with aqueous hydrogen peroxide using amphiphilic zeolite particles loaded with titanium oxide. *J. Catal.* **2001**, *204*, 402–408. [[CrossRef](#)]
218. Nur, H.; Ikeda, S.; Ohtani, B. Phase-boundary catalysts for acid-catalyzed reactions: The role of bimodal amphiphilic structure and location of active sites. *J. Braz. Chem. Soc.* **2004**, *15*, 719–724. [[CrossRef](#)]
219. Zeng, M.; Shah, S.A.; Huang, D.; Parviz, D.; Yu, Y.-H.; Wang, X.; Green, M.J.; Cheng, Z. Aqueous exfoliation of graphite into graphene assisted by sulfonyl graphene quantum dots for photonic crystal applications. *ACS Appl. Mater. Interfaces* **2017**, *9*, 30797–30804. [[CrossRef](#)] [[PubMed](#)]
220. Luo, J.; Zeng, M.; Peng, B.; Tang, Y.; Zhang, L.; Wang, P.; He, L.; Huang, D.; Wang, L.; Wang, X.; et al. Electrostatic-driven dynamic jamming of 2D nanoparticles at interfaces for controlled molecular diffusion. *Angew. Chem. Int. Ed.* **2018**, *130*, 11926–11931. [[CrossRef](#)]
221. Wang, X.; Zeng, M.; Yu, Y.H.; Wang, H.; Mannan, M.S.; Cheng, Z. Thermosensitive ZrP-PNIPAM Pickering emulsifier and the controlled-release behavior. *ACS Appl. Mater. Interfaces* **2017**, *9*, 7852–7858. [[CrossRef](#)] [[PubMed](#)]
222. Ikeda, S.; Nur, H.; Sawadaishi, T.; Ijio, K.; Shimomura, M.; Ohtani, B. Direct observation of bimodal amphiphilic surface structures of zeolite particles for a novel liquid-liquid phase boundary catalysis. *Langmuir* **2001**, *17*, 7976–7979. [[CrossRef](#)]
223. Leclercq, L.; Mouret, A.; Bauduin, P.; Nardello-Rataj, V. Supramolecular colloidosomes based on tri(dodecyltrimethylammonium) phosphotungstate: A bottom-up approach. *Langmuir* **2014**, *30*, 5386–5393. [[CrossRef](#)]
224. Mouret, A.; Leclercq, L.; Mühlbauer, A.; Nardello-Rataj, V. Eco-friendly solvents and amphiphilic catalytic polyoxometalate nanoparticles: A winning combination for olefin epoxidation. *Green Chem.* **2014**, *16*, 269–278. [[CrossRef](#)]
225. Pickering, S.U. Emulsions. *J. Chem. Soc. Trans.* **1907**, *91*, 2001–2021. [[CrossRef](#)]

226. Ramsden, W. Separation of solids in the surface-layers of solutions and “suspensions”. *Proc. R. Soc. Lond.* **1903**, *72*, 156–164.
227. Chevalier, Y.; Bolzinger, M.-A. Emulsions stabilized with solid nanoparticles: Pickering emulsions. *Colloid Surf. A* **2013**, *439*, 23–34. [[CrossRef](#)]
228. Finkle, P.; Draper, H.D.; Hildebrand, J.H. The theory of emulsification. *J. Am. Chem. Soc.* **1923**, *45*, 2780–2788. [[CrossRef](#)]
229. Destribats, M.; Gineste, S.; Laurichesse, E.; Tanner, H.; Leal-Calderon, F.; Héroguez, V.; Schmitt, V. Pickering emulsions: What are the main parameters determining the emulsion type and interfacial properties? *Langmuir* **2014**, *30*, 9313–9326. [[CrossRef](#)] [[PubMed](#)]
230. Leal-Calderon, F.; Schmitt, V. Solid-stabilized emulsions. *Curr Opin Colloid Interface Sci.* **2008**, *13*, 217–227. [[CrossRef](#)]
231. Leclercq, L.; Mouret, A.; Renaudineau, S.; Schmitt, V.; Proust, A.; Nardello-Rataj, V. Self-assembled polyoxometalates nanoparticles as Pickering emulsion stabilizers. *J. Phys. Chem. B* **2015**, *119*, 6326–6337. [[CrossRef](#)]
232. Leclercq, L.; Company, R.; Mühlbauer, A.; Mouret, A.; Aubry, J.-M.; Nardello-Rataj, V. Versatile eco-friendly pickering emulsions based on substrate/native cyclodextrin complexes: A winning approach for solvent-free oxidations. *ChemSusChem* **2013**, *6*, 1533–1540. [[CrossRef](#)] [[PubMed](#)]
233. Pacaud, B.; Leclercq, L.; Dechézelles, J.-F.; Nardello-Rataj, V. Hybrid core-shell nanoparticles by “plug and play” self-assembly. *Chem. Eur. J.* **2018**, *24*, 17672–17676. [[CrossRef](#)] [[PubMed](#)]
234. Potier, J.; Manuel, S.; Chambrier, M.-H.; Burylo, L.; Blach, J.-F.; Woisel, P.; Monflier, E.; Hapiot, F. Pickering emulsions based on supramolecular hydrogels: Application to higher olefins’ hydroformylation. *ACS Catal.* **2013**, *3*, 1618–1621. [[CrossRef](#)]
235. Potier, J.; Manuel, S.; Monflier, E.; Hapiot, F. Synergetic Effect of Randomly Methylated β -cyclodextrin and a Supramolecular hydrogel in Rh-catalyzed hydroformylation of higher olefins. *ACS Catal.* **2014**, *4*, 2342–2346. [[CrossRef](#)]
236. Chevry, M.; Vanbésien, T.; Manuel, S.; Monflier, E.; Hapiot, F. Tetronics/cyclodextrin-based hydrogels as catalyst-containing media for the hydroformylation of higher olefins. *Catal. Sci. Technol.* **2017**, *7*, 114–123. [[CrossRef](#)]
237. Yang, B.; Leclercq, L.; Schmitt, V.; Pera-Titus, M.; Nardello-Rataj, V. Colloidal tectonics for tandem synergistic Pickering interfacial catalysis: Oxidative cleavage of cyclohexene oxide into adipic acid. *Chem. Sci.* **2019**, *10*, 501–507. [[CrossRef](#)] [[PubMed](#)]



© 2019 by the authors. Licensee MDPI, Basel, Switzerland. This article is an open access article distributed under the terms and conditions of the Creative Commons Attribution (CC BY) license (<http://creativecommons.org/licenses/by/4.0/>).